NATIONAL TECHNICAL UNIVERSITY OF ATHENS
SCHOOL OF ELECTRICAL AND COMPUTER ENGINEERING DIVISION OF INFORMATION TRANSMISSION SYSTEMS AND MATERIAL TECHNOLOGY

Design and performance study of implantable and ingestible antennas

THESIS

Maria A.Riga

Thesis Advisor: Prof. Konstantina S. Nikita

Athens, February 2017

ΕΘΝΙΚΟ ΜΕΤΣΟΒΙΟ ΠΟΛΥΤΕΧΝΕΙΟ ΣΧΟΛΗ
ΗΛΕΚΤΡΟΛΟΓΩΝ ΜΗΧΑΝΙΚΩΝ ΚΑΙ ΜΗΧΑΝΙΚΩΝ
ΥΠΟΛΟΓΙΣΤΩΝ
ΤΟΜΕΑΣ ΣΥΣΤΗΜΑΤΩΝ ΜΕΤΑΔΟΣΗΣ ΠΛΗΡΟΦΟΡΙΑΣ
ΚΑΙ ΤΕΧΝΟΛΟΓΙΑΣ ΥΛΙΚΩΝ

Σχεδίαση και μελέτη επιδόσεων εμφυτεύσιμων, καταπόσιμων κεραιών

ΔΙΠΛΩΜΑΤΙΚΗ ΕΡΓΑΣΙΑ

Μαρία Α.Ρήγα

Επιβλέπων : Κωσταντίνα Σπ. Νικήτα
Αναπλ. Καθηγήτρια Ε.Μ.Π.

Αθήνα, Φεβρουάριος 2017

NATIONAL TECHNICAL UNIVERSITY OF ATHENS
SCHOOL OF ELECTRICAL AND COMPUTER ENGINEERING
DIVISION OF INFORMATION TRANSMISSION SYSTEMS AND MATERIAL TECHNOLOGY

Design and performance study of implantable and ingestible antennas

THESIS

Maria A.Riga

Advisory Board: Prof. Konstantina S Nikita
Prof. George Matsopoulos
Prof. Dimitrios Koutsouris

Approved by the Review Board on …..

……..	……..	……..
Konstantina S Nikita	George Matsopoulos	Dimitrios Koutsouris
Professor, NTUA	Professor, NTUA	Professor, NTUA
……..	……..	……..

Athens, February 2017

.....
Maria A.Riga

.....
Μαρία Α.Ρήγα

Abstract

The development of Biomedical Telemetry, through systems that are capable of transmitting data and physiological parameters of the patient in real time, has created a new perspective in the medical field, by promoting a an advanced healthcare system based on early diagnosis and treatment. Crucial part of these intelligent systems is the antenna integrated inside medical devices for wireless medical telemetry purposes. The aim of this diploma thesis is the design of a novel antenna, with miniaturized dimensions, for integration both in IMDs and WCE systems. In this thesis , the design of an implantable dual-band patch antenna of the literature is studied, which further enables the design of a novel patch antenna with optimized geometry and performance, that functions in the MedRadio (401-406 MHz) frequency band. Design of the novel antenna inside simplified tissue models are conducted, as well as performance evaluation of the antenna.

Keywords: Biomedical telemetry, Implantable antenna, Ingestible antenna, Injectable antenna, implantable medical device (IMD), Wireless Capsule Endoscopy (WCE), RFID tags (radio frequency identification), Injectable neurostimulators (InNS), MedRadio (Medical Device Radiocommunications Service) band, Industrial, Scientific and Medical (ISM) band, Microstrip - Patch antenna, Planar Inverted F-Antenna (PIFA), Finite Element (FE), optimization, Tissue Models

Περίληψη

Η ανάπτυξη της Βιοϊατρικής Τηλεμετρίας, και η εφαρμογή της μέσω συστημάτων τα οποία έχουν τη δυνατότητα να μεταδίδουν δεδομένα και φυσιολογικές παραμέτρους του ασθενή σε πραγματικό χρόνο, έχει δημιουργήσει μια νέα εικόνα στον κλάδο της υγείας, προωθώντας ένα προηγμένο συστήμα υγειονομικής περίθαλψης που βασίζεται στην έγκαιρη πρόληψη και θεραπεία. Ακρογωνιαίο τμήμα του συστήματος αυτού, αποτελεί η ύπαρξη κεραιών που ενσωματώνονται επί ιατρικών διατάξεων (εμφυτεύσιμων, καταπόσιμων, κ.α.), για την επίτευξη ασύρματης ιατρικής τηλεμετρίας. Στόχος της παρούσας διπλωματικής εργασίας είναι η σχεδίαση μιας πρωτότυπης κεραίας, μικροσκοπικών διαστάσεων,για εφαρμογές τόσο σε εμφυτεύσιμες ιατρικές διατάξεις όσο και σε κάψουλες καταπόσιμης ενδοσκόπησης. Στο πλαίσιο της εργασίας, μελετάται η πορεία σχεδίασης μιας εμφυτεύσιμης κεραίας μικροταινίας διπλής ζώνης της βιβλιογραφίας, η οποία αποτελεί τη βάση για τη σχεδίαση μιας πρωτότυπης κεραίας με βελτιστοποιημένη γεωμετρία και επιδόσεις και λειτουργία στη ζώνη συχνοτήτων MedRadio (401-406 MHz). Πραγματοποιείται σχεδίαση της πρωτότυπης κεραίας εντός απλοποιημένων μοντέλων ιστών, καθώς και μελέτη των επιδόσεων αυτής.

Λέξεις κλειδιά: Βιοϊατρική τεχνολογία, Εμφυτεύσιμη κεραία, Καταπόσιμη κεραία, Ενέσιμη κεραία,Εμφυτεύσιμη Ιατρική Συσκευή (IMD), ασύρματη ενδοσκοπική κάψουλα (WCE), ετικέτες ταυτοποίησης μέσω ραδιοσυχνοτήτων (RFID tags), Ενέσιμος νευροδιεγέρτης (InNS), Ζώνη Υπηρεσιών Επικοινωνίας Ιατρικών Εμφυτευμάτων (MedRadio band), Ζώνη Βιομηχανικών, Επιστημονικών και Ιατρικών Εφαρμογών (ISM band), Κεραία μικροταινίας, Επίπεδη κεραία ανεστραμμένου F (PIFA), Μέθοδος Πεπερασμένων Στοιχείων (FE), βελτιστοποίηση, Μοντέλα ιστού.

Εκτεταμένη Περίληψη

Ως Βιοϊατρική Τηλεμετρία ορίζεται η απόκτηση, μετάδοση και ερμηνεία διάφορων βιοσημάτων από σταθερά ή κινητά σημεία σε αποδεκτό κόστος. Η Βιοϊατρική Τηλεμετρία αποτελεί αναπόσπαστο κομμάτι της Τηλεϊατρικής και διαμορφώνει συνεχώς την εφαρμογή της δεύτερης στους ασθενείς μέσω τεχνολογικών εξελίξεων που αφορούν τον τομέα της πληροφορικής και τηλεπικοινωνιών , παρέχοντας τη δυνατότης μιας πιο προσανατολισμένης και εξατομικευμένης ιατρικής περίθαλψης.Προσφέρει ασύρματη, χωρίς περιορισμούς μετάδοση δεδομένων φυσιολογικών παραμέτρων χωρίς να απαιτεί τη χρήση αναισθησίας ή άλλων σημαντικών φυσικών περιορισμών. Τα συστήματα Βιοϊατρικής Τηλεμετρίας αποτελούνται απο ποικίλες ιατρικές διατάξεις με σκοπό να αποτελέσουν ένα δίκτυο ιατρικού αισθητήρα με εφαρμογές σε τομείς όπως αυτοί της Διάγνωσης, της Θεραπείας, της Αποκατάστασης κ.α. Αναπόσπαστο κομμάτι των ιατρικών αυτών διατάξεων είναι οι κεραίες που βρίσκονται ενσωματωμένες σε αυτές, και οι οποίες επιτρέπουν τη δυνατότητα επικοινωνίας με εξωτερικές διατάξεις επίβλεψης/ελέγχου.

Οι εμφυτεύσιμες ιατρικές συσκευές είναι μια κυρίαρχη κατηγορία στη Βιοϊατρική Τεχνολογία.Πρόκειται για συσκευές που τοποθετούνται εξ' ολοκλήρου ή μερικώς στα σώματα των ασθενών και οι οποίες παραμένουν στο σώμα για μερικές ώρες/έτη ή ακόμη και μόνιμα μετά από απαραίτητη χειρουργική επέμβαση. Από την εφεύρεση του πρώτου καρδιακού βηματοδότη και την επιτυχή του εμφύτευση το 1953, πολλές ηλεκτρονικές ιατρικές συσκευές έχουν κάνει την εμφάνιση τους, με χαρακτηριστικές διατάξεις όπως είναι: οι βηματοδότες, οι καρδιακοί απινιδωτές, τα κοχλιακά εμφυτεύματα, οι αντλίες ινσουλίνης, οι νευροδιεγέρτες, τα εμφυτεύματα αμφιβληστροειδούς, τα συστήματα μέτρησης της ενδοκρανιακής πίεσης, ο διαφραγματικός βηματοδότης κ.α.

Μεταξύ των πλεονεκτημάτων των Ασύρματων Δικτύων Περιοχής Σώματος (Wireless Body Area Networks, WBAN) και των Ασύρματων Δίκτυων Προσωπικής Περιοχής (Wireless Personal Area Networks, WPAN) συγκαταλέγονται η μειωμένη επεμβατικότητα και κατά συνέπεια ο μειωμένος κίνδυνος μόλυνσης, γρήγορη διάγνωση, κτλ. Σημειώνεται ότι ο όρος WBAN αναφέρεται στην επικοινωνία πολλαπλών ιατρικών διατάξεων τοποθετημένων επί ή εντός του ανθρώπινου σώματος με έναν επί του σώματος τοποθετημένο σταθμό βάσης, ενώ ο όρος WPAN αναφέρεται στην επικοινωνία διασυνδεδεμένων διατάξεων γύρω από ένα ανθρώπινο υποκείμενο, τυπικά σε απόσταση μικρότερη των 10 m. Ένα τυπικό σύστημα ασύρματης τηλεμετρίας για εμφυτεύσιμες ιατρικές διατάξεις μέσω κεραιών αποτελείται από έναν εξωτερικό σταθμό βάσης (φορετό ή σε κοντινή απόσταση από τον ασθενή) με τον οποίον επικοινωνούν δικατευθυντήρια οι εμφυτεύσιμες κεραίες. Ο σταθμός βάσης εκτελεί ποικίλες λειτουργίες, όπως: την επεξεργασία των ληφθέντων δεδομένων και τη λήψη αποφάσεων, την αποθήκευση ληφθέντων δεδομένων για

μελλόντικη επεξεργασία, την ειδοποίηση του ασθενή για ένα σημαντικό ιατρικό συμβάν, ή λοιπών εμφυτεύσιμων διατάξεων για την έγχυση κάποιου φαρμάκου.

Οι ασύρματες εμφυτεύσιμες συσκευές λειτουργούν σε διάφορα εύρη συχνοτήτων ανάλογα με τον απαιτούμενο ρυθμό δεδομένων, το εύρος λειτουργίας, τις απαιτήσεις ενεργειακής μεταφοράς, και τους εκάστοτε κυβερνητικούς κανονισμούς. Ευρέως διαδεδομένες ζώνες συχνοτήτων αποτελούν οι Ζώνες MedRadio και ISM (Industrial, Scientific and Medical). Στην Ζώνη MedRadio έχει ενσωματωθεί το υφιστάμενο φάσμα της ζώνης MICS (Medical Implant Communication Service) από 402-405 MHz και επιπλέον έχει προστεθεί το φάσμα στα 401 - 402 MHz και 405 - 406 MHz.

Η ζώνη MedRadio διατίθεται για ιατρικά εμφυτεύματα μακράς διάρκειας και επομένως έχει ελάχιστη ηλεκτρομαγνητική ρύπανση που μπορεί να προκαλέσει παρεμβολές στις συσκευές που λειτουργούν σε αυτές τις συχνότητες. Ωστόσο, τα μεγάλα μήκη κύματος που είναι αντιπροσωπευτικά της ζώνης αυτής, δημιουργούν προκλήσεις σχετικά με το μεγάλο μήκος της κεραίας, την απόδοση της ακτινοβολίας και το περιορισμένο εύρος λειτουργίας κτλ. Η πλέον συχνά χρησιμοποιούμενη ζώνη ISM για ασύρματη τηλεμετρία εμφυτεύσιμων ιατρικών διατάξεων είναι η ζώνη 2400.0–2483.5 MHz. Βασικό πλεονέκτημα των ζωνών ISM είναι το αυξημένο εύρος ζώνης, το οποίο επιτρέπει τη μετάδοση υψηλού ρυθμού δεδομένων (π.χ. μετάδοση βίντεο). Επιπλέον, η διείσδυση της ΗΜ ακτινοβολίας εντός του ανθρώπινου σώματος στις ζώνες ISM είναι αρκετά μικρότερη, λόγω μεγαλύτερων αποσβέσεων στις υψηλότερης συχνότητας λειτουργίας. Άλλες ζώνες λειτουργίας για ιατρική Τηλεμετρία που αναφέρονται είναι οι: Wireless Medical Telemetry Service (WMTS): (608 – 614MHz, 1395 – 1400MHz, 1427 – 1432MHz, Ultra-wideband technology (UWB) band 3.1-10.6 GHz.

Οι εμφυτεύσιμες κεραίες είναι ηλεκτρικά μικρές κεραίες που ακτινοβολούν μέσα στο ανθρώπινο σώμα το οποίο χαρακτηρίζεται απο μεγάλες απώλειες. Επομένως η σχεδίαση τους παρουσιάζει προκλήσεις προκειμένου να εξασφαλιστεί η βέλτιστη απόδοση της κεραίας και η ελαχιστοποίηση της πιθανότητας να επιδράσει αρνητικά στον οργανισμό. Οι πιο σημαντικοί παράμετροι που πρέπει να ληφθούν υπ’ όψιν κατά τον σχεδιασμό είναι: i) η σμίκρυνση των διαστάσεων της κεραίας (συμβάλλει στη μειωμένη επεμβατικότητα και δυσφορία του ασθενή), ii) η βιοσυμβατότητα (έτσι ώστε να μην προκαλούνται τοξικές αντιδράσεις ή φαινόμενα τραυματισμού κατά την επαφή τους με τους βιολογικούς ιστούς), iii) η ασφάλεια του ασθενή (απαραίτητη είναι η συμμόρφωση της διάταξης με τα όρια του Ειδικού Ρυθμού Απορρόφησης SAR όπως έχουν ορισθεί από τους διεθνείς οργανισμούς), iv) η τροφοδοσία της εμφυτεύσιμης διάταξης (προσανατολισμός σε μεθόδους που εξασφαλίζουν χαμηλότερη ενεργειακή κατανάλωση π.χ. επαγωγική σύζευξη για μεγαλύτερη διάρκεια ζωής της συσκευής), v) η απόδοση της κεραίας (έτσι ώστε να εξασφαλιστεί η αξιοπιστία της εμφυτεύσιμης διάταξης - ένας συμβιβασμός γίνεται μεταξύ του κέρδους της κεραίας στο μακρινό επίπεδο και των ενεργειακών περιορισμών προκειμενένου να διαφυλαχθεί ο ανθρώπινος οργανισμός από βλάβες της ηλεκτρομαγνητικής ακτινοβολίας).

Οι κυριότερες μεθοδολογίες σμίκρυνης των διαστάσεων της κεραίας είναι: i) η αύξηση της διαδρομής τού ρεύματος στην επιφάνεια της κεραίας, καθώς μειώνει

την επιτευχθείσα συχνότητα συντονισμού και επιτυγχάνει συμπαγέστερο μέγεθος για την εμφυτεύσιμη κεραία, ii) η προσθήκη αγωγού βραχυκύκλωσης, καθώς αυξάνει το ενεργό μέγεθος της κεραίας, μειώνοντας, εν συνεχεία, τις απαιτούμενες φυσικές διαστάσεις της για μία δεδομένη συχνότητα λειτουργίας, iii) η στοίβαξη ταινιών (η κατακόρυφη στοίβαξη δύο ή περισσότερων ταινιών συνιστά ένα τρόπο αύξησης του μήκους διαδρομής ρεύματος επί των ταινιών, μειώνοντας, παράλληλα, το συνολικό φυσικό μέγεθος της κεραίας) και iv) η χρήση διηλεκτρικών υλικών υψηλής σχετικής διηλεκτρικής σταθεράς. Η χρήση υλικών υποστρώματος και υπερστρώματος με υψηλή σχετική διηλεκτρική σταθερά (π.χ. κεραμική αλουμίνα, ROGER 3210) μειώνει το ενεργό μήκος κύματος της ακτινοβολίας και οδηγεί σε χαμηλότερες συχνότητες συντονισμού, συνεισφέροντας στη σμίκρυνση των διαστάσεων της κεραίας.

Οι καταπόσιμες κεραίες ταξιδεύουν κατά μήκος της πεπτικής οδού, ακολουθώντας πορεία από τον οισοφάγο στο στομάχι και από εκεί στο λεπτό έντερο μέχρι το παχύ έντερο και συμβάλλλουν στη διάγνωση ασθενειών του εντέρου,όπως καρκίνος, πολύποδες, νεοπλασίες του λεπτού εντέρου, συνδρόμα δυσαπορρόφησης, νόσος του Crohn, κοιλιακό άλγος και άλλες παθήσεις. Η κάψουλα στη συνέχεια αποβάλλεται από τον οργανισμό μέσα από την φυσιολογική διαδικασία εκκένωσης του οργανισμού. Η ιδιαιτερότητα της πεπτικής οδού περιορίζει την χρησιμοποίηση των σημερινών διαθέσιμων τεχνικών εξετάσης. Το πάνω τμήμα της γαστρεντερικής οδού μπορεί να εξετασθεί με γαστροσκόπηση.Τα δύο τελευταία μέτρα του παχέος εντέρου και του ορθού με κολονοσκόπηση. Στο ενδιάμεσο ωστόσο βρίσκονται 7 μέτρα ακανόνιστου λεπτού εντέρου στα οπόια δεν υπάρχει πρόβαση με τις προηγούμενες τεχνικές. Επομένως η μη-επεμβατική ενδοσκόπηση μέσω ασύρματης κάψουλας έρχεται για να επιτρέψει τη πλήρη οπτικοποίηση της γαστρεντερικής οδού. Η καταπόσιμη κάψουλα (στο μέγεθος δηλαδή ενός χαπιού βιταμίνης), εφοδιασμένη με μία κάμερα, φώτα LED, μικροσκοπική κεραία, μπαταρίες κ.α. συγκεντρώνει εικόνες, κατά μήκος της πεπτικής οδού και μεταδίδει τα δεδομένα ασύρματα σε μία εξωτερική βάση-σταθμό. Η εξωτερική συσκευή λήψης αποτελείται από ένα σύστημα αισθητήρων και έναν καταγραφέα δεδομένων που τοποθετούνται εξωτερικά στον εξεταζόμενο. Τα δεδομένα είναι διαθέσιμα σε πραγματικό χρόνο, αλλά μπορούν να αποθηκευτούν και για περαιτέρω ανάλυση και επεξεργασία από εξειδικευμένο προσωπικό με τη χρήση κατάλληλου λογισμικού. Οι πρώτες εφαρμογές ασύρματης καταπόσιμης ενδοσκόπησης αναφέρθηκαν για πρώτη φορά τη δεκαετία του ’50 για τη μέτρηση της θερμοκρασίας ,pH. Έκτοτε πολλά τέτοια συστήματα συναντιούνται στον εμπορικό τομέα. Ενδεικτικά αναφέρονται τα M2A, PillCam_SB, PillCam_ESO, PillCam COLON, Olympus Endoscope, Norika με εφαρμογές στη διαγνωση παθογένειας στον οισοφάγο,στο παχύ έντερο και άλλων εσωτερικών οργάνων. Όπως και στις εμφυτεύσιμες ιατρικές διατάξεις, κύριες συχνότητες λειτουργίας αποτελούν οι Ζώνες MICS (Medical Implant Communication Services, 402 MHz-405 MHz), ISM (2.40 GHz-2.48 GHz), WMTS (608 MHz-614 MHz, 1395 MHz-1400 MHz, 1427 MHz-1432 MHz) ή ακόμη χαμηλότερες συχνότητες (40 MHz). Οι σχεδιαστικές απαιτήσεις στη κατασκευή καταπόσιμων κεραιών περιλαμβάνουν την ανάγκη οι κεραίες να είναι μικροσκοπικών διαστάσεων και ταυτόχρονα να

λειτουργούν σε μεγάλο εύρος συχνοτήτων, προκειμένου να είναι δυνατή η μετάδοση εικόνων υψηλής ευκρίνειας και δεδομένων που σχετίζονται με φυσιολογικές παραμέτρους του ανθρώπινου σώματος (πίεση, θερμοκρασία, pH, συγκέντρωση οξυγόνου). Επιπλέον, η βελτίωση στην απόδοση της κεραίας θα πρέπει να συνοδεύεται από χαμηλή ενεργειακή κατανάλωση προκειμένου η ασύρματη κάψουλα να μπορεί να διατηρήσει τη λειτουργία της για όλο το διάστημα που παραμένει στο ανθρώπινο σώμα. Λόγω του «εχθρικού» περιβάλλοντος που αποτελεί το ανθρώπινο σώμα (εξαιτίας διαφορετικών χαρακτηριστικών και ηλεκτρικών ιδιοτήτων και διαστάσεων των διαφόρων τύπων ιστού) δημιουργούνται προβλήματα όπως είναι ο αποσυντονισμός (detuning) της κεραίας και η αστοχία στην προσαρμογή της αντίστασης (impedance mismatch) με επιπτώσεις στην επικοινωνία με την εξωτερική συσκευή και στο κέρδος της κεραίας (gain) αντίστοιχα. Όλα αυτά πρέπει να ληφθούν υπ'όψιν κατά τη διαδικασία σχεδιασμού της κεραίας. Επιπλέον, όπως και στη περίπτωση των εμφυτεύσιμων διατάξεων οι κάψουλες πρέπει να είναι βιοσυμβατές έτσι ώστε να μην προκαλέσουν βλάβες στον αθρώπινο οργανισμό και ταυτόχρονα εύρωστες ώστε τα υγρά του πεπτικού συστήματος να μην βλάψουν την κεραία. Τέλος, οι καταπόσιμες κεραίες πρέπει να είναι παγκατευθυντικές και να παρουσιάζουν κυκλική πόλωση, έτσι ώστε να δύνανται να μεταδίδουν σήματα ανεξάρτητα από τη θέση και τον προσανατολισμό τους. Αυτό συμβαίνει, γιατί η ακριβής θέση και ο προσανατολισμός της διάταξης που ταξιδεύει κατά μήκος ολόκληρης της γαστρεντερικής οδού, είναι άγνωστη. Ως εκ τούτου, μια ισοτροπική πηγή ακτινοβολίας απαιτείται για τον σχεδιασμό τους. Δεδομένων των παραπάνω απαιτήσεων συνήθως επιλέγονται κεραίες με ελικοειδή σχηματισμό.

Ο κυριότερος περιορισμός στην λειτουργία των καταπόσιμων κεραίων ασύρματης ενδοσκόπησης που βρίσκονται αυτή τη στιγμή σε χρήση, έγκειται στην αδυναμία ελέγχου της κίνησης της κάψουλας καθ' όλη τη διαδρομή της στο ανθρώπινο σώμα. Οι καταπόσιμες διατάξεις κινούνται παθητικά, λόγω των φυσικών περισταλτικών κινήσεων του εντέρου με αποτέλεσμα να μην μπορούν να επιστρέψουν σε κάποια περιοχή πιθανού ιατρικού ενδιαφέροντος, ενώ η ασυμμετρία του εντέρου μπορεί σε κάποιες περιπτώσεις να οδηγήσει σε πλήρη αβλεψία κάποιων σημαντικών πληροφοριών. Άλλοι περιορισμοί αφορούν την ανάλυση των ιατρικών εικόνων, τη διάρκεια ζωής των διατάξεων και την τοξικότητα πηγών ενέργειας που περιλαμβανονται σε αυτές (μπαταρίες).

Το επιστημονικό ενδιαφέρον προσανατολίζεται στη δημιουργία και διάθεση στο εμπόριο καταπόσιμων κεραιών με επαναφορτιζόμενες ή/και χωρίς μπαταρίες, που θα διαθέτουν μηχανισμούς ενεργής κίνησης, οι οποίοι θα επιταχύνουν, θα σταματούν ή θα επιβραδύνουν ανάλογα με τα τυχόν ευρήματα κατά τη πορεία της διάταξης στη γαστρεντερική οδό. Οι δύο κύριοι μηχανισμοί που έχουν αναπτυχθεί, είναι η ενσωμάτωση εσωτερικού μηχανισμού, η οποία θα βρίσκεται πάνω στην κάψουλα, και ο έλεγχος της κίνησης με εξωτερικό μηχανισμό που θα στηρίζεται στη λειτουργία μαγνητικών πεδιακών πηγών (Ciuti et al. 2016). Άλλες προσπάθειες γίνονται προς τη δημιουργία βελτιστοποιημένων αλγόριθμων που θα εξοικονομούν χρόνο μέσω αυτόματης ταυτοποίησης περιοχών της γαστρενετρικής οδού και τυχόν σημείων ύποπτα για αιμορραγίες ή άλλες κακώσεις (Farnbacher et al.2014). Τέλος,

προσπάθειες για τεχνικές απόκτησης ιστολογικών δειγμάτων από περιοχές του βλενογόννου του λεπτού εντέρου έχουν αναφερθεί στη βιβλιογραφία (Saurin et al. 2016). Τέτοιου είδους πρωτότυπες κεραίες θα επιτρέψουν τη λήψη βιοψίας και τη τοποθέτηση μηχανισμού αιμόστασης στο λεπτό έντερο. Ο συνδυασμός της Νανοτεχνολογίας με την Οπτική αναμένεται να δημιουργήσει διατάξεις επόμενης γενιάς στο τομέα της Ασύρματης Καταπόσιμης Ενδοσκόπησης που θα επιτρέψουν μηχανισμούς έγχυσης φαρμάκου επιτυγχάνοντας επιπλέον βελτίωση των θεραπευτικών και διαγνωστικών δυνατοτήτων των καταπόσιμων διατάξεων (Koulaouzidis et al. 2015).

Ένας πολύ σημαντικός τομέας που συγκεντρώνει το ενδιαφέρον των επιστημόνων είναι η κατασκευή ηλεκτρονικών συσκευών που είναι αρκετά μικρές έτσι ώστε να μπορούν να εισέλθουν στο ανθρώπινο σώμα σε ενέσιμη μορφή, μέσω σύριγγας. Οι κύριοι λόγοι που οδήγησαν στο προσανατολισμό αυτό, είναι η δυσφορία που προκαλείται στον ασθενή από συμβατικές, μεγάλες ιατρικές συσκευές καθώς επίσης και ο κίνδυνος μόλυνσης από ένα μετεγχειρητικό τραύμα. Ήδη από τις αρχές του’80, και αφού οι ετικέτες ταυτοποίησης μέσω ραδιοσυχνοτήτων (RFID tags) είχαν κατακλύσει την αγορά, οι επιστήμονες δημιούργησαν ενέσιμα ιατρικά εμφυτεύματα γνωστά ως μικρόμοναδες (micro-modules). Σημαντικό χαρακτηριστικό παράδειγμα αυτών, υπήρξε ο μικρο-διεγέρτης (micro-stimulator) που σχεδιάστηκε για εφαρμογές νευρομυϊκής διέγερσης. Τεχνολογικές εξελίξεις οδήγησαν στις αρχές του ’90 στη κατασκευή του BION (bionic neuron) της πρώτης συσκευής εμφυτεύσιμης ηλεκτρονικής διεπιφάνειας μυός-νεύρου. Επρόκειτο για ηλεκτρονικές συσκευές που εμπεριέχονταν σε ερμητικά κλειστή κάψουλα και ήταν αρκετά μικρές έτσι ώστε να εισαχθούν μέσω ένεσης, διαδερμικά στους μύες. Οι πρώιμες κατασκευές τροφοδοτούνταν εξωτερικά, δεδομένου ότι δεν υπήρχε μπαταρία κατάλληλη για τέτοιου είδους χρήση, ωστόσο τελικά η μέθοδος των αμοιβαίως συζευγμένων πηνίων εφαρμόστηκε ως τεχνική διατήρησης της ισχύος. Τέσσερις γενίες BION διεγερτών μπορούν να εντοπιστούν στη βιβλιογραφία (Carbunaru et al. 2004). Αυτές περιλαμβάνουν εφαρμογές όπως η χρήση επαναφορτιζόμενης μπαταρίας (Loeb et al. 2004) και προτάθηκαν με σκοπό να ανακουφίσουν τους ασθενείς από νευρολογικές διαταραχές συμπεριλαμβανομένων της ακράτειας ούρων, της φλεβικής θρόμβωσης, των χρόνιων κεφαλαλγιών, του περιφερικού πόνου, της στηθάγχης, της αποφρακτικής υπνικής άπνοιας κ.α.

Μια από τις κυριότερες εφαρμογές των ενέσιμων ιατρικών διατάξεων είναι η αποκατάσταση της μυϊκής λειτουργίας άκρων σε άτομα που είχαν χάσει τον μερικό ή ολικό έλεγχο της (π.χ. σε περίπτωση εγκεφαλικού) μέσω ενός μικροσκοπικού ενέσιμου εμφυτεύματος το οποίο εγχύεται κοντά σε μύες και περιφερικά νεύρα της περιοχής ενδιαφέροντος. Ένας τέτοιος τυπικός ενέσιμος νευροδιεγέρτης (Injectable neurostimulators InNS) αποτελείται από τουλάχιστον ένα ζεύγος ηλεκτροδίων. Τα κυριότερα μέρη μιας τέτοιας διάταξης είναι: i) ένας διεγέρτης ιστού-επιφάνειας, ii) μια κεραία για ιατρική τηλεμετρία, iii) μια ενθυλάκωση που εξυπηρετεί την σχέση λειτουργίας ιστού- ηλεκτρονικών εξαρτημάτων, iv) ένα βιοσυμβατό περίβλημα, v) κάποιοι αισθητήρες και vi) μερικές ενεργές διατάξεις (functional building blocks

FBBs) που παράγουν και ελέγχουν τους ηλεκρικούς παλμούς. Οι αισθητήρες είναι αυτοί που ανιχνεύουν και παρακολουθούν τις εφαρμοζόμενες τάσεις, την αντίδραση του νεύρου και άλλες παραμέτρους όπως πίεση κι θερμοκρασία μεταξύ της διεπιφάνειας ηλεκτροδίου-ιστού. Οι ενεργές διατάξεις FBBs περιλαμβάνουν τη μονάδα της ενεργειακής τροφοδοσίας και διαχείρισης της διάταξης, έναν πομποδέκτη δεδομένων, έναν μικρο-ελεγκτή, έναν μικρο-διεγέρτη, και μια νευρωνική μονάδα εγγραφής. Η νέα γενιά των ενέσιμων νευροδιεγερτών, μπορεί να τροφοδοτείται από μικρο- μπαταρία, από επαγωγική σύζευξη πηνίων, ή μέσω ασύρματης φόρτισης που επιτυχγάνεται με μετατροπέα ενέργειας ραδιοσυχνοτήτων (RF energy harvester).

Οι σημαντικότερες προκλήσεις στη δημιουργία ενέσιμων διατάξεων για Ιατρική Τηλεμετρία αφορούν το μέγεθος της διάταξης, την τροφοδοσία της, και την απόδοση της κεραίας που βρίσκεται ενσωματωμένη σε αυτήν. Η ενέσιμη μπαταρία πρέπει να είναι εξαιρετικά μικρή αλλά την ίδια στιγμή να έχει ισχύ για μεγαλύτερο χρόνο διέγερσης. Προς αυτήν τη κατεύθυνση έχουν προταθεί τεχνικές που αφορούν: επαναφορτιζόμενες μπαταρίες, μπαταρίες που αποτελούνται απο Λίθιο και χιλίαδες νανοκαλώδια (Li-ion microbattery), καθώς επίσης και μια καινοτόμος τεχνική που υποβλήθηκε το 2014 επονομαζόμενη “jellyroll” που επιτρέπει την συσσώρευση διπλάσιας ποσότητας ενέργειας, σε σχέση με τις, προηγμένης τεχνολογίας, μικρο-μπαταρίες (Honghao Chen et al. 2014). Στους ενέσιμους νευροδιεγέρτες (InNSs) που τροφοδοτούνται από επαγωγική σύζευξη πηνίων (ICL) ή από ολοκληρωμένους μετατροπείς ισχύος Ραδιοσυχνοτήτων (RF) σε ισχύ συνεχούς (DC) (RFEH radio-frequency energy harvesters) η χρήση μπαταριών μπορεί να παρακαμφθεί από έναν ενσωματωμένο πυκνωτή που δύναται να αποθηκεύει αυτόματα την μετατρεπόμενη ενέργεια και επιπλέον να μεταφέρει περισσότερη ισχύ σε σχέση με τις μπαταρίες. Όπως και στις εφαρμογές εμφυτεύσιμων και καταπόσιμων διατάξεων, ένας συμβιβασμός είναι απαραίτητος να γίνει μεταξύ του μεγέθους της κεραίας και της αυξημένης απόδοσης ακτινοβολίας. Η λειτουργία σε υψηλές συχνότητες κάποιων GHz μπορούν να αυξήσουν τις επιδόσεις της κεραίας, ωστόσο συνοδεύεται από μεγαλύτερη απορρόφηση από τους ιστούς γεγονός που αυτομάτως σημαίνει μικρό βάθος διείσδυσης της διάταξης.

Στην επόμενη γενιά, ενέσιμων νευροδιεγερτών αναμένονται επίσης σημαντικές ανακαλύψεις όσον αφορά τη χρήση μαλακών και ευλύγιστων υλικών, την αξιοπιστία, και τις μεθόδους ένεσης. Το περίβλημα των διατάξεων των InNSs και FBBs θα πρέπει να είναι από βιοσυμβατά υλικά όπως το γάλλιο, τα κράματα γάλλιου-ινδίου, κασσίτερου κ.α. Ωστόσο και η σιλικόνη θα μπορούσε να εφαρμοστεί ως ημιαγώγιμο υλικό, όντας τόσο βιοσυμβατή όσο και εύκαμπτη, καθώς μπορεί να κατασκευάζει κυκλώματα με υψηλή απόδοση. Προκειμένου να επιτευχθεί ευλυγισία στη διάταξη αλλαγές πρέπει να γίνουν όσον αφορά στο πάχος ή ακόμη και στη ύπαρξη του υποστρώματος. Μετάξι κολλαγόνο και άλλα βιοαποικοδομήσιμα πολυμερή θα μπορούσαν να χρησιμοποιηθούν για την παραγωγή εύκαμπτων και μαλακών ηλεκτροδίων. Σχετικά με την ενίσχυση της αξιοπιστίας τοξικά υλικά όπως τα οξείδια του χαλκού ή τα οξείδια του αρσενικού, όταν περιέχονται στα InNSs πρέπει να είναι σταθερά σφραγισμένα για τυχόν διαρροή στους ιστούς, ενώ επίσης κυκλώματα

παρακολούθησης για πιθανή υπερφόρτιση / εκφόρτωση, καθώς και βρόχων ανάδρασης για αυτο-ελέγχο και αυτο-βαθμονόμηση θα μπορούσαν να εισαχθούν.

Προς το παρόν, υπάρχουν δύο τρόποι για να εισαχθεί ο ενέσιμος νευροδιεγέρτης (InNS) στο σώμα: i) είτε με μονομίας εισαγωγή ολόκληρης της διάταξης στο στόχο ii) είτε μέσω διαδοχικής έγχυσης των βιοσυμβατών υλικών προκειμένου να σχηματίσουν εν τέλει την ηλεκτρονική συσκευή μέσα στον ιστό. Μια μέθοδος που αναφέρεται στη βιβλιογραφία, ότι δοκιμάστηκε σε in vivo και in vitro πειράματα, είναι η απευθείας έγχυση στον επιθυμητό ιστό, τρισδιάστατων ιατρικών ηλεκτρικών διατάξεων σε συνδυασμό με το αγώγιμο υγρό μέταλλο GaInSn. Η βιοσυμβατή ζελατίνη επιλέχθηκε ως το υλικό που θα περικλείει το ηλεκτρόδιο λόγω των κάταλληλων εύπλαστων και βιοαποικοδομήσιμων ιδιοτήτων της. Μέχρι τώρα η εφαρμογή είναι κατάλληλη για πολύ απλές ηλεκτρονικές διατάξεις. Συμπερασματικά καινοτόμες εξελίξεις αναμένονται στο τομέα των ενέσιμων κεραιών. Επιπρόσθετη σμίκρυνση της φόρμουλας που διαμορφώνει την διάταξη θα επιδιωχθεί, προκειμένου να γίνει δυνατή η άμεση ένεση σε νευρικές περιοχές, μέσω βελονών μεσαίου διαμετρήματος (π.χ. 16G ή 17G). Η πρόοδος στην ανάπτυξη των βιοϊατρικών αισθητήρων, των βιομιμητικών συστημάτων και των βιομοριακών ηλεκτρονικών είναι αυτή που θα καθορίσει την εξέλιξη της τεχνολογίας των InNSs.

Μια κεραία μπορεί να οριστεί ως η μεταβατική δομή μεταξύ ελεύθερου χώρου και μιας συσκευής καθοδήγησης (ομοαξονική γραμμή ή κυματοδηγός), η οποία χρησιμοποιείται για τη μεταφορά ηλεκτρομαγνητικής ενέργειας από την πηγή εκπομπής στην κεραία ή από την κεραία με το δέκτη. Για την περιγραφή της απόδοσης μιας κεραίας, διάφορες παράμετροι προσδιορισμού είναι: η ένταση ακτινοβολίας, το διάγραμμα ακτινοβολίας της κεραίας, η κατευθυντικότητα, η πόλωση, το κέρδος, η αντίσταση εισόδου, ο συντελεστής ανάκλασης, ο λόγος στάσιμου κύματος, το εύρος ζώνης λειτουργίας κ.α. Σε ένα προηγμένο ασύρματο σύστημα επικοινωνίας, μια κεραία, εκτός από τη μετάδοση ή τη λήψη σήματος, είναι υπεύθυνη για τη βελτιστοποίηση της έντασης ακτινοβολίας, καθώς επίσης και για την ενίσχυση της σε ορισμένες κατευθύνσεις και την καταστολή της σε άλλες. Για το λόγο αυτό, θα πρέπει να λειτουργεί ως μια κατευθυντική συσκευή και να παίρνει ποικίλες μορφές, ανάλογα με τις εκάστοτε απαιτήσεις.

Οι κεραίες μικροταινίας είναι ευρέως διαδεδομένες για εφαρμογές στην περιοχή των μικροκυματικών συχνοτήτων, όπου το μέγεθος, το κόστος, το βάρος και η επίδοση επιβάλλουν αυστηρούς περιορισμούς. Είναι απλές και συμβατές με επίπεδες και μη επιφάνειες, κατασκευάζονται εύκολα με τη σύγχρονη τεχνολογία τυπωμένων κυκλωμάτων, εμφανίζουν υψηλή μηχανική αντοχή, και εκδηλώνουν μεγάλη ευελιξία ως προς τη συχνότητα συντονισμού, την πόλωση, το διάγραμμα ακτινοβολίας και τη σύνθετη εμπέδηση. Επιπλέον, προσθέτοντας μεταξύ της ταινίας και της γείωσης κατάλληλες μεταλλικές ράβδους ή διόδους, μπορεί να ρυθμίζεται η συχνότητα συντονισμού, η σύνθετη εμπέδηση, και το διάγραμμα ακτινοβολίας. Η ταινία ακτινοβολίας μπορεί να είναι τετράγωνη, ορθογώνια, λεπτή λωρίδα (δίπολο), κυκλική, ελλειπτική, τριγωνική κλπ. (Εικόνα 2.2) ενώ συνηθέστερα χρησιμοποιούνται η τετραγωνική, η ορθογωνική, η κυκλική και η διπολική λόγω της

ευκολίας κατασκευής και ανάλυσης καθώς και λόγω των ελκυστικών χαρακτηριστικών ακτινοβολίας τους. Υπάρχουν διάφορες τεχνικές με τις οποίες μπορούμε να τροφοδοτήσουμε μια μικροταινιακή κεραία. Οι πιο διαδεδομένες είναι η τροφοδοσία με μικροταινιακή γραμμή (microstrip line), με ομοαξονικό καλώδιο (coaxial feed), με σύζευξη μέσω διαφράγματος (Aperture- coupled feed) και με σύζευξη λόγω γειτνίασης (proximity-coupled feed). Παρόλα αυτά παρουσιάζουν και κάποια λειτουργικά μειονεκτήματα όπως μικρή απόδοση, μικρή ισχύς και πολύ μικρό εύρος ζώνης συχνοτήτων τα οποία όμως με χρήση κατάλληλων μεθόδων μπορούν να βελτιωθούν σημαντικά. Προκειμένου να βελτιώσουν την απόδοση της κεραίας, οι σχεδιαστές εισήγαγαν αγωγούς βραχυκύκλωσης (shorting pins) μεταξύ της γείωσης (ground plane) και της αγώγιμης επιφάνειας σε διάφορα σημεία δημιουργώντας κατά αυτόν το τρόπο μια επίπεδη κεραία ανεστραμμένου F (Planar Inverted-F Antenna PIFA). Η προσθήκη των αγωγών αυτών, έχει σαν αποτέλεσμα τη μείωση των φυσικών διαστάσεων της κεραίας για δεδομένη συχνότητα συντονισμού. Στην βιβλιογραφία, ποικίλες εφαρμογές της Βιοϊατρικής Τεχνολογίας έχουν σχεδιαστεί με τη τεχνική αυτή, όπως παρουσιάζεται στον πίνακα 1 του κεφαλαίου 2, προκειμένου να επιτύχουν καλύτερη σμίκρυνση και βελτίωση του εύρους λειτουργίας τους. Οι πολυεπίπεδες (Multi-layered) μικροσκοπικές κεραίες έχουν ιδιαίτερα πλεονεκτική δομή όσον αφορά τη μείωση των διαστάσεων της κεραίας. Οι πολυεπίπεδες δομές περιλαμβάνουν κατακόρυφη στοίβαξη ταινιών (vertically stacked radiating patches), αυξάνοντας έτσι το μήκος διαδρομής ρεύματος επί των ταινιών, μειώνοντας, ως αποτέλεσμα, το συνολικό φυσικό μέγεθος της κεραίας. Η πολυστρωματική αυτή δομή είναι εύκολη στην κατασκευή και διασφαλίζει καλύτερα τα επιθυμητά χαρακτηριστικά της κατευθυντικότητα και απόδοσης της κεραίας σε σχέση με αλλες δομές που αναφέρονται στη βιβλιογραφία. Επιπλέον, οι ακτινοβολητές αυτοί έχουν ευρύ φάσμα λειτουργίας λόγω ισχυρής αλληλεπίδρασης του Η/Μ κοντινού πεδίου με τους ανθρώπινους ιστούς.

Προκειμένου να βελτιστοποίησουμε το στενό εύρος λειτουργίας των κεραιών Μικροταινίας, διάφορες τεχνικές έχουν προταθεί. Αυτές περιλαμβάνουν: i) Την επίδραση του υποστρώματος. Η μείωση της διηλεκτρικής σταθεράς βελτιώνει το εύρος ζώνης της κεραίας. Ένα υπόστρωμα με μεγαλύτερη διηλεκτρική σταθερά ή που είναι παχύτερο θα υποφέρει από αυξημένη διέγερση επιφανειακών κυμάτων, η οποία θα μειώσει την απόδοση της κεραίας. Επιπλέον, η αύξηση του πάχους του υποστρώματος δεν είναι ιδανική λύση για τις εμφυτεύσιμες διατάξεις, αφού αυξάνεται ο όγκος, το βάρος και το κόστος της κεραίας. ii) Την επίδραση εισαγωγής εγκοπών στην ταινία. Η τεχνική εισαγωγής εγκοπών (slotted patch) αποτελεί μία αποτελεσματική μέθοδο ελέγχου της συχνότητας συντονισμού και του εύρους ζώνης των κεραιών, διατηρώντας παράλληλα μικρό το μέγεθος. Η βασική ιδέα της τεχνικής είναι η αύξηση της διαδρομής του ρεύματος πάνω στην επιφάνεια της ταινίας δημιουργώντας σιγμοειδή μονοπάτια με τη χάραξη εγκοπών πάνω στην ταινία. Η τεχνική μπορεί να υλοποιηθεί με τομές στις άκρες της ταινίας, είτε με αυλάκωση είτε με περικοπή των γωνιών. Με δεδομένη τη συχνότητα συντονισμού είναι δυνατό να επιτευχθεί μείωση των διαστάσεων της κεραίας. Οι εγκοπές μπορεί να είναι σχήματος U, E, H κτλ.

Ένας άλλος τρόπος αύξησης της ευρυζωνικότητας της κεραίας είναι με τη χρήση παρασιτικών τεχνικών. Υπάρχουν δύο υλοποιήσεις παρασιτικής γεωμετρίας: i) η ομοεπίπεδη και ii) η στοιβαγμένη γεωμετρία. Στην πρώτη υλοποίηση η κεραία αποτελείται απο πολλές ταινίες ενωμένες με μια κύρια ταινία, η οποία είναι και η μόνη που έχει διεγερθεί. Κατά μήκος και πλάτος μιας κεραίας Μικροταινίας, κάποιες από τις ακμές της ακτινοβολούν και κάποιες όχι. Όταν οι παρασιτικές ταινίες τοποθετούνται κοντά στην ενεργή ταινία, τότε οι πρώτες συντονίζονται, λόγω διαταραχής και ηλεκτρομαγνητικής σύζευξης (Multiresonator MPA). Στη στοιβαγμένη γεωμετρία οι παρασιτικές ταινίες τοποθετούνται η μια πάνω στην άλλη (πολυεπίπεδη διάταξη) και ο συντονισμός όλων επιτυγχάνεται λόγω διαφραγματικής σύζευξης ή ηλεκτρομαγνητικής σύζευξης (Multilayer broadband MSA).

Ανάλογα με το είδος του ιστού και τη συχνότητα του Η/Μ κύματος οι παράμετροι της διηλεκτρικής επιτρεπτότητας και αγωγιμότητας των βιολογικών ιστών επηρεάζονται αντίστοιχα. Στο κεφάλαιο 2-πίνακες 2&3, αναφέρονται ενδεικτικά οι τιμές των διηλεκτρικών σταθερών που συναντώνται συχνά σε εμφυτεύσιμες και καταπόσιμες ιατρικές διατάξεις. Για να μπορέσουμε να αξιολογήσουμε την απόδοση μίας κεραίας εντός του ανθρώπινου οργανισμού χρησιμοποιούμε μοντέλα προσομοίωσης του ανθρώπινου σώματος. Τα μοντέλα αυτά διακρίνονται σε δύο μεγάλες κατηγορίες τα αριθμητικά και τα φυσικά (phantoms).

Στην κατηγορία των αριθμητικών μοντέλων ανήκουν τα κανονικά (canonical models) και τα ανατομικά μοντέλα (anatomical models). Τα κανονικά μοντέλα, έχουν απλή γεωμετρία και χρησιμοποιούνται ευρέως καθώς μειώνουν αρκετά τον υπολογιστό κόστος της προσομοίωσης προσφέροντας παράλληλα αξιόπιστα αποτελέσματα. Συνήθως αποτελούνται από ένα ή περισσότερα στρώματα σε απλή γεωμετρική διάταξη (ορθογώνιο κουτί, κύλινδρος, σφαίρα κ.α.). Τα ανατομικά μοντέλα χρησιμοποιούνται όταν θέλουμε να εκτιμήσουμε τις αποδόσεις της κεραίας κάνοντας χρήση πιο ρεαλιστικών προσομοιώσεων. Τα ανατομικά μοντέλα προκύπτουν από το συνδυασμό δεδομένων Μαγνητικής Τομογραφίας (MRI) ή/και Υπολογιστικής Τομογραφίας (CT) με τις ηλεκτρικές ιδιότητες των ιστών του ανθρώπινου σώματος. Η χρήση αυτών των μοντέλων απαιτεί ισχυρά υπολογιστικά συστήματα και ο χρόνος προσομοίωσης αυξάνεται σημαντικά. Τέλος τα φυσικά μοντέλα χρησιμοποιούνται στη πράξη, με σκοπό την πειραματική επαλήθευση των αποτελεσμάτων που προέκυψαν από τα αριθμητικά μοντέλα. Μπορεί να έχουν οποιοδήποτε σχήμα, ακόμα και ανατομικό, και η σύσταση τους μπορεί να είναι είτε ομοιογενής είτε μη ομοιογενής.

Για την πρόβλεψη των επενεργειών της ηλεκτρομαγνητικής ακτινοβολίας η μέθοδος των πεπερασμένων στοιχείων (Finite Element Method, FEM) είναι αυτή που εφαρμόστηκε στη παρούσα διπλωματική εργασία. Σύμφωνα με τη μέθοδο FE, το ΗΜ πρόβλημα, το οποίο αποτελείται από τη γεωμετρία της πηγής, τη μοντελοποίηση της διέγερσης, τους σκεδαστές και τις συνθήκες απορρόφησης, διακριτοποιείται με μεταβλητό τρόπο. Για την περιγραφή των πολύπλοκων γεωμετριών, χρησιμοποιούνται μικρά στοιχεία πλέγματος, ενώ για πιο ομοιόμορφες περιοχές χρησιμοποιούνται μεγαλύτερα πλεγματικά στοιχεία. Τα στοιχεία που επιλέγονται

είναι απλού σχήματος (εδώ τετραεδρικά). Η υπολογιστική σχεδίαση και μελέτη της κεραίας πραγματοποιούνται στο λογισμικό Ansoft HFSS (High Frequency Structure Simulator) με τη βοήθεια της μεθόδου των Πεπερασμένων Στοιχείων. Το δομικό πλεγματικό στοιχείο του λογισμικού HFSS έχει σχήμα τετραέδρου, το οποίο επιτρέπει την ακριβή μοντελοποίηση και ταχεία επίλυση καμπύλων γεωμετριών, όπως οι προτεινόμενες κεραίες κυκλικής γεωμετρίας. Το πλέγμα διακριτοποίησης του υπό προσομοίωση ΗΜ μοντέλου βελτιστοποιείται αυτόματα από το λογισμικό με επαναληπτικό τρόπο. Το πλέγμα μεταβάλλεται κατά, το πολύ, 30% σε κάθε επανάληψη. Οι επαναλήψεις σταματούν όταν η μέγιστη διαφορά στον υπολογισμό του μέτρου του συντελεστή ανάκλασης της κεραίας ($|S_{11}|$) μεταξύ δύο επαναλήψεων είναι μικρότερη του 0.02 (κατ' απόλυτη τιμή), ή όταν ο αριθμός των επαναλήψεων είναι μεγαλύτερος του 10. Για λόγους ευστάθειας της αριθμητικής επίλυσης, η κεραία περιβάλλεται από αέρα σε διάστημα ($\lambda_0/4$, όπου λ_0 είναι το μήκος κύματος στον ελεύθερο χώρο στη συχνότητα συντονισμού). Στα όρια της περιοχής επίλυσης θεωρούνται οριακές συνθήκες απορρόφησης οι οποίες προσομοιώνουν την ακτινοβόληση στον ελεύθερο χώρο απείρων διαστάσεων.

Στο κεφάλαιο 3 μελετήθηκε μια μικροσκοπική πολυεπίπεδη κεραιά, η οποία λειτουργεί σε δύο εύρη συχνοτήτων, στη Ζώνη Υπηρεσιών Επικοινωνίας Ιατρικών Εμφυτευμάτων (MedRadio band 401- 406 MHz), και στη Ζώνη Βιομηχανικών, Επιστημονικών και Ιατρικών Εφαρμογών (ISM band 2.4-2.483 GHz) για εμφυτεύσιμες εφαρμογές. Η κεραία τοποθετείται σε τρία κανονικά μοντέλα που προσομοιώνουν τις διηλεκτρικές ιδιότητες του μυός, του ανθρώπινου κεφαλιού, και της τριστρωματικής απλοποιημένης εκδοχής του σώματος (μυς-λίπος-δέρμα) και μελετώνται παράμετροι που αφορούν το συντελεστή ανάκλασης S_{11} , το κέρδος της κεραίας, το διάγραμμα ακτινοβολίας κ.α. Η κεραία αποτελείται από τέσσερα κάθετα στοιβαγμένα υποστρώματα με σπιροειδή ορθογώνια επιμετάλλωση απο χαλκό, πάχους 35μm και διαστάσεων που παρουσιάζονται στην εικόνα 3.5. Το υλικό που χρησιμοποιήθηκε για αυτά είναι το Roger TMM 10 (αλουμίνα) λόγω της μεγάλης διηλεκτρικής του επιτρεπτότητας ε_r=9.2 και του χαμηλού συντελεστή απωλειών tanδ=0.0022. Η διάταξη περικλείεται μέσα σε μια κυλινδρική κάψουλα από βιοσυμβατό υλικό PEEK (Polyetheretherketones) πάχους 0.8mm. Ο συνολικός όγκος της κεραίας είναι $\pi \; x 5^2 x \; 32.1 \, mm^3$. Προκειμένου να προσομοιωθεί ρεαλιστικά η επιθυμητή υποδόρια εμφύτευση η κεραία τοποθετείται έκκεντρα στο κυλινδρικό κανονικό μοντέλο (25mm κατά τον x-άξονα & 17mm κατά τον y- άξονα).

Τα αποτελέσματα, όταν η κεραία προσομοιώνεται στη Ζώνη MedRadio βρίσκονται σε συμφωνία με όσα αναμένονταν ως προς τις παραμέτρους του συντελεστή ανάκλασης, κέρδους, κατευθυντικότητας, ωστόσο η κεραία συντονίζεται εκτός των ορίων της MedRadio (401-406 MHz). Συγκεκριμένα, ο συντονισμός της κεραίας επιτυγχάνεται μεταξύ του εύρους συχνοτήτων 385-390 MHz. Δεδομένου, ότι όλα τα βήματα της διαδικασίας σχεδιασμού της διάταξης, ακολουθήθηκαν με προσοχή, ποικίλες τεχνικές προτάθηκαν προκειμένου να καμφθεί αυτή η απόκλιση. Η πιο ελκυστική, είναι η αντικατάσταση του υλικού του υποστρώματος από το Roger TMM 10, στο Roger TMM 6 (χαμηλότερης διηλεκτρικής επιτρεπτότητας). Όπως

διαφαίνεται στις γραφικές παραστάσεις που παρουσιάζονται στην εικόνα 3.14 η συχνότητα συντονισμού, μετακίνειται τότε προς την επιθυμητή Ζώνη Λειτουργίας. Στην Ζώνη ISM, τα αποτελέσματα των προσομοιώσεων είναι ικανοποιητικά, όπως παρουσίαζεται στις εικόνες 3.15-3.18.

Στη συνέχεια μελετάται η επίδραση που έχουν οι αλλαγές κάποιων παραμέτρων στην απόδοση της κεραίας. Εξετάζονται μεταβλητές που αφορούν: το διηλεκτρικό υλικό των υποστρωμάτων, το πάχος των μεταλλικών λωρίδων, το σημείο τροφοδοσίας της κεραιάς.Τα αποτελέσματα της παραμετροποίησης παρουσιάζονται στις εικόνες 19-27 του κεφαλαίου 3. Τέλος, πραγματοποιείται βελτιστοποίηση των παραμέτρων της μεταλλικής διαδρομής της κεραίας με χρήση του αλγόριθμου Quasi-Newton (QN method). Η μέθοδος λαμβάνει ως παραμετρικές εισόδους τα πλάτη και τα μήκη των μεταλλικών λωρίδων της κεραίας, και με δεδομένο κριτήριο τερματισμού, το πλάτος του συντελεστή ανάκλασης να είναι μικρότερο από -20dB στη συχνότητα συντονισμού, πραγματοποιεί διαδοχικά 350 επαναλήψεις προκειμένου να επιτύχει το βέλτιστο αποτέλεσμα (Εικόνες 3.28 3.29. 3.31). Ο βαθμός σύγκλισης στο ζητούμενο αποτέλεσμα φαίνεται σε κάθε επανάληψη από τη συνάρτηση κόστους, η οποία επιστρέφει μηδέν όταν ο αλγόριθμος έχει ικανοποιήσει τα κριτήρια αναζήτησης και μεγάλες τιμές όταν δεν ικανοποιούνται τα κριτήρια. Ως βέλτιστη λύση του προβλήματος επιλέχθηκε αυτή με το μικρότερο κόστος (cost=2.835), από τη στιγμή που σε καμία επανάληψη δεν ικανοποιήθηκε το κριτήριο τερματισμού.

Στο κεφάλαιο 4 παρουσιάζεται ο σχεδιασμός και η μελέτη των επιδόσεων μιας πρωτότυπης κεραίας που στηρίχθηκε στην υλοποίηση της πολυεπίπεδης κεραίας του κεφαλαίου 3. Η νέα κεραία είναι ακόμη πιο μικροσκοπικών διαστάσεων και απαιτείται η λειτουργία της στη Ζώνη Συχνοτήτων MedRadio. Η διάταξη αποτελείται πλέον απο τρία υποστρώματα αντί για τέσσερα, διηλεκτρικού υλικού Roger TMM 10, ενώ ο συνόλικος όγκος της κεραίας είναι $2018\,mm^3$ έναντι του αρχικού $2529\,mm^3$. Το πάχος κάθε υποστρώματος μειώνεται ελαφρά όπως επίσης και το μήκος της διάταξης κατά 2mm. Το πλάτος της μεταλλικής διαδρομής του ρεύματος αυξάνεται καθώς επίσης και το μήκος της, όσον αφορά κυρίως τις διαστάσεις της στο πρώτο υπόστρωμα. Όπως και πρίν, την κεραία περικλείει βιοσυμβατή κάψουλα, κυλινδρικού σχήματος, από υλικό PEEK.

Η κεραία, στο πρώτο σετ προσομοιώσεων, τοποθετείται σε τρία κανονικά μοντέλα που προσομοιώνουν τις διηλεκτρικές ιδιότητες του μυός, του ανθρώπινου κεφαλιού, και της τριστρωματικής απλοποιημένης εκδοχής του σώματος (μυς-λίπος-δέρμα) προκειμένου να ελεγχθεί για εφαρμογές σε εμφυτεύσιμες διατάξεις. Τα αποτελέσματα καταδεικνύουν εύρωστη λειτουργία. Η κεραία συντονίζεται στα 405MHz με μέτρο συντελεστή ανάκλασης ($|S_{11}|$) που ξεπερνάει τα 20dB και στις τρείς περιπτώσεις. Τα μέγιστα κέρδη της κεραίας υπολογίζονται στα -24.2 dB, -28.06 dB, και -25.49 dB στα τρία κανονικοποιημένα μοντέλα αντίστοιχα.

Εξαιτίας του μικροσκοπικού μεγέθους και της ισοτροπικής της ακτινοβολίας, η κεραία στο δεύτερο σετ προσομοιώσεων ελέγχεται για εφαρμογή σε καταπόσιμες διατάξεις. Εξαρτήματα όπως μικροηλεκτρονικά κυκλώματα, αισθητήρες, κάμερα,

φώτα LED, μπορούν να τοποθετηθούν στον κενό χώρο που βρίσκεται κάτω και πίσω από την κεραία (βλ. Εικόνα 4.1). Η διάταξη τοποθετείται σε κανονικά μοντέλα που προσομοιώνουν τις διηλεκτρικές ιδιότητες των ιστών τις γαστρεντερικής οδού (ισοφάγου, στομάχου, λεπτού και παχέως εντέρου). Στον ισοφάγο, στο στομάχι και στο παχύ έντερο η κεραία συντονίζεται στα 401.5 MHz, 395 MHz, 405 MHz αντίστοιχα με συντελεστή S_{11} που ξεπερνάει τα -20dB και στις τρείς περιπτώσεις. Στο λεπτό έντερο η κεραία φαίνεται να επηρεάζεται έντονα από φαινόμενα αποσυντονισμού, το οποίο ενδεχομένως να οφείλεται στη υψηλή διηλεκτρική του αγωγιμότητα τοι ιστού, με αποτέλεσμα ο συντελεστής ανάκλασης να είναι μειωμένος. Παρ΄ολα αυτά σε πιο ρεαλιστικά μοντέλα προσομοιώσεων, τα φαινόμενα αυτά αναμένεται να καμφθούν. Συνολικά η πρωτότυπη κεραία εμφανίζει μια εύρωστη λειτουργία τόσο σε εμφυτεύσιμες όσο και σε καταπόσιμες εφαρμογές.

Μελλοντική εργασία θα μπορούσε να περιλαμβάνει τον επανασχεδιασμό της κεραίας προκειμένου να επιτευχθούν: επιπλέον σμίκρυνση, ακριβής προσαρμογή (έτσι ώστε η διάταξη να λειτουργεί με επαρκείς αποδόσεις σε όλα τα απλοποιημένα μοντέλα), μελέτη άλλων διηλεκτρικών υλικών που θα μπορούσαν ενδεχομένως να χρησιμοποιηθούν για την ενίσχυση της απόδοσης της κεραίας, καθώς επίσης και πειραματική κατασκευή και μέτρηση της κεραίας σε φυσικά μοντέλα.

To my parents ,Ms. Evgenia Sioziou and Mr. Athanasios Rigas
and my siblings, Evelina and Trifonas, for supporting me through all these years.

Acknowledgements

I would like to deeply thank my thesis advisor, Prof. K.S. Nikita, for her trust and support all along this thesis.

A special thank you goes to my wonderful parents for standing next to me, with constant support and encouragement. Mom, this song, like all of this, this song is for you.

Table of Contents

LIST OF FIGURES

List of Tables

Chapter 1

Introduction

The first chapter is introductory and depicts the current state-of-the-art in implantable, ingestible and injectable medical devices for medical telemetry. One of the most major components of these devices, are the antennas embedded in such systems, which enable the transmission of physiological signals at a certain distance .The challenging request of wireless performances for implantable / ingestible devices reflects on the difficulties of the design of these antennas. The subject of this thesis is presented, which is the design of an optimized antenna for data telemetry.

1.1 Biomedical telemetry and applications

Recent advances in information and communications technology (ICT) enable the acquisition, transmission, and interpretation of different biosignals, from fixed or mobile locations, at an acceptable cost. This is what biotelemetry is about. It can support better prevention and well-being and provide valuable and prompt diagnostic tools in various application domains, ranging from home care to emergency care, or situations in which a second or a specialist opinion is required before taking a clinical decision.[1]

Biomedical telemetry offers wireless, restraint-free, simultaneous, real-time, long-term data gathering of physiological variables in conscious, unrestrained humans. Biomedical telemetry systems consist of various medical and other devices to create a medical sensor network that can be used in various application domains such as:

• Diagnostic Applications: In order to gather biomedical, physiological or histological, data from the sensors within or around the body in order to identify and diagnose any kind of pathologies (i.e. eye implants to measure intraocular pressure to diagnose low tension glaucoma, endoscopic wireless camera-pill to capture images from the digestive tract,..)

• Therapeutic Applications: In order to alleviate certain symptoms and help in the treatment of a disease (i.e. drug delivery systems, ePatch, ECG holders,..)

• Rehabilitative Applications: Rehabilitative biotelemetry systems used to substitute a lost function, such as vision, hearing, or motor activity (i.e. neuromuscular microstimulator to stimulate paralyzed muscle groups, visual prosthetic device designed to stimulate ganglion cells in retina in order to restore vision to people, fall detection sensors, etc.) [2]

1.2Biomedical telemetry link to Telemedicine

Telemedicine (also referred to as "telehealth" or "e-Health") is defined as the delivery of health care and sharing of medical data over distance using communication technologies. Current telemedicine systems are supported by state of the art technologies like interactive video, high resolution monitors, biomedical telemetry data acquisition systems, high speed computer systems, expert clinical decision support systems, electronic patient record systems , and telecommunications systems including fiber optics, wireless networks, satellites and cell phones .

Telemedicine services have become successful in delivering and exchanging health care information, and it is widely recognized that modern wireless technology has an important role in making that possible. It is obvious that the delivery of health care and health care organizations are converted by advances in biomedical telemetry technologies. These advances trigger a range of improvements in the way in which healthcare services are delivered. Patient-specific healthcare is a research field that has recently garnered much more attention due to the benefits of better services provided to patients and a reduction of healthcare costs. A series of emerging technologies and the exploitation of Information and Communications Technologies (ICT) aim to emphasize the provision of personalized healthcare services to patients [3][4][5].Preventive medical care will be highlighted for individual health management, data will regularly be transmitted to the hospital via built-in sensor and monitoring systems, while mobile and wireless technologies will, support the acquisition, integration, analysis, and storage of clinical data in all its forms.

1.3 Implantable Medical Devices

The field of IMDs (Implantable Medical Devices) is one major category of Biomedical Telemetry. These devices, permit the measurement of physiological signals at a distance, through either wired or wireless communication technologies. Electronic implantable

medical devices (IMD) are designed to be fully or partially implanted in the human bodies through surgeries [6], and remain in bodies for several hours to several years or even permanently after the surgical intervention. From the invention of the cardiac pacemaker with its first implantation in 1953, a bunch of electronic IMDs for both therapeutic and diagnostic applications have emerged over the last decades. Especially in recent years, there have been significantly increasing demands on electronic IMDs. In today's clinical application, well known IMDs include cardiac pacemakers, implantable defibrillators, cochlear and retinal implants, nerve stimulators (Functional Electrical Stimulation- FES), limb function stimulation, ,bladder stimulators, sphincter stimulators, diaphragm stimulators, implantable infusion pumps for drug delivery, blood-glucose sensors such as Continuous Glucose Monitoring (CGM) Biosensor , Intracranial pressure sensor system (ICP), bio-monitoring devices such as temperature monitors or the capsule endoscope. Some of these devices are presented below:

Cardiac Pacemakers

Pacemaker is an implantable medical device including a small battery and placed beneath the epidermal tissue of the chest. Electrical impulses are sent by the pacemaker to stimulate the muscles of the heart, in order to contract and produce a heartbeat. Most pacemakers work just when they're needed - on demand. Some pacemakers send out impulses all of the time - this is called fixed rate. [7]

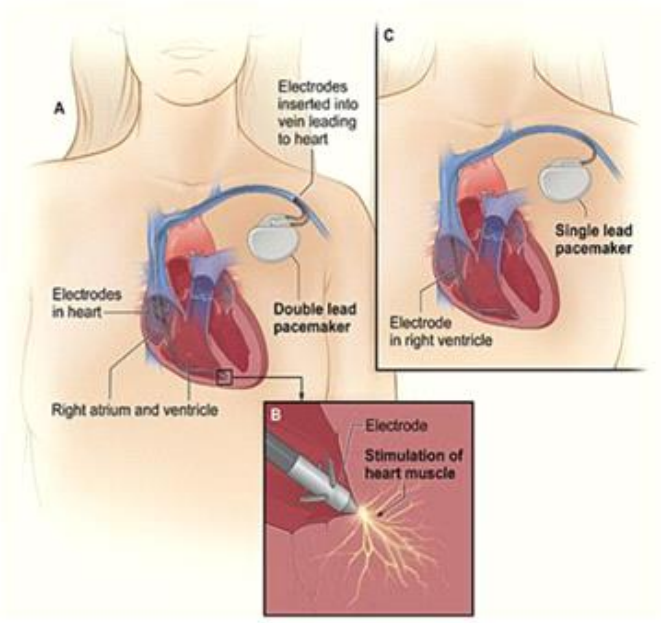

Figure 1.1 Pacemaker

Cochlear Implant

A cochlear implant (CI) is a surgically implanted electronic device that provides a sense of sound to a person who has a severe or profound hearing loss; Cochlear implants bypass the normal hearing process; they have a microphone and some electronics that reside outside the skin, generally behind the ear, which transmits a signal to an array of electrodes placed in the cochlea, which stimulate the cochlear nerve. [8]

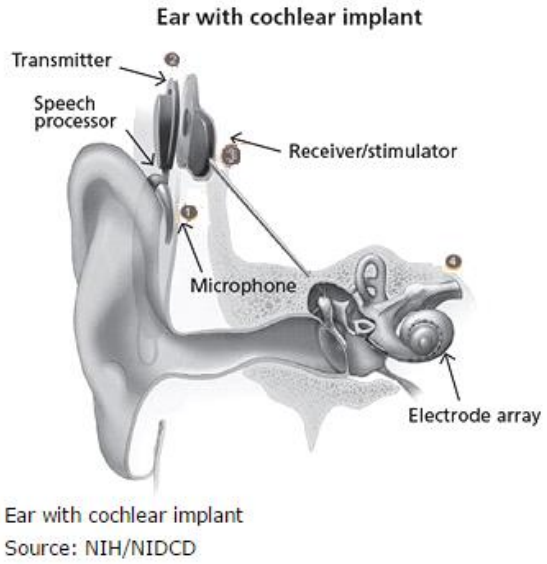

Figure 1.2. Cochlear Implant. [9]

1. A sound processor worn behind the ear or on the body, captures sound and turns it into digital code. The sound processor has a battery that powers the entire system.
2. The sound processor transmits the digitally-coded sound through the coil on the outside of your head to the implant.
3. The implant converts the digitally-coded sound into electrical impulses and sends them along the electrode array placed in the cochlea (the inner ear).
4. The implant's electrodes stimulate the cochlea's hearing nerve, which then sends the impulses to the brain where they are interpreted as sound.[10]

Retinal Implant

Retina implant technology involves the use of microelectronics and microchip electrodes surgically implanted into the back of the eye (retina) to restore the function of the damaged light-activated cells found there. Via electrical stimulation of retinal neurons, degenerated photoreceptors are being bypassed, achieving, to some degree, restoration of the patient's vision.

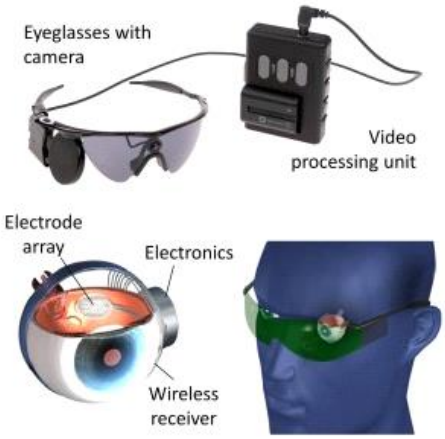

Figure 1.3.Retinal Implant [11]

Continuous Glucose Monitoring (CGM)

CGM is a way to measure glucose levels in real-time throughout the day and night. A tiny electrode called a glucose sensor is inserted under the skin to measure glucose levels in tissue fluid. It is connected to a transmitter that sends the information via wireless radio frequency to a monitoring and display device. The device can detect and notify you if your glucose is reaching a high or low limit.

Figure 1.4. Figure 1.4 CGM system [12]

Diaphragm Pacing Stimulation (DPS)

Diaphragm pacing ,also known as phrenic nerve pacing , is the rhythmic application of electrical impulses to the diaphragm to provide ventilation support for respiratory failure or sleep apnea. At present, diaphragmatic pacing systems are still cumbersome, though work is being done on more portable miniature systems. All currently available systems involve an external transmitter and an implanted receiver. Fully implantable diaphragmatic pacing systems are being developed.

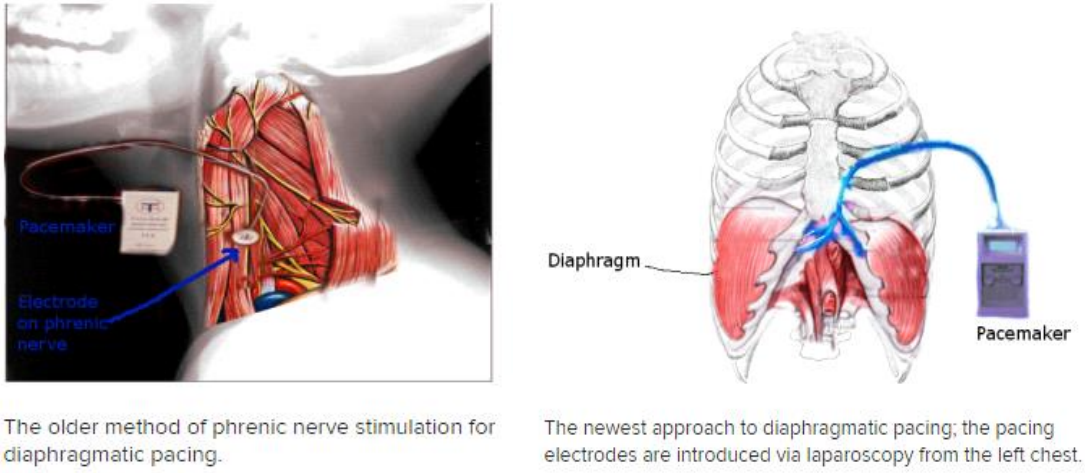

Figure 1.5. Diaphragmatic pacing systems [13]

Intracranial pressure sensor system (ICP)

Intracranial pressure (ICP) monitoring uses a device, placed inside the head. The monitor senses the pressure inside the skull and sends measurements to a recording device. There are 3 ways to monitor pressure in the skull (intracranial pressure).

i) *The intraventricular catheter* is the most accurate monitoring method. To insert an intraventricular catheter, a hole is drilled through the skull. The catheter is inserted through the brain into the lateral ventricle. This area of the brain contains liquid (cerebrospinal fluid or CSF) that protects the brain and spinal cord.

ii) *Subdural screw.* This method is used if monitoring needs to be done right away. A hollow screw is inserted through a hole drilled in the skull. It is placed through the membrane that protects the brain and spinal cord (dura mater). This allows the sensor to record from inside the subdural space.

iii) *Epidural sensor* .An epidural sensor is inserted between the skull and dural tissue.

The epidural sensor is placed through a hole drilled in the skull. This procedure is less invasive than other methods, but it cannot remove excess CSF.[14]

Figure 1.6. Telemetric ICP Measurement. RAUMEDIC®

Functional Electrical Stimulation (FES)

Functional electrical stimulation (FES) is a technique that uses small electrical currents to stimulate the nerves that connect to the paralyzed muscles. This causes the muscles to contract. FES can be used to stimulate nerves in the arms, legs, trunk and buttocks that have been traumatized or affected by a stroke, in order to achieve a range of functional movements .The FES current is generated by a small battery-powered electronic device. There are two ways of delivering the current to the nerve:

1) Surface (external) FES: The most common way is to use electrodes placed on the skin over the nerve. It is important that the electrodes are accurately placed each time FES is used if the correct movement is to be produced.
2) Implanted FES: This involves surgery in which the electrodes are placed directly onto the nerves and controlled by a small implant placed under the skin. The FES device activates the implant through a wireless antenna worn on the outside of the body. Implanted devices remove the need to position electrodes on the skin each day. They also significantly reduce or eliminate the sensation associated with external stimulation.[15]

Figure 1.7.Spinal Cord Stimulator [16]

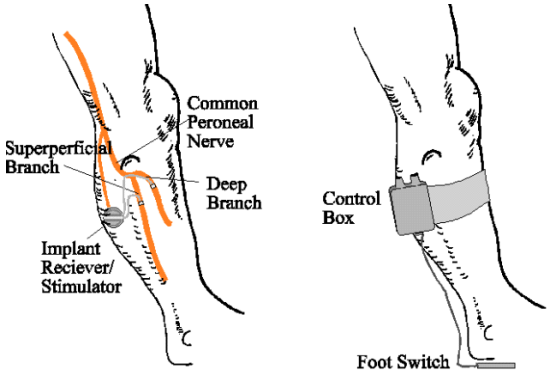

Figure 1.8.Implanted Dropped Foot Stimulator [17]

1.3.1 Wireless Medical Implantable System for Data Telemetry

The wireless body area networks (WBANs) can be seen as an integration of intelligent networks, which permits devices and sensors to work together to obtain a series of critical physiological parameters, such as blood flow velocity and heartbeat frequency[18]. Recently, implant WBANs for biomedical applications have brought about a revolutionary change due to the development of antenna technologies and wireless communication systems. Ubiquity, reduced risk of infection and early diagnosis of a health risk are among the advantages of the WBANs with implant devices.[19] Modern wireless technology has provided the capability of a less invasive and disturbing biotelemetry and has gained a lot of approval among medical implementations for a number of reasons, including low power consumption, simple structure requirements and potentially fast transmission data rates [20][21]. The main aim of a healthcare monitoring system, with a wireless implantable device, is to provide reliable information from inside of the human body to an external Base Station (BS) or subsequently a smartphone. Physiological signals are obtained by means of appropriate transducers, then postprocessed, and eventually transmitted to exterior monitoring/control equipment for analysis by the operator. The components of a typical wireless biomedical telemetry system are:

1. Base Station (or Smartphone) – consisting of several sub-systems such as :
a)a controller to drive the entire system and store the measurements
b)a receiver which encloses antennas;
c)a connector to the data collecting system.

2. Channel Propagation

The analysis of the Electromagnetic (EM) propagation from the implanted device to the Base Station is of great importance .Due to mostly indoor applications of IMDs, the study of the multi-path propagation of the radiated EM waves and the scattering because of nearby objects is crucial, as it can evidently improve the performance of the entire system.

3. Human Body

The complex, dispersive and highly lossy characteristics of the human body inevitably affect the analysis, design, realization and characterization of implantable antennas, thus the wireless performances of the entire system.

4. Insulation

The human body is a hostile environment for the Radio Frequency (RF) radiation. Thus, biocompatible insulation is necessary for any implantable device, in order to avoid any undesirable reaction with the living tissues. Moreover, placing insulating layers around the antenna or on the surface of the human skin, can enhance the EM transmission from an implantable radiator to the Base Station.

5. Implantable Antennas

The design of the radiator is essential for an implantable device operating in a WBAN of a few meters range. Factors such as radiation efficiency, bandwidth characteristics, coupling with the lossy biological material and optimal use of accessible volume must be taken into consideration.

6. Power supply and Electronics

The power supply takes up the most space within the device and its degradation determines the longevity of the device. To extend the life span of IMDs several options are being explored including; the use of internal power supplies; transferring power wirelessly from an external source; and blood sugar energy harvesting.

Electronics of an IMD are responsible for exchanging data and providing signal processing, as well as regulating the power demand, that is required to make the unit operational.

7. Bio-sensors and Bio-actuators

Depending on the purpose they need to serve, IMDs either include biosensors, which utilize biological material to monitor physiological process, or bio-actuators to stimulate a physiological reaction to perform a bodily function. In some cases, IMDs work both as sensors and as stimulators.

8. Characterization and Experiments –Compliance with Regulations

All devices constituting the healthcare monitoring system, must strictly conform to regulations regarding patient's and operator's safety. They must also, undergo extensive testing in order to validate the accuracy and reliability of the results. Thus, in vitro and in vivo testing on animals is required before human testing can commence.

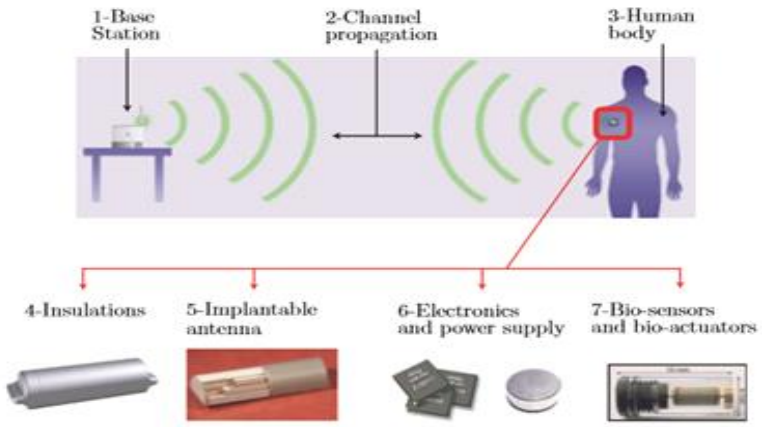

Figure 1.9. Wireless Implantable system for data telemetry [22]

1.3.2 Frequency bands

Wireless implantable devices operate in several frequency bands depending on the required data rate, working range, power transfer capability and different government standards. The prevailing frequency bands include the Medical Implant Communications Service (MICS) band (402-405 MHz) and the Industrial, Scientific and Medical band (ISM) (2.400 - 2.500 GHz).

Medical Implant Communications Service,(MICS)

Until recently, no globally accepted frequency band had been given over to biotelemetry for IMDs' applications. In order to overcome range limitations in the mid-1990s, Medtronic, petitioned the U.S. Federal Communications Commission (FCC) for spectrum dedicated to medical implant communication. The 402-405 MHz Medical Implant Communication Service (MICS) band was recommended for allocation by ITU-R Recommendation SA1346 in 1998. The FCC established the band in 1999 with similar standards following in Europe. In March 2009, the FCC announced the establishment of

the MedRadio Service (401 – 406 MHz) under Part 95 of the Commission's rules, following earlier European regulatory approval in 2007. The creation of the MedRadio Service incorporated the existing MICS spectrum at 402 – 405 MHz and added additional spectrum at 401 – 402 MHz and 405 – 406 MHz for a total of five megahertz of spectrum for implanted devices as well as devices worn on the actual body [23]. MICS is permitted to operate at an Effective Isotropically Radiated Power (e.i.r.p.) level of -16dBm (25 microwatts) or less in a reference bandwidth of 300 kHz in order to provide adequate protection to the Meteorological Aids Systems [24]. The MedRadio band is available for long term medical implants, and therefore has minimal electromagnetic pollution that can cause interference in this band. However, caused by long wavelength for MedRadio band, antenna design at MedRadio band would cause some challenging problem, such as large antenna size, low radiation efficiency, and narrow operating bandwidth. [25]

Industrial Scientific and Medical,(ISM)

The industrial, scientific, and medical radio band (ISM band) refers to a group of radio bands or parts of the radio spectrum that are internationally reserved for the use of radio frequency (RF) energy intended for scientific, medical and industrial requirements rather than for communications. ISM bands are generally open frequency bands, which vary according to different regions and permits. The 2.45 GHz ISM band (2.400–2.4835 GHz) with the mature circuit technologies, wide support for connecting to smart phones and other mobile devices, convenient access to the network, is also widely used for implantable medical systems [26]. According to ETSI EN 300 328 [ETSI, 2004] Standard, ISM has an effective radiated power of up to -10 dBW (100 mW). A great advantage of the ISM band is the enlarged bandwidth which enables higher data transmission rate (i.e. video transmission).
Note however, that higher frequencies suffer from greater body attenuation. The industrial, scientific and medical bands (ISM) are heavily used by other systems (i.e. Bluetooth devices, ZigBee, cordless phones, Wi-Fi computer networks etc.) and they are generally less favorable for the communication of medical data.

Other frequency bands designated for biotelemetry devices:
-Wireless Medical Telemetry Service (WMTS): (608 – 614MHz, 1395 – 1400MHz, 1427 – 1432MHz) is a wireless service specifically defined in the United States by the Federal Communications Commission (FCC) for transmission of data (except voice and video) for remote monitoring of a patient's health.

- Ultra-wideband technology (UWB) :Several countries (US 2002, Singapore 2003, Australia 2004, New Zealand 2005, Hong Kong 2005, Japan 2005, Europe 2006, and South Korea 2006) have adopted domestic UWB rules that permit medical imaging devices in portions of the band 3.1-10.6 GHz. However, these rules are not harmonized worldwide. The UWB frequency band is a promising candidate due to its simple structure, multipath fading, and high data speed. Nevertheless, the weaknesses of UWB are that it only offers short-range of coverage and it experiences higher energy attenuation. [27]

1.3.3 Design challenges for Implantable Antennas

Implantable antennas are electrically small antennas radiating into a lossy medium (human body), which has a relevant impact on the design of an efficient implantable antenna. In order to perform a successful design, the following requirements and constraints must be taken into consideration:

▪ Implantable Antenna Biocompatibility

For the IMD not to be rejected by the patient's body ,the implantable antenna must be biocompatible. Furthermore, human tissues are conductive, and would short circuit the implantable antenna if they were in direct contact with its metallization [28].The prevailing method for preserving the biocompatibility of the antenna-while simultaneously separating the metal radiator from the human tissue – is to cover the structure with a superstrate dielectric layer as shown in Fig 10.

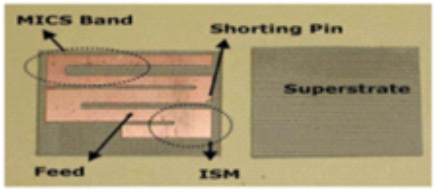

Figure 1.10.Biocompatibility issues for implantable patch antennas: the addition of a superstrate.

Frequently used biocompatible materials are Teflon (permittivity ε_r =2.1, dielectric loss tangent, tanδ= 0.001) , MACOR ®(ε_r =6.1, tanδ= 0.005), and ceramic alumina (ε_r =9.4, tanδ= 0.006) [29].Although, it is essential to highlight that ceramic substrates are not the most suitable choice for drilling and round cuts .Another commonly used technique for

making the IMD biocompatible is the encapsulation of the antenna by using a thin layer of low-loss biocompatible coating. Commonly used materials include zirconia (ε_r =29, tanδ≃0), PEEK (ε_r =3.2, tanδ= 0.01), and Silastic (ε_r =3.3, tanδ≃0). High permittivity and low loss encapsulation materials (zirconia) allow the near fields of the antenna to concentrate inside the encapsulation layer, thus mitigating power loss. However, PEEK and Silastic are much easier to manufacture and handle.

▪Miniaturization

Miniaturization becomes one of the greatest challenges in implantable-antenna design, with new developments aiming at ultra-small antennas that however preserve the desirable EM performances. The use of microstrip (patch) antennas enables some further miniaturization techniques, since they appear to be highly flexible in design shape and conformability. The aim is to decrease the antenna physical size, while increasing its electrical size.[30]
The main design strategies are:
1) Lengthening of the current flow path on the patch surface; longer effective current-flow paths can reduce the resonance frequency, and achieve a more-compact size for the implantable antenna.
2) Addition of shorting pins; inserting a shorting pin between the ground plane and patch increases the effective size of the antenna, which consequently, reduces the required physical dimensions.
3) Patch stacking; vertically stacking two radiating patches reduces antenna size by increasing (nearly doubling) the length of the current-flow path [31].
4) Use of high-permittivity dielectric materials for both substrate and superstrate. Their use shortens the effective wavelength and leads to lower resonance frequencies, thus assisting in antenna miniaturization [32].

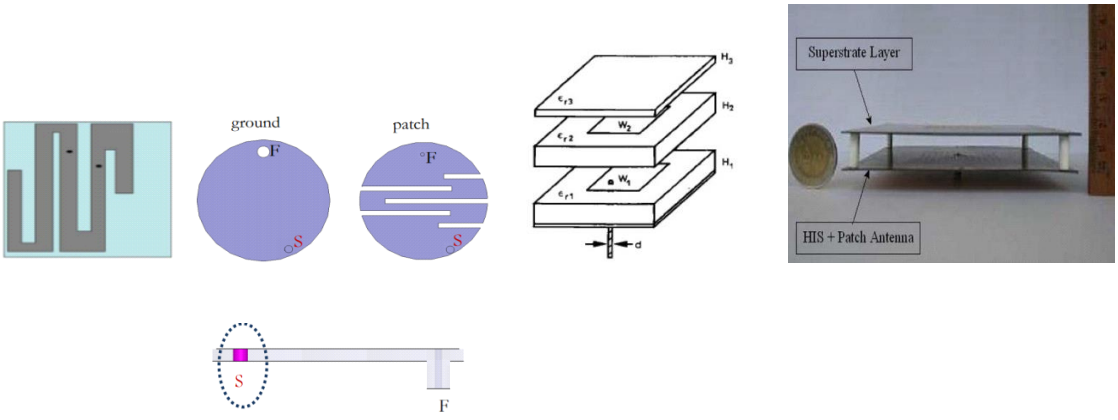

Figure 1.11. (1) **(2)** **(3)** **(4)**

Table 1.1

Various implantable antennas reported in the literature.

Substrate	Substrate Shape	Patch Shape	Frequency Band [MHz]	Implantation Tissue	Miniaturization Technique	Vol. [mm^3]
Rogers 3210	Rectangular	Spiral	402-405	Skin	-	10240
RT Duroid 6002	Rectangular	Waffle	402-405	2/3 Muscle	Shorting Pin	6480
Rogers 3210	Rectangular	Spiral	402-405	Skin	Shorting Pin	6144
ARLON 1000	Square	SRR coupled spiral	402-405 2400-2480	Skin	Shorting Pin	1375.4
Rogers 3210	Rectangular	meandered	402-405	Skin	Shorting Pin	1200
Rogers 3210	Rectangular	Π-shaped	402-405	Muscle	Shorting Pin	790.9
Rogers 3210	Circular	Hook-slotted	402-405	Skin	Shorting Pin and Patch stacking	335.8
Rogers 3210	Square	Spiral	402-405	Viterous humor	Shorting Pin and Patch stacking	273.6
Rogers 3210	Square	Spiral	402-405	Skin	Shorting Pin and Patch stacking	190
Rogers 3210	Circular	Hook-slotted	402-405	Skin	Shorting Pin and Patch stacking	149.2
Rogers 3210	Circular	meandered	402-405	Skin	Shorting Pin and Patch stacking	110.4
Alumina	Circular	meandered	402-405	Skin	Shorting Pin and Patch stacking	32.7

▪Patient's safety

The rate at which power is absorbed by the human body [W/kg]:

$$SAR(x,y,z) = \frac{\sigma(x,y,z)E^2(x,y,z)}{2\rho(x,y,z)} \ ,$$

ρ: tissue density [kg/ m^3]
σ: tissue conductivity
E: electric field amplitude [V/m]

Power limitations are necessary to prevent hazardous heating of biological tissue as defined with peak spatial-average Specific Absorption Rate (SAR) limits. Indeed, the maximum input power for the transmission from any implantable device must comply with the SAR limitations, presented below:

Table 1.2

	IEEE C95.1-1999	IEEE C95.1-2005	ICNIRP
whole-body average	0.08 W/kg	0.08 W/kg	0.08 W/kg
partial-body average	1.6 W/kg	2 W/kg	2 W/kg
	averaged over 1g of tissue in the shape of a cube	*averaged over 10g of tissue in the shape of a cube*	*averaged over 10g of contiguous tissue*

▪Power supply

Towards the direction of lower power consumption, in order to extend the lifetime of the implantable medical device , alternative solutions have been proposed, investigated and developed. Nonetheless, inductive power transmission across the body tissue is currently the prevailing solution to deliver sufficient power to various kinds of IMDs with miniaturized dimensions [33].This method is based on a mutual inductance between two coils in which one is located outside the body while the other is integrated with the implanted device. As the external antenna transmits a varying electromagnetic signal, a voltage would be induced in the receiver coil . The wireless power efficiency depends on the resonance frequency (or operating frequency), distance, alignment, and coupling matching between the transmitter and the receiver coils [34]. Furthermore, power scavenging sources including motion, vibration, air flow, temperature difference, light and infra-red radiation have been suggested.[35]

▪Efficiency

Far-Field Gain, indicates the desired receiver sensitivity for achieving reliable biotelemetry communication. There is a tradeoff between the size of the implantable antenna and the far-field gain. Very small-sized antennas indicate low levels of gain, which subsequently means low radiation efficiency. On the other hand, antennas with high levels of gain, are of greater proportions. Thus, a compromise must be made regarding those two parameters and the existing power limitations of the implantable antenna.

1.4 Ingestible antennas

1.4.1Wireless Capsule Endoscopy, (WCE)

These are the antennas inside the capsule that travels through the digestive tract and other parts of the internal organs and diagnoses GI related cancers , tumours, Crohn's Disease, Celiac Disease, OGIB (Obscure Gastrointestinal Bleeding) ,inflammatory bowel disease (IBD),etc. [36]. Studies are also extending the indication of CE to protein loss, growth failure, abdominal pain, suspected polyp or graft-versus-host disease (GVHD) and regular follow-up for the known small bowel diseases. The particularity of the alimentary tract restricts the utilization of the current available examine techniques. The upper gastrointestinal tract can be examined by Gastroscopy. The bottom 2 meters makes up the colon and rectum, and can be examined by Colonoscopy. In between, lays the small intestine being very long (average 7 meters) and very convoluted. However, this part of the digestive tract lies beyond the reach of the two previously indicated techniques. Therefore, the non-invasive technique, 'Wireless Ingestible Capsule Endoscopy (WCE)' enables the visualization of the whole GI tract cable freely [37]. The swallowable pill endoscope is a miniature telecamera that acquires images as it travels through the gastrointestinal tract. The imaging system consists of a swallowable capsule, a data recorder, and a workstation. The patient swallows the capsule, which contains a color video camera, LED lights, wireless radio frequency transmitter, antenna and battery. The capsule acquires images and transmits video signals to receiver. These capsules move through the digestive tract by the natural motility of the tract itself. WCE takes images in its 8-hour journey through the digestive tract, after it is swallowed by the patient. The capsule is then excreted naturally in the patient's bowel movement, and the data it contains is retrieved and interpreted. Fig. 12 shows the human GI tract consisting of four main parts, that is, the esophagus, stomach, small intestine/bowel, and large intestine or colon.

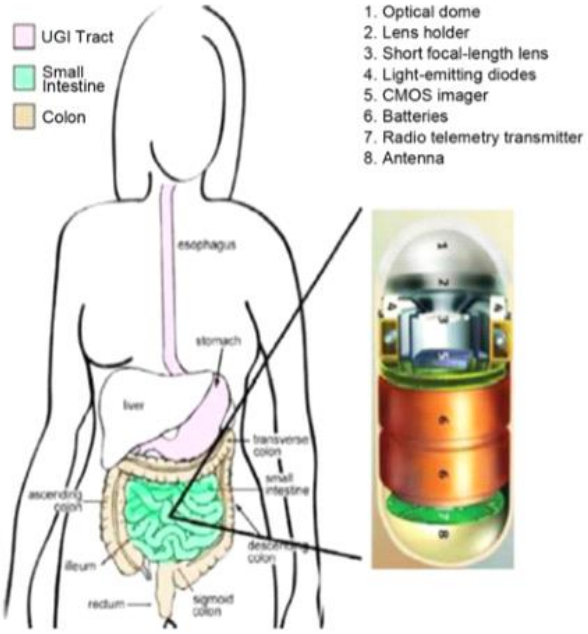

Figure 1.12.Complete GI path of a bio-telemetric capsule and typical components found within an imaging capsule system.

1.4.2 Applications

The first examples of wireless medical capsules were developed beginning in the late 1950s and measured temperature, pressure, or pH. Little further progress was made until the recent development of a video capsule. However, video is only one of the several measurements that physicians wish to obtain from the GI tract. Accurate measurements of temperature, pressure, pH and other ion concentrations can reveal pathologies that are undetectable by video.

M2A

The very first capsule-type endoscope, that was designed, called the M2A, was developed and commercialized in 2001 by Given Imaging Inc., Israel [38]. It is 10 mm in diameter and 26-mm long with a charge coupled devices (CCD) camera, an RF module, illuminating LEDs, and a battery integrated. It can be swallowed and can transmit wireless still and moving images from the gastrointestinal tract.
In 2002 the company introduced M2ATM Plus, making it possible to know the location

of the capsule, with an accuracy of about ± 3 cm, by means of a triangulation process of the signal strength received by three adjacent aerials. Then, the suspected blood indicator (SBI) utility was implemented in order to decrease the time to interpret WCE recordings.[39]

Figure 1.13. M2A Capsule and schematic diagram of its components

PillCam_SB

M2A was renamed PillCam SB (meaning "small bowel"; Fig. 14) after the advent of esophageal CE (PillCam ESO; Fig. 15), also developed by Given Imaging [40]. PillCam SB was approved by the Ministry of Health, Labor and Welfare of Japan in April 2007, and finally reimbursement for CE costs was approved by Social Insurance Agency of Japan in October 2007. The PillCam SB system has three components: a capsule endoscope body, an external receiving antenna with attached portable hard disc drive (data recorder), and a customized PC workstation (RAPID: reading and processing images and data) with dedicated software for review and interpretation of images [41]. The PillCam SB capsule (11 mm × 26 mm, 3.64 g) contains among others a CMOS chip imager, two watch batteries, and a UHF band radio telemetry transmitter. The activated PillCam SB capsule provides images at a frequency of 2 frames per second until the battery expires, after about 8 hours, which enables the device to take up to 55000 still images (JPEG format).[42]

PillCam_ESO

Besides PillCam SB, Given Imaging produces PillCam ESO (Fig. 15), marketed in the U.S. by the InScope Division of Ethicon Endo-Surgery Inc., Johnson & Johnson Group, Cincinnati, Ohio (USA), [43]. The body of PillCam ESO harbors two cameras, one on each side and, while it proceeds along the esophagus, it captures 14 images per second. Other features, concerning dimensions, field of view and resolution, are the same as the PillCam SB. The PillCam ESO acquires images which are directly transmitted to the sensor arrays and then to the storage unit.

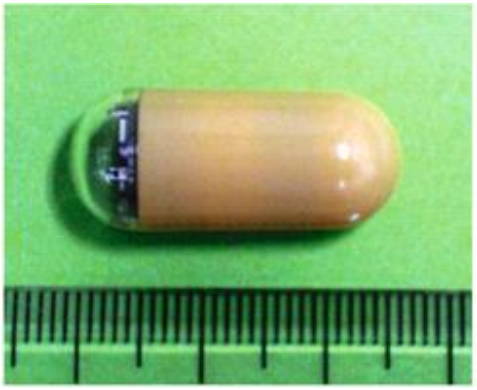

Figure 1.14. PillCam SB(11x26mm); a first line tool for the detection of abnormalities of the small bowel

Figure 1.15.PillCam ESO (11x26MM); capsule endoscope for investigating esophageal diseases

PillCam COLON

PillCam COLON (Fig.16, 11 mm × 31 mm) was developed by Given Imaging to detect colonic neoplasia. Interestingly, some polyps can be detected by PillCam COLON that are missed by a traditional colonoscopy, according to this interim analysis [44].

Figure 1.16.PillCam COLON

Olympus Endoscope

In October 2005 Olympus Corporation, Tokyo (Japan), launched in Europe EndoCapsule, a disposable and passive pill for small bowel endoscopy, 26 mm in length and 11 mm in diameter, with a CCD sensor camera (Fig. 17) and an operational time of 8h.An antenna sends two images per sec to the recorder. Moreover, thanks to the Real Time Viewer monitor (Fig. 17), physicians can view real-time images and estimate the capsule position. Then, the EndoCapsule Software allows the management of the acquired data. Its main features are: a multi display function for optimal observation, structure enhancement and enlargement display function to highlight the tiniest details, red color detection function to highlight suspected bleeding symptoms, and auto speed adjustment function to optimize the review speed.

Figure 1.17. Olympus WCE system: EndoCapsule & Real Time Viewer

Norika

Another wireless type endoscope called Norika V3 is being developed by RF System Co., Japan (Fig.18). It does not have any battery module in its body, and thus requires a smaller volume. .The diagnostic system includes a pill, 23 mm in length and 9 mm in diameter, a camera, 4 LEDs for illumination, an external controller, a transmitter vest and a workstation. It receives the energy externally through transmitted microwaves. Besides being able to transmit images, it can change the view point of the camera with a rotating mechanism based on rotor coils. [45] The newly developed capsule-type endoscopes have an advantage in reducing pain and discomfort of the patient due to its wireless nature. However, they must move passively from the mouth to anus by the peristaltic waves. Thus, no active diagnosis is possible due to the lack of a locomotive mechanism.

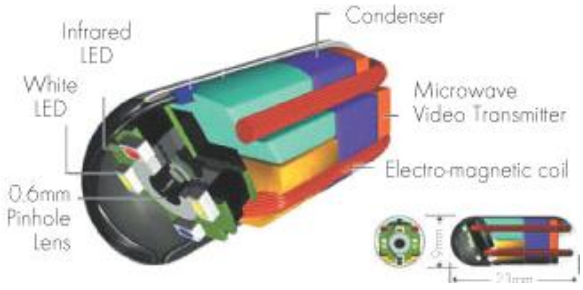

Figure 1.18.The Norika3 capsule endoscope

1.4.3 Frequency Bands

Ingestible antennas operate in the following bands:

• Dual band MICS (Medical Implant Communication Services): 402 MHz-405 MHz
• ISM band: 2.40 GHz-2.48 GHz
• WMTS bands (608 MHz-614 MHz, 1395 MHz-1400 MHz, 1427 MHz-1432 MHz)
• Or even lower frequencies: 40 MHz

1.4.4 Design requirements for ingestible antennas

• The antenna should have enough bandwidth to transmit high-resolution images and large amount of real-time data such as temperature, pressure, pH and oxygen concentration of GI tract. Thus, antennas with a miniature size but wide bandwidth are required.
• The enhancement of antenna efficiency should facilitate lower power consumption , in order to maintain the communication link given the power requirements imposed by international safety guidelines (IEEE Std C95.1-1999 and Std C95.1-2005).[46]
•The antenna should drain a fairly small amount of energy so that the wireless capsule can maintain its operation during the entire GI tract (typically 8 - 9 h). A future option , could be the wirelessly transmission of power to ingestible antennas using principles of magnetic induction in order to avoid the use of batteries that limits the lifetime of such systems
• The endoscopic capsule operates inside the dissipative multi-layer human body . So the electric properties of this medium (high dielectric constant, conductivity different from zero) are going to modify the antenna performances such as radiation pattern, resonant

frequency, radiation efficiency, and must be considered while designing the antenna
• Same as for implantable antennas, ingestible antennas must be biocompatible so that they do not harm the patient and durable so that the body fluids do not harm the antenna. These requirements constitute packaging of the ingestible antennas inside a shell. Capsule casings and circuitry have been found to have a minor effect on the performance of the ingestible antenna. Therefore, taking the effects of casing into account while modeling the antenna is not necessarily compulsory.
•Different from implantable antennas, the ingestible antenna needs to be omnidirectional and exhibit circular polarization in order to transmit signals independent of its position and orientation. That's because the exact position and orientation of the capsule device travelling along the entire GI tract, is unknown. Therefore, an isotropic radiation pattern is required for ingestible antennas. [47]

Given the above considerations, normal mode helical antennas are most commonly employed for such applications (Fig 19.a).

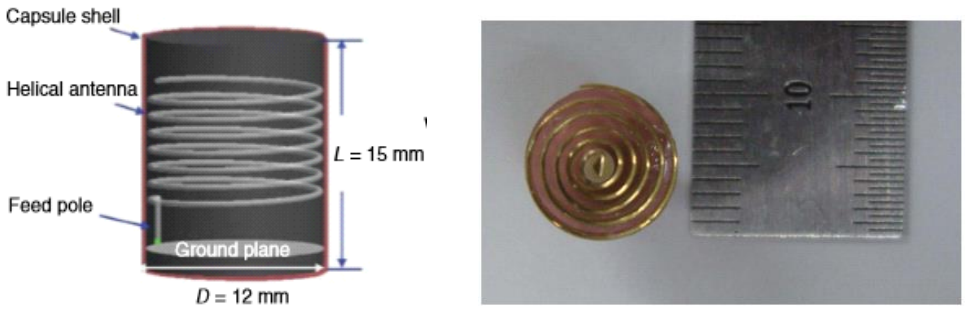

Figure 1.19. Example of ingestible antennas: (a) helical (48), (b)spiral (49) geometries.

1.4.5 Limitations of present capsules

Present capsule endoscopes do not provide high image resolution and frame rates. Although the limited power is an issue, a highly efficient transceiver chip can boost the data rate with the optimized power. The most concerning limitation however, is the limited control of the movement of the capsule. Current WCE models are passive devices and their motion relies on natural bowel peristalsis, which implicates the risk of failing to capture images of significant regions, since the practitioner cannot control capsule/camera orientation and motion. The system is incapable of repeated examination of the same area, and the asymmetrical bowel transit (slow or fast) increases the likelihood important information chance not to be detected [50]. For this reason, present

capsules are commonly used for inspecting the small bowel. When applied to the examination of the large bowel, robotic endoscopic capsules may overcome the drawbacks of pain and discomfort, but they still lack in reliability, and –overall– fail due to their inherent inability to combine therapeutic functions with common screening aims [51][52]. In addition, all of the capsules are powered by two coin-cell batteries, so, if transit is too slow for any reason, the batteries may be depleted before the examination is completed [53]. Furthermore, the usage of an internal power source, such as a battery, is a critical issue as to toxicity and length. In particular, the latter sets a limit on the amount of available energy devoted to the acquisition of pictures. This affects the choice of the image sensor: CMOS technology may be preferable since it ensures a lower power consumption than CCD, but at a price of a poorer image quality [54]. Moreover, the limited energy provided by a battery makes it impossible to add other functional modules to endoscopic capsules, especially those for the locomotion and control of movement.

1.4.6 Future prospects of WCE

The primary focus of CE research in recent years has been enabling active CE locomotion and extension of the technology to therapeutic functionality (i.e. the integration of sensors could make other diagnostic and therapeutic tasks feasible, e.g. biopsy and drug delivery.)

Locomotion

If a capsule had an active locomotion it could vary its speed, hence reducing the transit time, and with stop mechanisms it might stay at a specific point of diagnostic interest for a prolonged time. This would enable the physician to conduct a more thorough analysis, whenever he spots interesting sites. The main issue in that is related to technological integration. It is difficult to embed a locomotion module into a swallowable capsule because of the size of actuation and power constraints. Two main strategies allow the implementation of active locomotion in an endoscopic swallowable capsule: one consists in embedding on-board a miniaturized locomotion system(s), i.e. internal locomotion; the other requires an external approach, i.e. external locomotion. This latter approach generally relies on magnetic field sources [55].

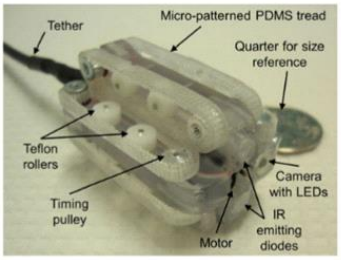

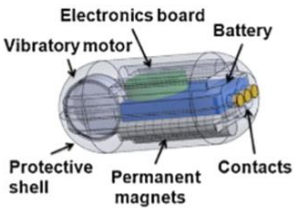

B

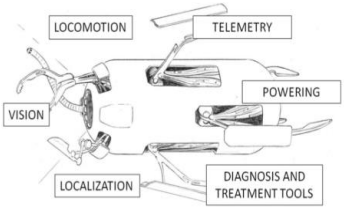

Figure 1.20.a)Internal locomotion platform Mattoli **b) External locomotion platform magnetically-driven capsule with vibration by Ciuti** **c) System architecture of a robotic capsule Courtesy of Virgilio Mattoli**

Reading time and identification of lesions

Capsule recordings are of extraordinary length, therefore, requiring significant time for analysis of the examiner. Improvements and enhancements of software algorithms will allow for more time-sparing approaches by automatically identifying gastric, duodenal and cecal landmarks and by automatically scanning images for bleeding-suspicious or lesion-suspicious images.[56]

Therapeutics

Two technical possibilities have been proposed for obtaining histological evaluation of the small bowel mucosa with a capsule: (1) real samples could be obtained through aspiration/cutting or (2) virtual histological images could be obtained by using confocal imaging or optical coherence tomography [57]. Novel capsule prototypes will allow obtainment of mucosal biopsies and placement of clips for hemostasis.[58] The Nano-based capsule-Endoscopy with Molecular Imaging and Optical biopsy project by Given Imaging Ltd. and a global consortium ultimately intends to develop a capsule system that will combine optical and nano-technologies in order to further improve diagnostic and therapeutic possibilities. Other innovative capsule models, intended to be used for drug delivery in the next-generation wireless CE include the micro-robot; developed by Woods and Constandinou the micro-positioning mechanism allows a needle to be positioned within a segment of a cylindrical capsule and be extendible by up to 1.5 mm outside the capsule body (Fig. 21.a), the intelliCap, the Enterion Drug Delivery Capsule(Fig.21.b), etc. [59]

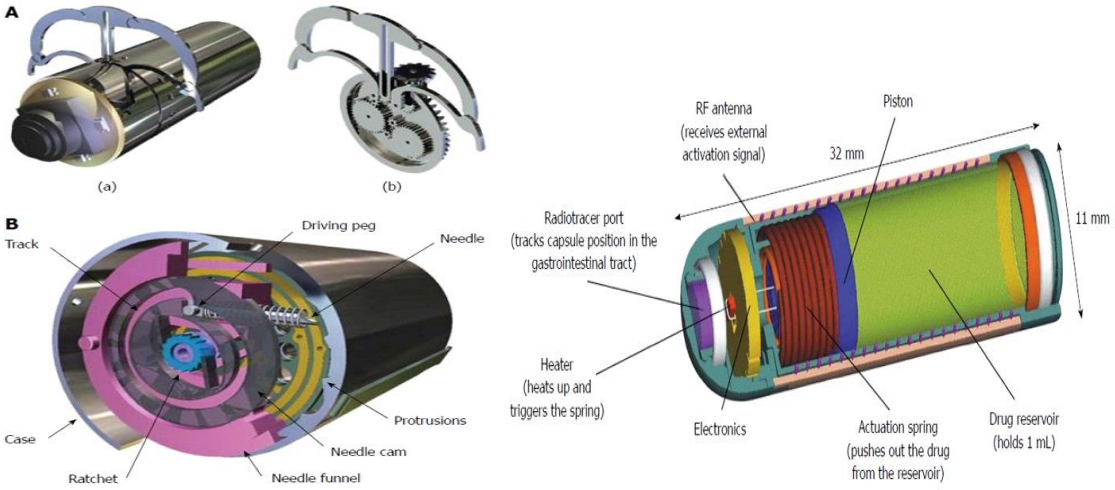

Figure 1.21.a)The micro-robot capsule for: A) Stabilization of positioning and B) Drug delivery, with permission **b)Enterion drug delivery capsule, with permission.**

Powering

At least, externally rechargeable batteries (using radio frequency, microwave, ultrasound or electric induction) or even 'battery-free' capsule endoscopy systems are under development to extend retention times and enable activities like capsule movements or clip placements.[60]

1.5 Injectable antennas-applications

A major field of interest, that is constantly gaining more ground among researchers , is the development of tiny electronic devices that are small enough to be injected trough a syringe. The main reasons behind this scientific orientation, are the side effects, provoked by conventional, large implantable medical devices such as discomfort , risk of infection and post-surgery trauma.

Since the early-1980s, and after millions of RFID tags, (radio frequency identification tags), have been sold, research laboratories have developed injectable medical implants, known as micromodules. The RFID tag was a subminiature glass capsule containing a solenoidal coil and an integrated circuit, used for livestock, pet, laboratory animal, and endangered-species identification. Due to the electronic and implant-packaging research progress, the development of a variety of injectable micromodular electronic implants

was made possible. A significant representative of these micromodules ,was the microstimulator, designed for use in functional-neuromuscular stimulation.[61]

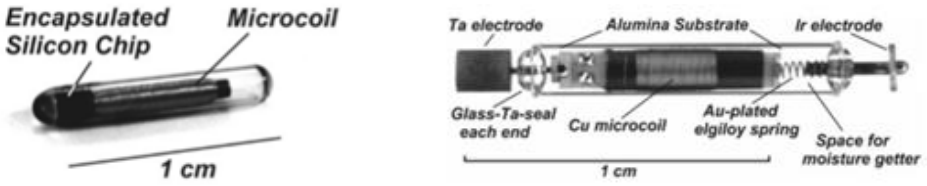

Figure 1.22.a)Commercial injectable radio frequent (RFID) metal transponder. Within the glass capsule is a microcoil connected to an integrated circuit. **1.22.b) Microstimulator. At each end ,a stimulating electrode exits the glass capsule**

Technological advances led, in the early-1990s, to the design of the first device of implantable electronic interfaces with nerve and muscle. BIONs (bionic neurons), hermetically encapsulated, leadless electrical devices, were small enough to be injected via a percutaneous procedure into muscles. They received their power and digital addressing and command signals from an external transmitter coil that could be worn by or placed under the patient [62].They were aimed to be used at various patterns of therapeutic stimulation, in order to build strength and bulk in hypotrophic muscles, e.g. following stroke, spinal cord injury, major trauma and orthopedic reconstructions. Early designs were externally empowered as there was no battery suitable for such a purpose at that time. Ultimately, an inductively coupled link (ICL) was inserted for power and data telemetry. Four generations of BION technology can be seen in Figure 23.a. BION1: RF-powered, continuously controllable, BION2: RF-powered, continuously controllable stimulators and sensors , BION3: Rechargeable battery-powered, programmable stimulators BION4: Rechargeable battery-powered, intercommunicating stimulators and sensors [63] .Other implementations such as the rechargeable battery-powered bion® microstimulator ,that can be seen in Fig.23.b), was applied in order to alleviate patients from neurological disorders ,including urinary incontinence, prevention of deep vein thrombosis ,fecal incontinence, chronic headaches, peripheral pain, angina and obstructive sleep apnea [64].

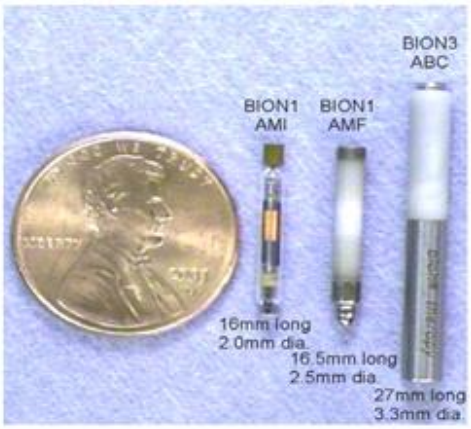

Figure 1.23.a)BIONs now in clinical use b)BION microstimulator, measuring only 28mmx3.2mm

1.5.1 The InNS Concept

Functional recovery of limb movement requires feedback signals about ongoing movement, for which attention was drawn to the development of next generation BIONs that provide outgoing telemetry of such data .In order to restore the motor function to paralyzed limbs by functional electrical stimulation (FES) , the BION was developed to enable neuromuscular stimulation through a miniature, self-contained implant designed to be injected in or near muscles and peripheral nerves[65].BION was the first prototype of the injectable neurostimulator [66].

A neurostimulator is a biomedical electronic device that provides low-frequency pulses, thus stimulating electrically the nerves in order to palliate neurological symptoms and rehabilitate nerve or muscle function [67]. Injectable neurostimulators (InNSs) are currently applied in clinical trials to replace the dominant bulky implantable neurostimulators (ImNS) . Due to its smaller size, wireless-updatable software, and wireless power supply, the injectable neurostimulator is indubitably less invasive, 'smarter', and has a longer lifetime. Moreover, its smaller power consumption, leads to less heating is of the tissue. A typical InNS consists of at least a pair of electrodes. InNS components:

•a stimulator tissue-interface
•an optional antenna for power and data telemetry
•a package that serves both the electronics-tissue interface
•a protective layer that shields the electronics from the body
•some sensors , and
•several functional building blocks (FBBs) in order to generate and control the electrical pulses.

The sensors detect and monitor supplied voltages , electrode impedance ,neural signals' behavior, temperature or pressure of the interface between the InNS and the tissue .The FBBs
include the power supply and power management module ,a data transceiver , a microcontroller, a microstimulator and a neural recording module. Unlike the ImNS, the InNS has no electrode extension leads, because of direct delivery to the stimulation target.
The new generation of InNSs can be powered from a microbattery, a radio-frequency energy harvester, or an inductive coupling link as shown in Fig. 24.

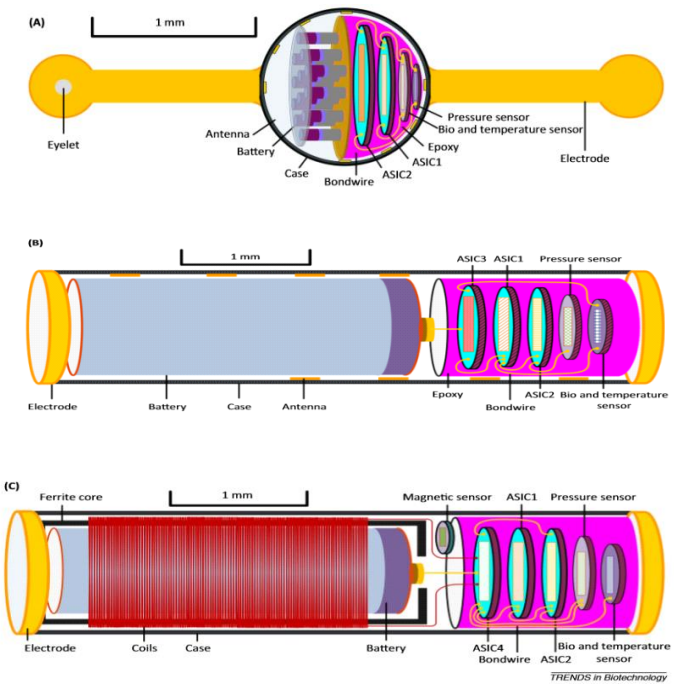

Figure 1.24.Conceptual architecture of the new generation of InNSs to be powered by (A) a battery, (B) a RFEH (ASICS3) for low-threshold stimulation , (C) an ICL

1.5.2 Implementation Challenges and development trends

There are many challenges for researchers to embrace as far as the realization of the InNs is concerned. Obstacles include the implementation of injectable batteries, injectable antennas, and radio-frequency energy harvesters (RFEH).

▪The injectable battery needs to be exceptionally small, but at the same time needs to have high power capacity for longer stimulation time. Towards this direction, a rechargeable battery has been introduced, which can make Bion last for one or more weeks before running out [68], and also the Li-ion microbattery consisting of Lithium and thousands nanowires[69].An innovative technique, called the " jellyroll" technique was also submitted in 2014 ,which enables double energy packing, comparing to the so far advanced microbatteries [70]

▪In RFEH- and ICL-powered InNS , batteries can be sidestepped by a built-in capacitor ,that both conserves instant harvested power and conveys more power than batteries.[71]

▪Regarding the injectable antenna, a tradeoff stands between small size antenna and high efficiency. The RFEH-powered InNS demands an injectable antenna of few millimeters length to meet both its power and data telemetry needs .High frequencies (microwave frequencies of few GHz) increase radiation efficiency, but simultaneously experience more intensive absorption by the tissues leading to limited penetration depth [72]. Thus, a compromise must be made between the two parameters.

The realization of InNSs also awaits breakthroughs in soft and bendable materials, reliability, and the mode of injection.

•The FBBs and packages of the InNS can utilize biocompatible materials such as gallium, or gallium-indium alloys and tin as conductive materials [73]. Nevertheless, Silicon could be applied as a semiconducting material, being both biocompatible and flexible, due to its ability to build circuitry with high performance. In order to achieve bendiness in silicon-composed InNs, alterations should be made to the thickness or even presence of the substrate. Silk, collagen and other biodegradable polymers could be used to produce bendable and soft electrodes and FBBs [74].Nonetheless new materials and new types of ASICs (application-specific integrated circuits) are yet required to build genuinely bendable InNSs.

•In terms of reliability, toxic materials like copper oxides or arsenic oxides, when contained in the InNSs must be firmly sealed to prevent harmful chemicals from leaking into the tissues [75]. In addition, battery monitoring circuitry in essential for possible overcharging /over-discharging, as well as feedback loops for auto-control and self-calibration. Software and connection failures, materials' efficiency, and isolation layers must be also put rigidly under control, in order for reliability to boost.

•Currently there are two methods of injecting an InNs into the body:
1)either inject the whole device into the target ,all at once,
2)or inject biocompatible materials into the tissue step by step, in order to form an entire electronic device and then design an operative InNs from several such devices.
Another method that was attempted recently, in both in vivo and in vitro experiments, was the direct injection of 3-D medical electronics into the target biological tissues combined with conductive liquid metal.[76]Fig.25 .The liquid metal used was GaInSn because of its desirable properties; low melting temperature, well controlled wettability, and high electrical conductivity .The biocompatible gelatin was selected as the packaging material, owning to its excellent bio-degradable and injectable properties, while a green dye has also been employed to enhance the identification of the used packaging material. Nonetheless, until now this application is only suitable for simple electronic devices .

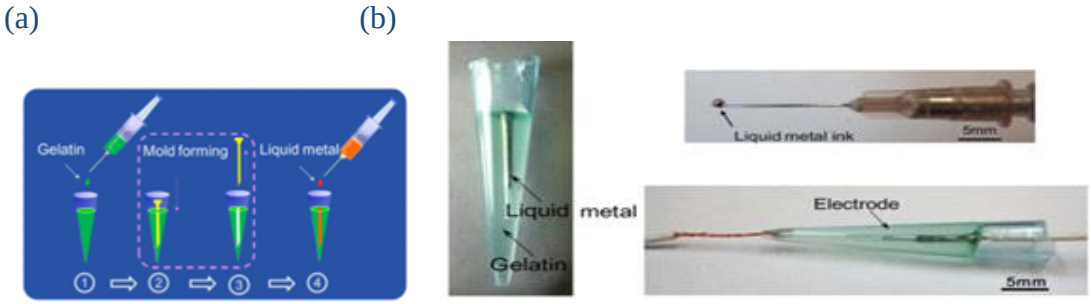

Figure 1.25.Injectable packaged bio-electrode in a 1 ml pipette pin. a) Schematic illustration of the fabrication process: During the procedure of (2) and (3) a syringe needle with a diameter of 1 mm was employed to shape the electrode mold. And through injecting the GaInSn-based liquid metal ink, an electrode with diameter of 1 mm was fabricated in the final step of (4*).* **b) Formed electrode [140]**

To sum up, the liquid metal based 3-D injected fabrication technique opens the way for minimally invasive medical implantation. It offers a much superior tool in a variety of biological and medical applications, for instance fabricating a RFID (Radiofrequency Identification) (Fig. 26). Through a precise control of the injector's shifting and injection speed, a much complex RFID antenna can be easily fabricated inside the biological body. Future research in InNSs, will focus on next generation microbatteries with high power density, innovative antennas for power and data transmission in vivo, and new materials to create truly bendable InNSs. Moreover, further miniaturization of form factor will be pursued, so that direct injection into nerve sites can be made possible, by means of middle-gauge needles (e.g. 16G or 17G).It is all up to developments of biomedical

sensors[77][78] biomimetic systems[79] and biomolecular electronics [80] that will define the evolution of InNS technology.

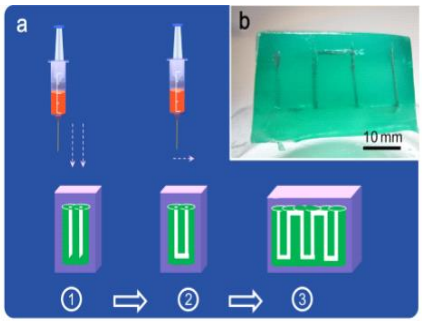

Figure 1.26. Profiles for injectable 3-D RFID antenna.

(a) Schematic illustration for the fabrication procedure of injected RFID antenna within the biological tissue.

(b) A 3D RFID antenna fabricated by injecting the liquid metal into the packaging domains.

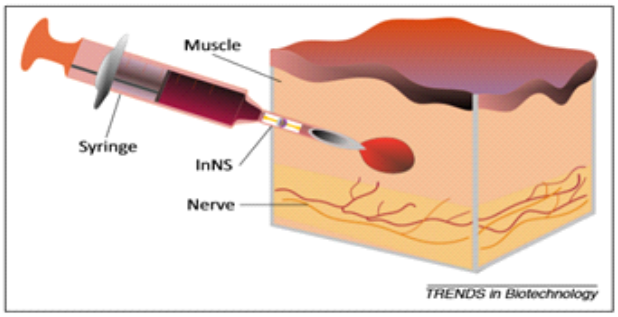

Figure 1.27.An InNS being injected into a muscle site by means of a syringe with a 16G needle. [81]

Chapter 2

Antenna Theory and Modeling Features

This chapter outlines the theoretical framework and research background necessitated to design an implantable/ingestible antenna .Initially, the properties and operating principles of microstrip, and PIFA antennas are presented alongside with Antenna Performance parameters and their modification by certain miniaturization techniques .The analysis exhibited in this chapter serves as a common base for all the investigations and results presented later on. Moreover, the Biological Tissue Properties are displayed, since the biological environment is essential to the operation of an implantable medical device.

2.1 Antenna Performance parameters

An antenna can be defined as the transitional structure between free space and a guiding device (coaxial line or waveguide), which is used to transport electromagnetic energy from the transmitting source to the antenna or from the antenna to the receiver. To describe the performance of an antenna, definitions of various parameters are necessary [82].The definitions are taken from IEEE Standard Definitions of Terms for Antennas, IEEE Std 145-1983.:

▪*An antenna radiation pattern* is defined as a graphical representation in three dimensions of the radiation properties of the antenna as a function of angular direction. In most cases, the radiation pattern is determined in the far-field region (*that region of the field of an antenna where the angular field distribution is essentially independent of the distance from the antenna*). Antenna radiation performance is usually measured and recorded in two orthogonal principal planes (such as E-plane and H-plane or vertical and horizontal planes) and the pattern is usually plotted either in polar or rectangular coordinates. The pattern of most base stations contains a main lobe, containing the direction of maximum radiation, and several minor lobes, named side lobes. The minor lobe that occupies the hemisphere in a direction opposite to that of the major (main) lobe is called back lobe.

▪ *Radiation intensity* is defined as "the power radiated from an antenna per unit solid angle." The radiation intensity is a far-field parameter, and it can be obtained by simply multiplying the radiation density by the square of the distance. In mathematical form it is expressed as:

$U = r^2 W_{rad}$, where

$U =$ radiation intensity (W/unit solid angle)

$U_{\max} =$ maximum radiation intensity (W/unit solid angle)

$U_o =$ radiation intensity of isotropic source (W/unit solid angle)

P_{rad} = total radiated power (W)

W_{rad} = radiation density (W/m^2)

For an isotropic source U will be independent of the angles θ and φ, as well as for W_{rad} . Thus the radiation intensity of an isotropic source can be written as:

$$U_0 = \frac{P_{rad}}{4\pi}$$

▪ *Antenna directivity* of an antenna defined as "the ratio of the radiation intensity in a given direction from the antenna to the radiation intensity averaged over all directions" .If the direction is not specified, the direction of maximum radiation intensity is implied. The average radiation intensity is equal to the total power radiated by the antenna divided by 4π. The directivity of any source; other than isotropic, is always greater than unity. In mathematical form, it can be written as:

$$D = \frac{U}{U_o} = \frac{4\pi U}{P_{rad}} \quad , \; D_{\max} = D_o = \frac{U_{\max}}{U_o} = \frac{4\pi U_{\max}}{P_{rad}}$$

D = directivity (dimensionless)

D_o = maximum directivity (dimensionless)

▪ *Antenna Polarization*: The polarization of a wave radiated by an antenna in a specified direction at a point in its far field, is defined as " the polarization of the (locally) wave which is used to represent the radiated wave at that point"." At any point in the far-field of an antenna the radiated wave can be represented by a plane wave whose electric field strength is the same as that of the wave and whose direction of propagation is in the radial direction form the antenna. Polarization may be classified as linear, circular, or elliptical.

▪*Antenna Efficiency*: The total antenna efficiency is related to losses at the input terminals and within the structure of the antenna. These losses are owed to the two following losses:

a) Reflections because of mismatch between the feeding transmission line and the

antenna and b) conduction and dielectric losses IR^2

▪*Antenna Gain*: The maximum gain of an antenna is defined as the product of the directivity and the efficiency e of the antenna.

$G(\theta,\varphi) = e\ D(\theta,\varphi)$

If the efficiency is not 100 percent, the gain is less than the directivity. When the reference is a lossless isotropic antenna, the gain is expressed in dBi, the efficiency is e =1 and is the same as the directivity of the antenna. When the reference is a half wave dipole antenna, the gain is expressed in dBd (1 dBd = 2.15 dBi).

▪*Far-field region*: "that region if the field of the antenna where the angular field distribution is essentially independent of the distance from specified point in the antenna region". The radiation pattern is measured in the far field.

▪*Input Impedance* Z_{in}: "The impedance presented by an antenna at its terminals or the ratio of the voltage to current at a pair of terminals or the ratio of the appropriate components of the electric to magnetic fields at a point". The input impedance is a complex function of frequency with real and imaginary parts.

▪ *Coaxial antenna*: "An antenna comprised of an extension to the inner conductor of a coaxial line and radiating sleeve which in effect is formed by folding back the outer conductor of the coaxial line".

▪*Directional antenna:* "An antenna having the property of radiating or receiving electromagnetic waves more effectively in some directions than others.

▪*Omnidirectional antenna*: "An antenna having an essentially non-directional pattern in a given plane of the antenna and a directional pattern in any orthogonal plane".

▪*Reflection Coefficient* S_{11} of an antenna is defined as the ratio of the reflected wave's amplitude to the amplitude of the incident wave. The reflection coefficient is zero (S_{11} =0dB) if the transmission line impedance is the complex conjugate of the antenna impedance; then all the power is reflected from the antenna and nothing is radiated. Sometimes it is written as gamma: Γ or return loss.

Γ =voltage reflection coefficient at the input terminals of the antenna= $\dfrac{Z_{in} - Z_o}{Z_{in} + Z_o}$

[Z_{in} = antenna input impedance, Z_o = characteristic impedance of the transmission line]

▪*Front-to-back ratio*: “The ratio of the maximum directivity of an antenna to its directivity in specified rearward direction”. Sometimes the directivity in the rearward direction is taken as the average over an angular region

▪*Voltage Standing Wave Ratio (VSWR)*: The radio of the maximum/minimum values of standing wave pattern along a transmission line to which a load is connected. VSWR value ranges from 1 (matched load) to infinity for a short or open load. For most base station antennas the maximum acceptable value of VSWR is 1.5. VSWR is related to the reflection coefficient as shown below:

$$\text{VSWR} = \text{voltage standing wave ratio} = \frac{1+|\Gamma|}{1-|\Gamma|}$$

▪*Frequency Bandwidth*: “The range of the frequencies ,on either side of a center frequency, within which the performance of the antenna, conforms to a specified standard ,with respect to some characteristics (e.g., input impedance, reflection coefficient, etc.)”. VSWR of an antenna is the main bandwidth limiting factor.

2.2 Operating principles of implantable antennas

In addition to transmitting or receiving energy, an antenna in an advanced wireless system is usually required to optimize or accentuate the radiation energy in some directions and suppress it in others.[82]Thus, the antenna must also serve as a directional device in addition to a probing device. It must then take various forms to meet the particular need at hand, and it may be a piece of conducting wire, an aperture, a patch, an assembly of elements (array), a reflector, a lens, and so forth.

2.2.1 Microstrip - Patch Implantable Antenna

Microstrip antennas are becoming very widespread within the wireless communication market. Patch antennas are low cost, light weight, have a low profile and are easily fabricated using modern printed-circuit technology. They are, mechanically robust, compatible with MMIC designs, and their thin profile configurations enable conformability to mounting hosts [83]. According to the patch shape and mode selected, they are adaptable as far as resonant frequency, polarization, pattern, and impedance are concerned. Moreover, by adding loads between the patch and the ground plane (pins, varactor diodes, etc.), adaptive elements with shifting resonant frequency, impedance,

polarization, and pattern can be designed.[84]However, microstrip antennas also have some limitations including; low efficiency, narrow bandwidth and associated tolerance problems ,lower power handling capability, poor polarization purity , complex feed structures for high-performance arrays, extraneous radiation from feeds and junctions, excitation of surface waves etc. There are ways to minimize the effect of some of these limitations by certain structures and techniques as mentioned below.
The following drawing shows a patch antenna in its basic form: a flat plate over a ground plane (usually a Printed Circuit board).

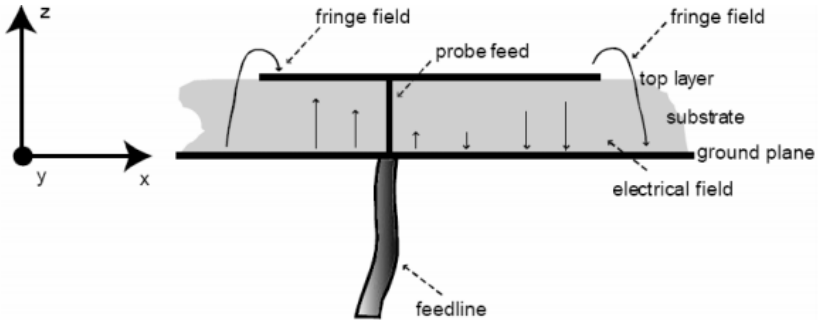

Figure 2.1. Basic form of patch antenna

The electric field is zero at the center of the patch, maximum (positive) at one side, and minimum (negative) on the opposite side. The minimum and maximum continuously change side according to the instantaneous phase of the applied signal. The electric field does not terminate brusquely at the patch's periphery as in a cavity; rather, the fields extend the outer periphery to some degree. These field extensions are referred as fringing fields and cause the patch to radiate. [85]
As shown in Fig.2, a microstrip antenna consists of a very thin radiating strip (patch) placed on one side of a dielectric substrate, with a ground plane on the other side. The patch is generally made of conducting material such as copper or gold and can take any possible shape. There are various substrates that can be used for the design of microstrip antennas, and their dielectric constants (ε_r) usually range between 2.2 and 12. The thicker a substrate is, the lower value ε_r has, so better efficiency and larger bandwidth are achieved on the downside of larger antenna size. [86]
The frequency of operation of the rectangular patch antenna of Figure 1 is determined by the length L. The center frequency will be approximately given by:

$$f_c = \frac{c}{2L\sqrt{\varepsilon_r}} = \frac{1}{2L\sqrt{\varepsilon_r \varepsilon_o \mu_o}} \qquad (2.1)$$

The above equation says that the microstrip antenna should have a length equal to one half of a wavelength within the dielectric (substrate) medium. Other parameters that will influence the resonant frequency:

· Ground plane size
· Metal (copper) thickness
· Patch (impedance) width

The width W of the microstrip antenna controls the input impedance. It is given by:

$$W = \frac{c}{2 f_r} \sqrt{\frac{2}{\varepsilon_r + 1}} \qquad (2.2)$$

Larger widths also can increase the bandwidth. By increasing the width, the impedance can be reduced. However, to decrease the input impedance to 50 Ohms often requires a very wide patch antenna, which takes up a lot of valuable space. The width further controls the radiation pattern.

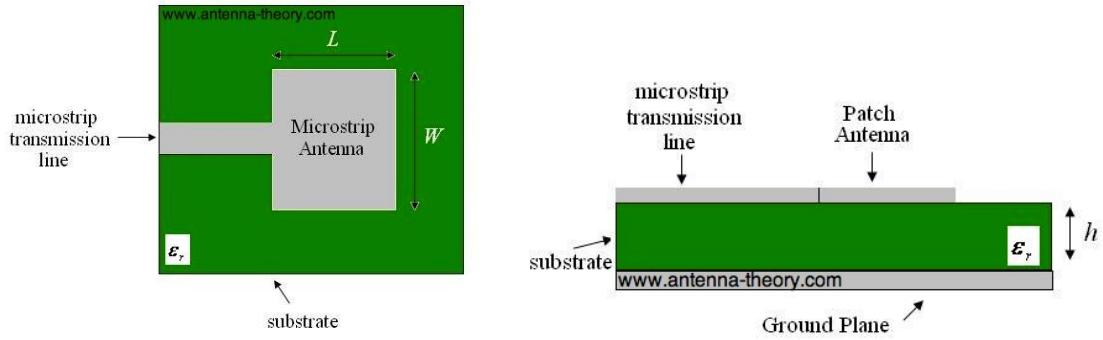

Figure 2.2.Geometry of Microstrip (Patch) Antenna.

The radiating patch may be square, rectangular, thin strip (dipole), circular, elliptical, triangular, or any other configuration, as illustrated in Figure 2. The first three are the most common because of ease of analysis and manufacture, and their desirable radiation characteristics, especially low cross-polarization radiation. Microstrip dipoles are preferred due to their inherent possession of a large bandwidth and less space occupation, which makes them attractive for arrays [82]. Linear and circular polarizations can be obtained with either single elements or arrays of microstrip antennas. Arrays of

microstrip elements, with single or multiple feeds, may also be used to introduce scanning capabilities and achieve greater directivities.

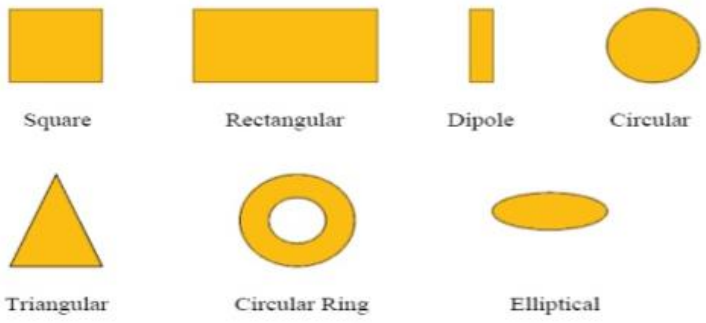

Figure 2.3.Common shapes of microstrip patch elements

Prominent feeding techniques of microstrip antennas are ; coaxial feed (probe coupling), microstrip line (coplanar feed) ,proximity-coupled feed, aperture –coupled feed and coplanar waveguide feed.[83]

2.2.2 Probe-Fed Shorted Patch or Planar Inverted F-Antenna (PIFA)

In order to improve antenna's performance ,designers introduced in patch antenna design shorting pins (from the patch to the ground plane) at various locations, which led into the Planar Inverted-F Antenna (PIFA). The Planar Inverted-F Antenna is popular, and is widely used in wireless communication because it has a low profile and an omnidirectional pattern. Owing to the fact that the patch is shorted at the end, the current at the end of the patch antenna is no longer forced to be zero. Subsequently, this antenna actually has the same current-voltage distribution as a half-wave patch antenna (resonant at a quarter-wavelength). However, the fringing fields which are responsible for radiation are shorted on the far end, so only the fields nearest the transmission line radiate. Consequently, the antenna gain is reduced, but the patch antenna maintains the same basic properties as a half-wavelength patch, but is reduced in size 50%.

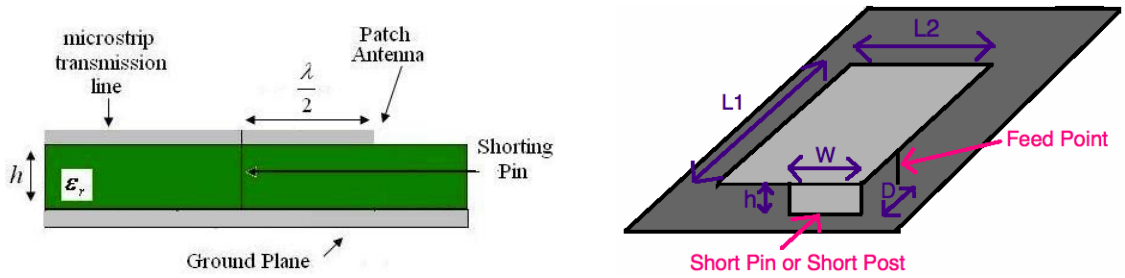

Figure 2.4.The Planar Inverted-F Antenna (PIFA).

The impedance of the PIFA can be controlled via the distance of the feed to the short pin (D). The closer the feed is to the shorting pin, the impedance will decrease; the impedance can be increased by moving it farther from the short edge. In addition, the shorting pin can become capacitive if instead of extending all the way to the ground plane, it is left floating a small amount above. This introduces another design parameter to optimize performance.

2.2.3 Literature Review of Antenna Designs

In literature, most of the antennas for biomedical telemetry applications have been designed by embracing the stacked planar inverted-F antenna (PIFA) structure in order to achieve better size reduction and bandwidth enhancement. Many of the proposed antennas include the rectangle stacked PIFA [87] [88]the spiral PIFAs [89] , the spherical stacked PIFA [90], and the meandered PIFA [91][92] etc. Nevertheless, among these antennas, even though the antenna reported in [93] has the most compact size with only volume 26.4 mm^3 (11 mm×8 mm×0.3 mm) and that presented in [94] is as small as $\pi \times 4^2 \times 0.65 \simeq 32.7\, mm^3$, the two antennas are still suffering from inherent detuning effects and subsequent low return loss or can only provide a narrow bandwidth to become a dominant block to the fabrication of both implantable and ingestible medical devices.

Multi-layered stacked design has proven to be advantageous to reducing the radiator's size. Multi-layer structures including vertically stacked radiating patches increase the length of the current flow and further contribute to miniaturization. Multilayer structure also presents a simple realization process that assures both better directivity and efficiency comparing to other typologies mentioned in literature. These radiators have a

wide bandwidth behavior because of the strong interaction of the EM near field terms with the human tissues.

In the article [95] (2015), a new compact three-layer stacked PIFA antenna was proposed for use in the biotelemetry communication when operating at the 402 - 405 MHz frequency band. The proposed antenna is a modification of Planar Inverted-F Antenna (PIFA), consisting of \ ground, lower patch, and upper patch. The design has an overall size of only $\pi \times 4.5^2 \times 1.27\, mm^3$, which reaches a size reduction of 57.5%, comparing with the reported work in [88].With a spiral structure etched on the patch surface and with the insertion of a shorting pin between the two lower patches ,not only reduction in antenna size but also good resonant performance was obtained.

The design proposed in [96] (2016) has an overall size of 2 cm x 1 cm x 3.81 mm^3.The skill of meandering the radiating patches was applied to lengthen the effective current path and thus achieving wider bandwidth and more compact size than those reported in [90], [97] making this antenna more suitable for implantable biometry devices.

As the antenna dimensions shrink, the effect of fabrication issues becomes even more critical. Other reported stacked PIFAs occupy miniaturized volumes of 762 [96] (2016), 416 [98] (2012), 273.6 [99] (2011), 110.4 [92] (2011) etc. A detailed table of the majority of the literature from the recent years is presented as follows.

Table 2.1 Various antennas reported in the literature.

Ref	Year	Substrate Shape	Application	Implantation tissue	Vol [mm^3]	Frequency Band [MHz]	Miniaturization techniques			
							Dielectric material	Patch Shape	Shorting pin	Patch Stacking
[91]	2016	square	Biomedical telemetry	Skin-fat-muscle	67.5	402-405	Silicon wafer	meandered	-	-
[96]	2016	Rectangular	Biomedical telemetry	Skin Tissue	762	402-405 2400-2480	Rogers 3210	meandered	YES	YES
[90]	2015	cylindrical	Leadless Pacemaker	heart	1440.1	402-405	polyamide	spiral	-	-
[100]	2015	square	Biomedical Telemetry	Skin Tissue	200	402-405	LTCC	spiral	YES	-
[93]	2015	Rectangular	scalp implantable Biotelemetry	Skin Tissue	26.4	402-405	Rogers RT/duroid 6010	serpentine	YES	-
[101]	2015	Rectangular	Wireless Biotelemetry	2/3 Human Muscle	461.25	402-405	FR-4	meandered	YES	-
[95]	2015	Cylindrical	Biomedical telemetry	Skin-fat-muscle	80.75	402-205	Rogers 3210	circular	YES	YES
[97]	2014	Rectangular	Breast Implanation	Skin-fat Tissue	1950.7	402-405	Rogers 4350	spiral	YES	-
[89]	2014	circular	Intraocular transceiver	Vitreous Humor	334.4	402-405	Rogers RO3010	spiral	-	-
[102]	2013	Rectangular	Biomedical telemetry	Skin Tissue	366	402-405 2400-2480	Rogers RO3210	Spiral	-	-
[98]	2012	Rectangular	Implantable biomedical telemetry	2/3 Human Muscle	416	402-405	LTCC	meandered	YES	YES
[94]	2011	Circular	Head implantation	Skin Tissue	32.7	402-405	Alumina	meandered	YES	YES
[103]	2012	Rectangular	Biomedical telemetry	Skin-fat-muscle	188.4	1350-1710	Roger 5880	meandered	YES	-
[92]	2011	Circular	Skin implantation	Skin Tissue	110.4	402-405	Rogers 3210	meandered	YES	YES
[99]	2011	Square	Retinal prosthesis	Vitreous humor	273.6	402-405	Rogers 3210	Spiral	YES	YES
[104]	2010	Square	Implantable biomedical telemetry	Skin Tissue	1375.4	402-405 2400-2480	ARLON 1000	SRR coupled Spiral	YES	-
[88]	2008	Square	Biotelemetry	Skin Tissue	190	402-405	Rogers RO3210	Rectangular spiral	YES	YES

2.3 Bandwidth enhancement

In order to optimize the narrow bandwidth (BW) of the MPA (Microstrip Patch Antennas), which can be as low as 1% [105], different techniques have been proposed. Some of these techniques are cited below.

2.3.1 Substrate Effect on Bandwidth

The most straightforward way to improve the MPA bandwidth is to increase the patch-ground plane separation by using a thicker substrate [106]. Thus, given the mathematical form: $BW = \frac{VSWR - 1}{Q\sqrt{VSWR}}$, where Q is the quality factor of the antenna $Q = \frac{Energy\_stored}{Power\_lost}$ it is easy to conclude that BW will increase monotonically with thickness. Another important substrate parameter that influences the bandwidth is the permittivity. The bandwidth of a patch antenna increases with decreasing substrate permittivity. By using low dielectric constant and thick substrate ($h/\lambda o > 0.1$), the bandwidth can be reached 10%. (Fig.5) [107]

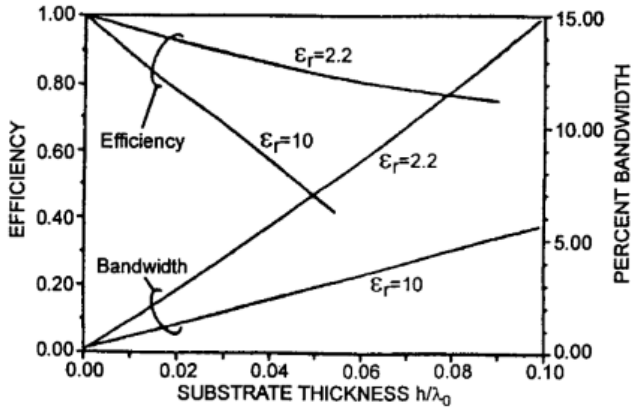

Figure 2.5.Effect of substrate thickness and dielectric constant on the impedance bandwidth (VSWR) and radiation efficiency

Unfortunately, the thick substrate except from an certain increase in the volume of the antenna, will support surface wave modes that will increase mutual coupling in antenna arrays [85]. Mutual coupling will result in serious degradations in impedance mismatch, large radiation loss, polarization distortion and scan blindness in phased array antennas [108].

2.3.2 Slotting Patch antennas

Considering the fact that smaller area is preferable, the technique of modifying the topology of patches is most attracted. The basic idea is to introduce slots into a common patch, bringing new resonant frequencies and resulting in the enhancement of bandwidth. Slotting is most commonly used for bandwidth, gain improvement, broadband operation, and size reduction. The basic concept of this technique is the lengthening of the current flow path on the patch surface, by cutting slots in the patch [109]. Slots are suitably embedded in the printed patch along the radiating edges of a patch. Their dimensions and positions are properly selected in order to the first two broadside-radiation modes of the patch be perturbed such that their resonance frequencies get close to each other to form a wide impedance bandwidth[110][111]. The slots may be rectangular, square, circular, triangular, U shaped, H shaped, E shaped, diamond shaped [112]. Typical examples are the U-shaped slots and the Parallel Dual Slots (also called E-shaped patches)

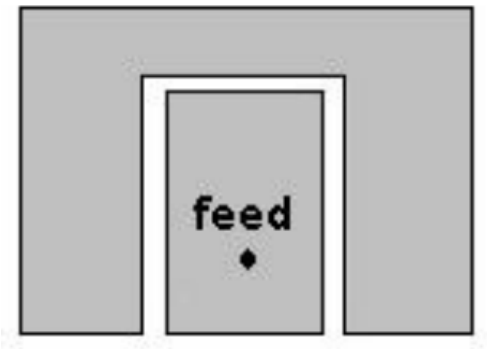

Figure 2.6. u-slot in rectangular patch [113]

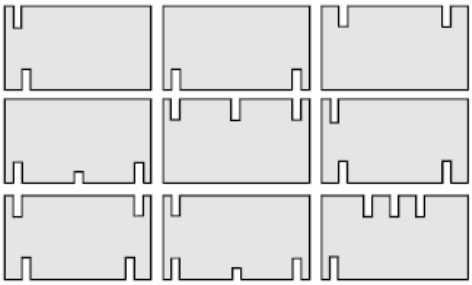

Figure 2.7.Different number of slots with different positions to optimize the best bandwidth [113]

2.3.3 Broadbanding using parasitic techniques

Another way to improve the bandwidth of an MPA is to create several resonant structures into one antenna by adding more layers, more patches or more extra components (shorting pins, additional strips etc.)

There are two configurations of the parasitic geometry: the coplanar geometry and the stacked geometry. The coplanar geometry consists of many patches incorporated coplanar on the dielectric substrate and they are coupled to the main patch (only one patch has been excited). For a Microstrip antenna edges along the width and length are known as radiating and non-radiating edged respectively. When parasitic patches are

placed close to the active patch, resonance occurs in them due to the perturbation and electromagnetic coupling. (Multiresonator MPA) [113]. If the resonances of the both patch are close to each other broad bandwidth is achieved. The parasitic
patches are used in various combinations.

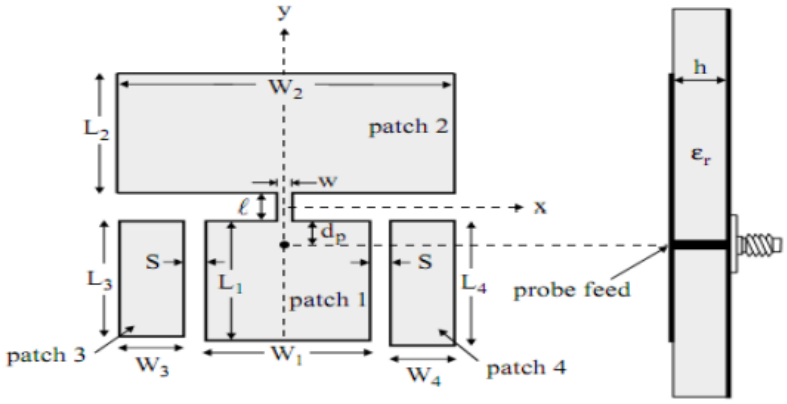

Figure 2.8.Geometry of multi-resonator patch antenna [114]

For stacked geometry, the patch radiators are employed one above the other with intervening dielectric layers. In this multiple-layer, resonance occurs in the patches due to either aperture or electromagnetic coupling. (Multilayer broadband MSA).

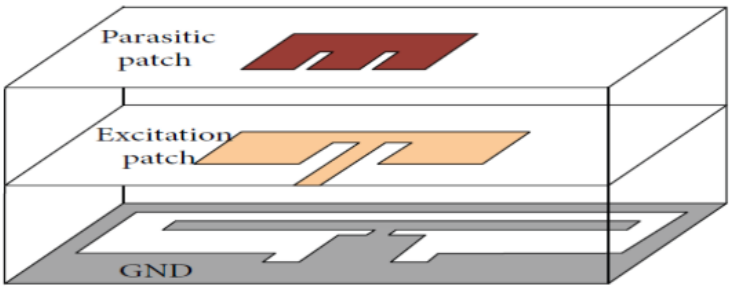

Figure 2.9.Geometry of stacked patch antenna [115]

The stacked patch configuration has the following advantages:
•It does not increase the surface area of the element
•It can be used in array configurations without the danger of creating grating lobes. Its radiation patterns remain relatively constant over the operating frequency band
The drawbacks of stacked patch configuration are:
•It has a large number of parameters which make the design and optimization process is very complex

•It requires >1 substrate layer to support the patches**,** so the overall height of the antenna is increased. [116]

Note that other parameters, such as feeding techniques and patch shapes also affect the broadbanding of MPAs.[107]

2.4 Biological Tissues Properties

Both implantable and ingestible antennas are required to operate within a complex biological environment that the human body is, and this feature significantly differentiates the design of the antennas, which are not intended to operate in free space. Commonly reported issues include antenna detuning (shift of the resonance frequency and change in the input impedance of the antenna), distortion of the radiation pattern, and degradation of the radiation efficiency [117].In such cases, one or more characteristics of the antenna can be changed to such degree that the original design specifications and demands are no longer met. Hence, the analysis of complex biological environment in advance, is crucial, in order to evaluate all those parameters that will lead to a correct design giving the antenna the desired characteristics.

2.4.1 Electrical Properties of Human Tissue

The medium in which the antenna is radiating influences the performance of the antenna. Therefore, when the antenna is inserted into human skin (tissue), the radiation field and the impedance of the antenna will change according to the electrical properties of the tissue and the implementation of the antenna. When we place the antenna inside the tissue, we are radiating in a high permittivity and conductivity media. The effect of the material on the antenna radiation depends on the dielectric constant or the complex permittivity of the material.

The permittivity ε, permeability μ and conductivity σ of a linear, homogeneous and isotropic medium are in general complex quantities

$$\varepsilon = \varepsilon_o (\varepsilon'_r - j\varepsilon''_r) \qquad (2.1)$$

$$\mu = \mu_o (\mu'_r - j\mu''_r) \qquad (2.2)$$

$\sigma = \sigma' - j\sigma''$ (2.3)

where ε_o and μ_o are the permittivity and permeability of vacuum, respectively.

The imaginary terms ε''_r and μ''_r account for the losses due to the damping of the vibrating dipole moments (electric and magnetic) and to the time lag responses of the medium [118]. The human body does not have any particular magnetic properties (μ'_r = 1, μ''_r =0).Therefore focusing on (2.1) and (2.3), we can define the real relative effective permittivity ε'_e and conductivity σ'_e as:

$$\varepsilon'_e = \varepsilon'_r - \frac{\sigma''}{\omega\varepsilon_o} \quad (2.4)$$

$\sigma'_e = \sigma' + \omega\varepsilon_o\varepsilon''_r$ (2.5) , where ω= 2πf , frequency dependency

Adjusting the previous expressions into Maxwell's equations one can define the complex effective permittivity as:

$$\varepsilon'_e = (\varepsilon'_e - j\varepsilon''_e) = \varepsilon_o(\varepsilon'_e - j\frac{\sigma''}{\omega\varepsilon_o}) \quad (2.6)$$

The EM power dissipation in a medium is often indicated by the loss tangent;

$$\tan\delta = \frac{\sigma'_e}{\omega\varepsilon_o\varepsilon'_e} \quad (2.7)$$

Dielectric properties of the biological tissues are taken from the innovative work of Gabriel [119] via the mathematical form:

$$\varepsilon(\omega) = \varepsilon_\infty + \sum_{m=1}^{4}\frac{\Delta\varepsilon_m}{(j\omega\tau_m)^{1-a_m}} + \frac{\sigma_j}{j\omega\varepsilon_o}$$

where, ε_∞ is the permittivity in the terahertz frequency range, σ_j is the ionic conductivity, τ_m for each dispersion region is the relaxation time , a_m, ε_m tissue parameters

Table 2.2. ***Dielectric Properties of Different Body Tissues at 404.5 MHz (MedRadio Band)***

Body Tissue	ε'_e	σ [S/m]	tanδ
Muscle	57.09	0.797	0.621
Fat	5.58	0.041	0.328
Skin (dry)	46.71	0.689	0.658
Head	43.5	0.87	0.799
Small intestine	66.02	1.905	1.282
Colon	62.51	0.86	0.611
Esophagus	*67.45*	1.004	0.662

Table 2.3. ***Dielectric Properties of Dfferent Body Tissues at 2.4 GHz (ISM)***

Body Tissue	ε'_e	σ [S/m]	tanδ
Muscle	52.729	1.739	0.242
Fat	5.28	0.105	0.145
Skin (dry)	38.007	1.464	0.283
Head	39.2	1.80	0.337
Small intestine	54.425	3.173	0.428
Colon	53.879	2.038	0.277
Esophagus	62.158	2.211	0.261

It can be seen that both the dielectric constant and conductivity of biological tissues depend significantly on the type of tissue and the frequency of the electromagnetic wave.

2.5 Numerical Investigation

2.5.1 Tissue Models & Body Phantoms for Medical Analysis

In numerical simulations, implantable and ingestible antennas are analyzed inside inhomogeneous lossy media that simulate biological tissues. Biological tissues have their own permittivity (ε'_e), conductivity (σ), and mass-density values. Canonical tissue models are often used to reduce the simulation time, and to use analytical formulae. Moreover, they provide standard and easy to realize conditions for the radiator measurements. These may be either a single-layer, thus accounting for a generic tissue

antenna, or multilayer, thus providing a simplified model of a specific implantation site inside the human body. Examples of canonical tissue models, used in the literature, for the simulation of ingestible and implantable antennas are shown below:

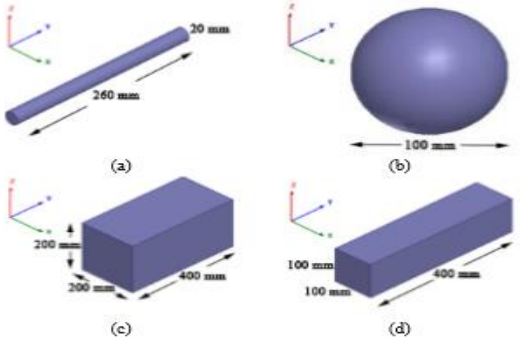

Figure 2.10.i The proposed canonical models for an ingestible serpentine antenna.(a) Esophagus, (b) Stomach, (c) Small Intestine, and (d) Large Intestine.[120]

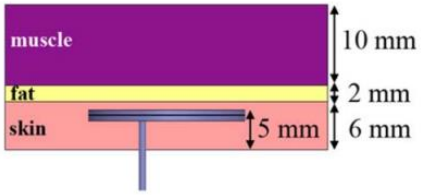

Figure2.10.ii)A three-layer (skin/fat/muscle) canonical tissue model for an implantable patch antenna [121].

To obtain more realistic results, anatomical tissue models (e.g., Fig.11[122]), produced by the combination of magnetic-resonance imaging (MRI) or computer tomography (CT) data with the electrical properties of human body tissues, can also be applied. The modeling of the human body or parts of it, is made using cubic boxes (voxels) homogeneously containing the dielectric properties of the tissue. Just like the pixels of a digital image contain the necessary information, voxels integrate the equivalent data regarding the electrical properties of the biological tissue. The smaller the size of the voxel is, the closer to the actual characteristics of the body the anatomical model is. Typical examples of anatomical models are "Visible Human Project", "Virtual Family", and "Virtual Classroom". These phantoms describe precisely the human body geometry while taking under consideration the parameters of different body constitutions (according to age and gender). Anatomical tissue models used in the literature for simulation of implantable patch antennas are shown in Table 4 [123][124].

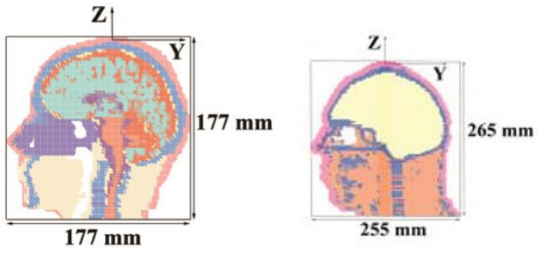

Figure 2.11.Anatomical human head tissue models [122][125].

Anatomical Tissue Model		
Body Part	**# of Tissues**	**Max Dimensions [mm]**
chest	30	286 × 320 × 584
shoulder	31	180 × 190 × 390
head	13	160 ×177 × 177
	30	200 × 256 × 280
head with shoulders	30	288 × 400 × 620

Table 2.4.Anatomical tissue models used in the literature for analysis of implantable patch antennas.

Regarding the antenna design, we should note that multilayer canonical models have been proven to provide an acceptable model for the human body. Highly alike return-loss characteristics have been observed for antennas inside a three-layer planar geometry and a realistic model of the human chest, as well as inside a three-layer spherical and an anatomical model of the human head [122].

Finally, physical phantoms have been used for testing the antennas' performance and evaluating the effects of radiation on tissues. As in numerical models, they can be distinguished in canonical and more complex phantoms. The geometric characteristics range from simple spherical, cylindrical and rectangular containers containing liquid or semi-solid (gel) mixtures with stable properties, to more complex shapes (headforms, limbs, etc.) [126] .Note, that the intended implantation site determines the types and structure of the tissues surrounding the antenna, and, therefore, its dielectric loading. For example, skin-implantable antennas might operate in a different way while implanted within the skin-tissue of different parts of the body.[127] Canonically-shaped phantoms have so far been used for testing of implantable patch antennas (e.g., Figure 12a,b). In this case, the main challenge lies in the formulation and characterization of tissue-emulating materials. Example phantoms reported in the literature are being presented

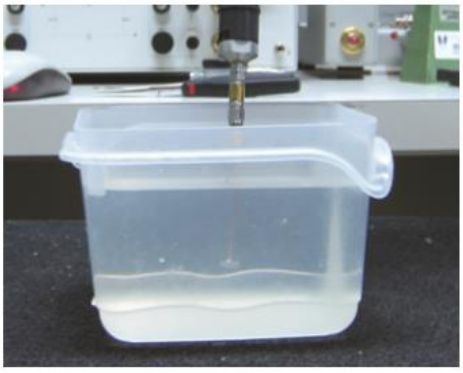

Figure 2.12 A liquid canonical phantom used phantom for testing of implantable patch antennas.[122]

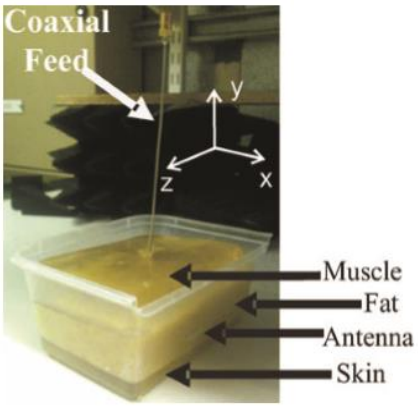

Figure 2.13 A multilayer gel canonical used for testing of implantable patch antennas

2.5.2 Numerical Methods & HFSS Simulation Software

Analytical methods can only be applied for analyzing the performance of simplified antennas positioned inside canonical tissue models. The electromagnetic field solvers that are most commonly used in the literature for implantable and ingestible antenna design are based on the Finite-Element Method (FEM) (e.g., Ansoft HFSS) [128][129]. The Finite-Difference Time-Domain (FDTD) Method is also applied in some studies, because

it exhibits simplicity in the implementation of inhomogeneous media and assessment of bio-electromagnetic interactions, while enabling efficient modeling of detailed anatomical human body parts.

FEM

The finite element method is a numerical procedure for obtaining solutions to boundary-value problems. The principle of the method is to replace an entire continuous domain by a number of subdomains in which the unknown function is represented by simple interpolation functions with unknown coefficients. Thus, the original boundary-value problem with an infinite number of degrees of freedom is converted into a problem with a finite number of degrees of freedom, or in other words, the solution of the whole system is approximated by a finite number of unknown coefficients. Therefore, a finite element analysis of a boundary-value problem should include the following basic steps:

1. Discretization or subdivision of the domain
2. Selection of the interpolation functions (to provide an approximation of the unknown solution within an element)
3. Formulation of the system of equations (also the major step in FEM. The typical Ritz variational and Galerkin methods can be used.)
4. Solution of the system of equations. (Once we have solved the system of equations, we can then compute the desired parameters and display the result in form of curves, plots, or color pictures

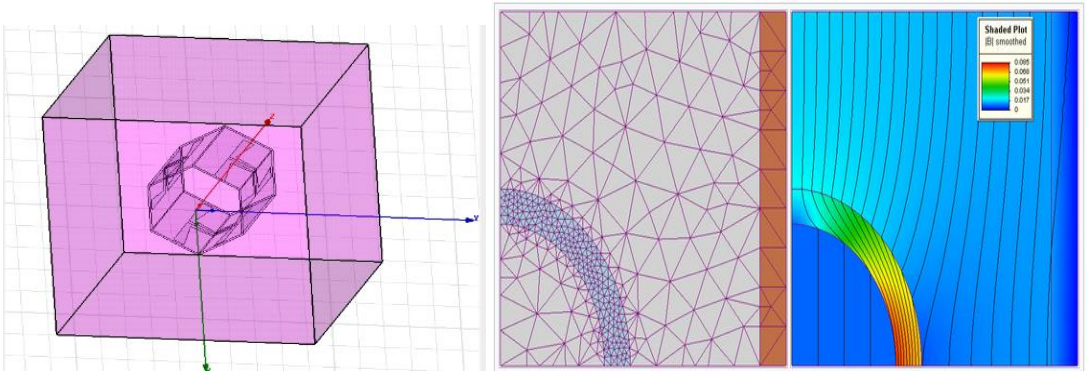

Figure 2.14. FEM mesh created in an HFSS geometry

FE numerical simulations are carried out in this study using the software HFSS .The FE solver of HFSS performs iterative tetrahedron-meshing refinement automatically with the mesh being perturbed by 30% between each pass. The mesh refinement procedure has been set to stop when the maximum change in the reflection coefficient magnitude (|S11|) between two consecutive passes is less than 0.02, or when the number of passes exceeds

10. The solver performs usually a 400 point-frequency sweep by ±100MHz around the center frequency of MedRadio Band (404.5 MHz). Radiation boundaries are set $\lambda_0/4$ (λ_0 is the free space wavelength, f_0 = 404.5 MHz) away from all simulation set-ups to extend radiation infinitely far into space and guarantee stability of the numerical simulations [130].

2.6 HFSS Software Package -(High Frequency Structure Simulator)

HFSS is a high-performance full-wave electromagnetic(EM) field simulator for arbitrary 3D volumetric passive device modeling that takes advantage of the familiar Microsoft Windows graphical user interface. It integrates simulation, visualization, solid modeling, and automation. Ansoft HFSS, whose basic mesh element is a tetrahedron, employs the Finite Element Method (FEM) and adaptive meshing to calculate parameters such as S-Parameters, Resonant Frequency, and Fields.

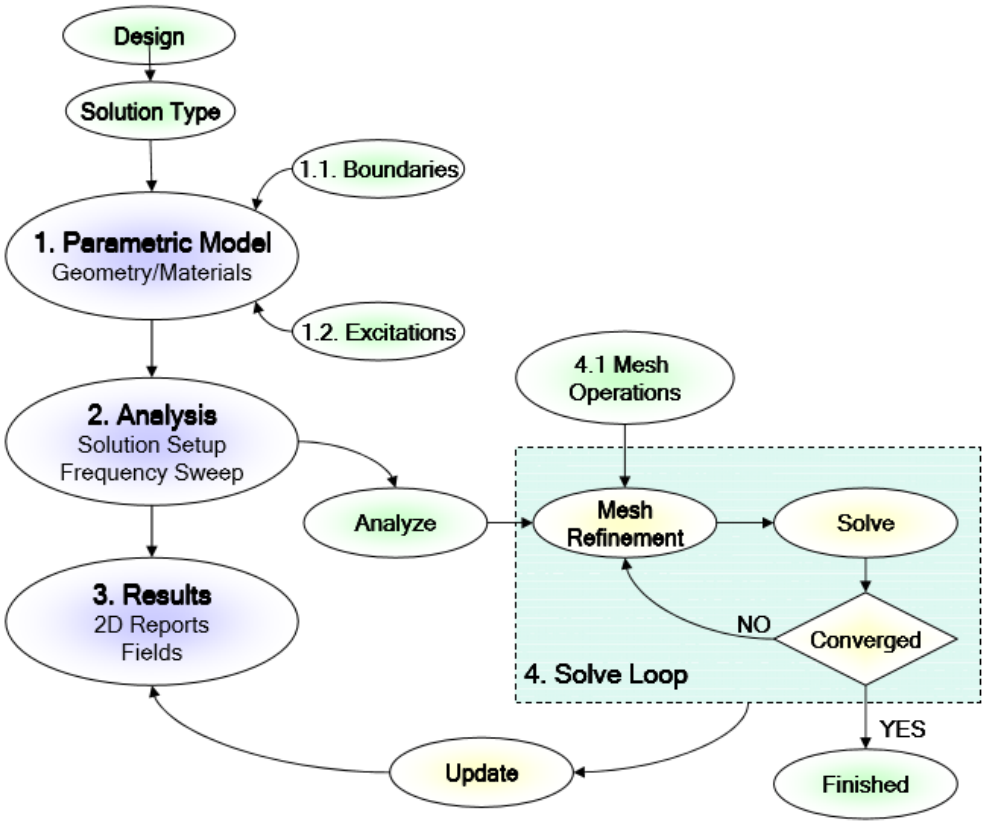

Figure 2.15.Schematic diagram of the antenna design procedure. [131

2.6.1 Antenna Simulation Steps

The following summarizes the input necessary for antenna calculations:

• Selecting the Solution Type.*[1.Driven Mode (preff.) 2.Driven Terminal 3.Eigenmode]*

• Setting Units of Measurement for the Model

• Assigning Materials

• Assigning HFSS-IE Boundaries

• Define structure (*microstrip antenna, define layers, patches, ground, feeding etc.)*

• Assigning Waveport *(Definition of excitation ports)*

•Define radiation Box

• Analysis Setup (*i.e. setting frequency range, solution frequency, Maximum Number of Passes is Adding Frequency Sweep etc.)*

•Start simulation *(Simulation will stop as soon as the results converge)*

•Analyze results (*i.e. create reports of S Parameters, input impedance, Gain, etc.)*

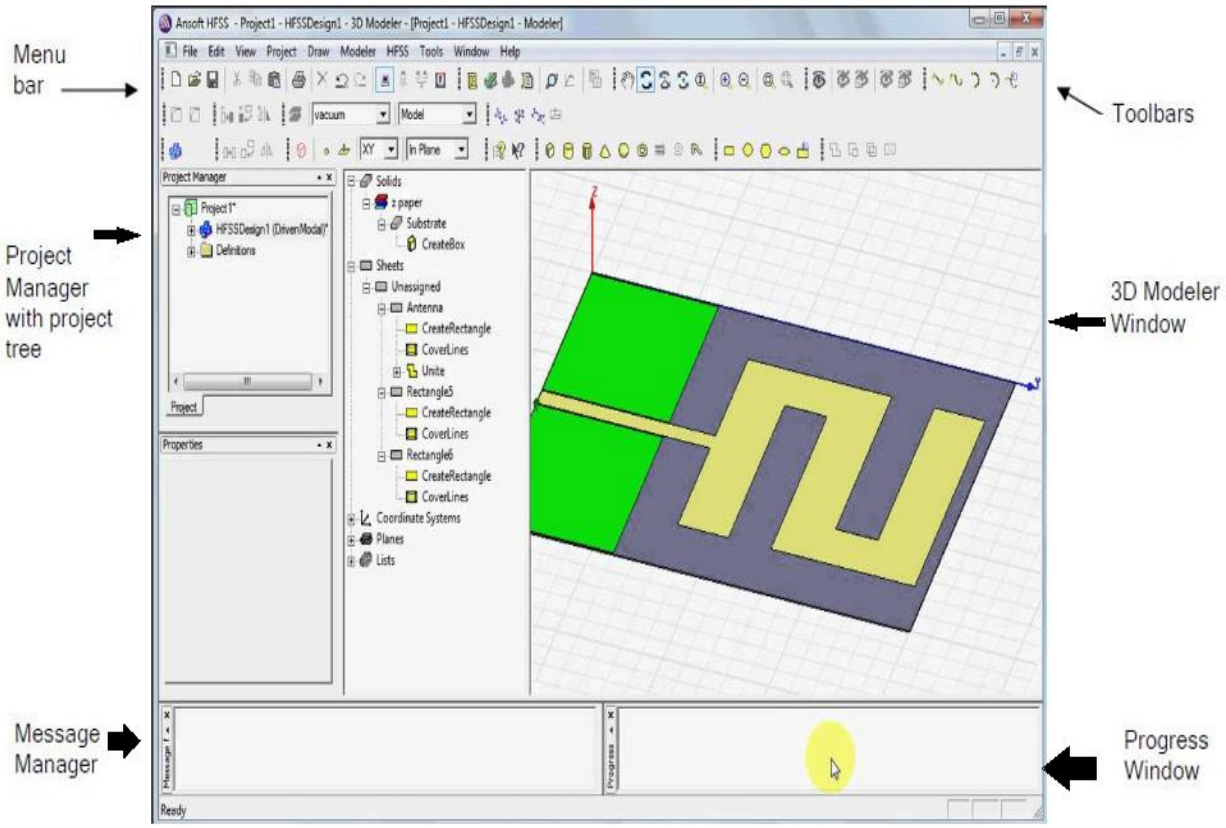

Figure 2.16.Typical Ansoft HFSS software environment

Chapter 3

Performance study of a dual band implantable antenna

In this chapter, a miniature dual band antenna, that can been found in literature [132], for applications in Implantable Wireless Communications Systems is being studied and redesigned according to the configurations given, and simulated in Ansoft HFSS Software in order to verify and compare their return-loss characteristics as well as their performance to the ones shown in [132].The antenna is located inside three different canonical models; muscle, head and three-layer model (muscle, fat, skin) and parameters such as return loss, gain, input impedance etc. are examined. Later on, the antenna is optimized and the results that have emerged are being evaluated.

3.1 Antenna Design

According to [132], a multilayer design was designed for implantable medical device inside the human body .This typology was preferred over the spherical spiral and meander topologies. The spherical case suffered from more accentuated omnidirectional radiation and consequently lower directivity without any significant efficiency. The meander and spiral topologies were both declined, despite the notable increase in radiation efficiency and directivity of the latter [133][134][135], due to excessive space needed for their metallizations, which reached over the battery-housing region. This very short distance between the ground plane of the antenna and the metallizations does not facilitate the radiation. On the contrary, the multilayer spiral design accomplishes the desired resonance and provides the most performing typology in terms of directivity and efficiency; therefore this arrangement was selected for the making of the design.

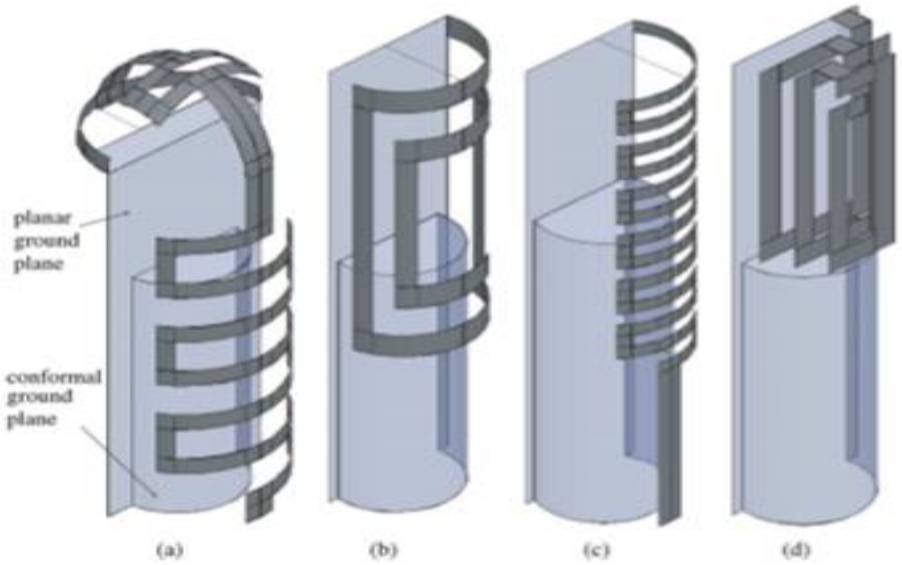

Figure 3.1.First investigated typologies in free space: (a)spherical, (b)spiral, (c)meander and (d) multilayered. The ground plane (in light color), consists of a rectangular section and a conformal part (half hollow cylinder). Delta-gap excitations are indicated with dashed lines.

The radiator works in both the Medical Device Radiocommunication Service (MedRadio, 401-406 MHz) and the Industrial Scientific and Medical (ISM, 2.4-2.5 GHz) bands. The dual band capability is obtained with the transceiver produced by Zarlink Semiconductors [136].Via this component, the power consumption is minimized as the sensor can be awaken from sleeping state by receiving a signal in the 2.4-2.5 GHz band. Hence, data are transmitted only in the MedRadio band.

A dense packaging is required to reduce the implant volume, so that a single antenna feeding point is selected in order to reduce the assembly complexity. The structure is made of four stacked dielectric substrates in pyramidal arrangement. The material chosen is Roger TMM 10 (alumina) with 35μm copper metallization due to its high relative dielectric constant (ε'_r=9.2), and low loss (tanδ=0.0022). As depicted in chapter 1, this high-permittivity material was used, as it results in lower resonance frequencies, thus assisting in antenna miniaturization. The pyramidal structure is united with the conformal ground plane - a half hollow cylinder as presented in Fig.3.2.

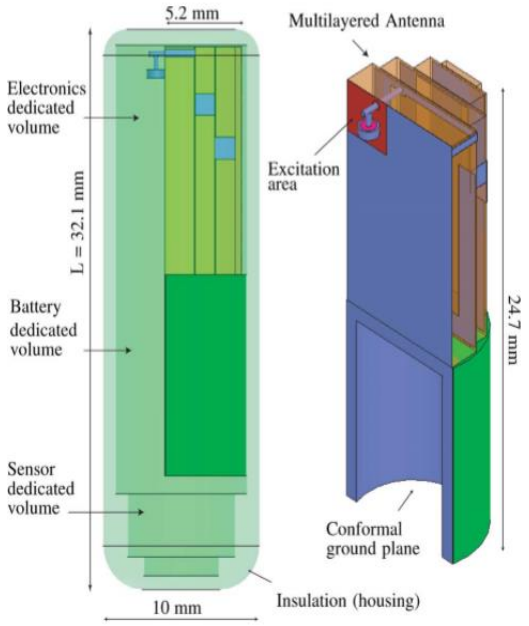

Figure 3.2. Design of the proposed prototype.

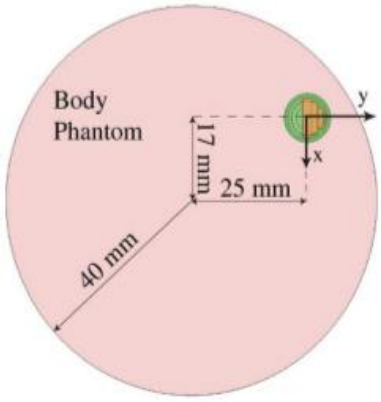

Figure 3.3. Antenna off-centered placement in the cylindrical homogenous phantom.

The antenna was encapsulated with a biocompatible material to evade adverse tissue reaction [137],short – circuiting effects deriving from the highly conductive human tissues and to overall enhance the antenna's performance. The material used for both the conformal ground plane and the biocompatible insulation was PEEK (Polyetheretherketones, ε'_r =3,2 , tanδ=0.01) ,mainly due to its practical qualities, since it is flexible, durable and strong in nature, it does not harm body or skin and is easy to manufacture and metallize. The thickness of the insulation was set to 0.8mm, while the volume of the entire implant (i.e., the antenna, insulation, electronics, batteries and biosensors) must fit in a cylindrical housing of an external diameter of 10mm and 32.1mm height .Overall volume of the implant is $\pi \times 5^2 \times 32.1\, mm^3$ .To mimic the targeted subcutaneous implantation, the antenna is then placed off-centered in the cylindrical body phantom of radius 40mm and height 110mm, respectively(Fig.3).

Typology	Res. Freq. [GHz]	Gain [dBi]	Directivity [dBi]	Rad. Eff. [%]
Spherical	1.035	-7.6	1.2	13.182
Spiral	1.029	-3.8	1.8	27.542
Meander	1.038	-7.9	1.3	12.022
Multilayered	1.058	-1.8	1.8	43.651

Table 3.1.Comparison of the radiation performances for four antenna typologies in free space.

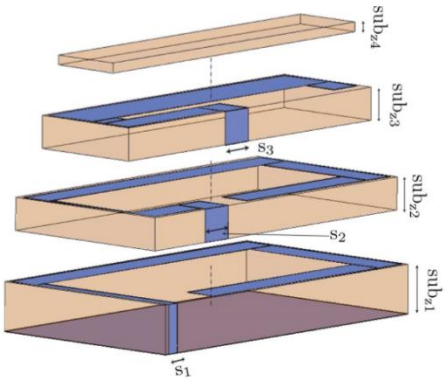

Figure 3.4.Assembling of the 4 ROGER TMM substrates to create a pyramidal structure.

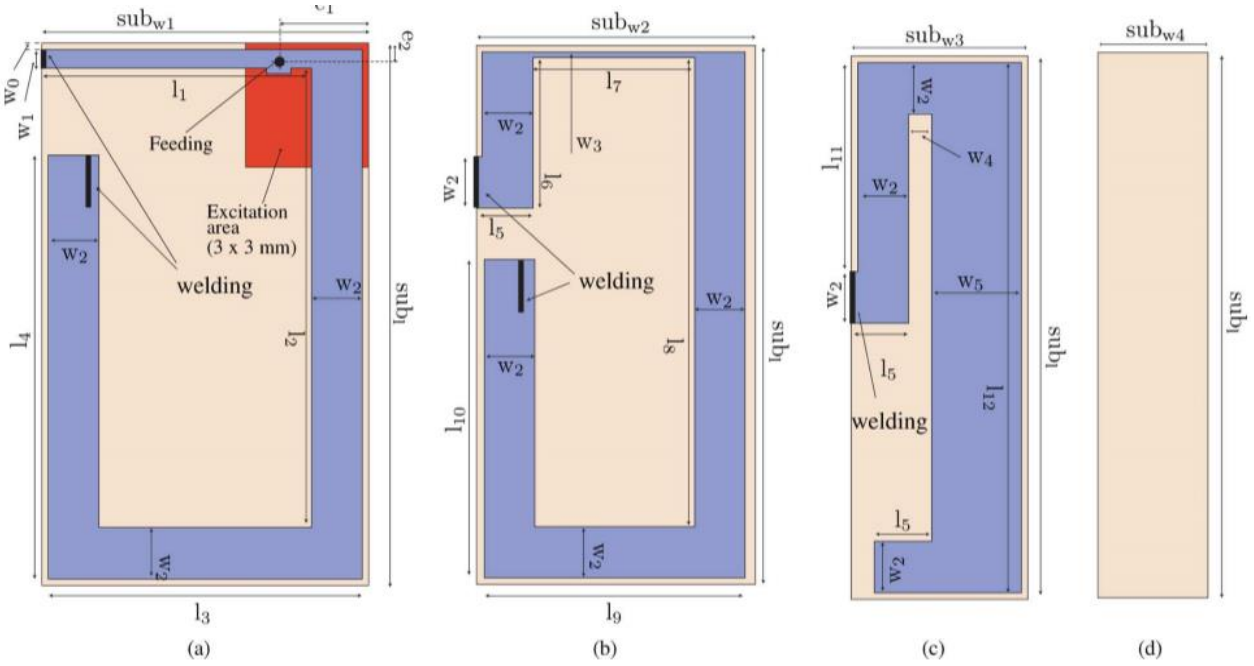

Figure 3.5.Top view of Roger TMM substrates: (a) first (double layer) with the excitation area, (b) second (single layer), (c) third (single layer) and (d) fourth (no metallization).Thick black lines indicate where the welding (with the vertical metallizations) occurs.

Table 3.2.Values of the design parameters indicated in Figs. 4,5

Parameter	Value [mm]	Parameter	Value [mm]	Parameter	Value [mm]	Parameter	Value [mm]
subw1	8.000	**l4**	10.250	**w0**	0.150	**e1**	2.200
subw2	6.900	**l5**	1.400	**w1**	0.450	**e2**	0.450
subw3	4.300	**l6**	3.650	**w2**	1.250	**s1**	0.450
subw4	2.700	**l7**	4.000	**w3**	0.150	**s2,3**	1.250
subz1	1.905	**l8**	11.400	**w4**	0.550	**rp**	5.000
subz2	1.270	**l9**	6.450	**w5**	2.200	**rg**	3.500
subz3	1.270	**l10**	7.750	**l1**	6.6.17	**Pk**	0.800
subz4	0.381	**l11**	5.050	**l2**	11.100	**hg**	10.750
sub1	13.100	**l12**	12.800	**l3**	7.700	**Wd**	1.000

The very first simulation realized, was the one where the antenna was simulated in free space without any biocompatible insulation. That simulation was made in order to observe where the multilayer spiral antenna resonates. The results agree with the reported performances of Table 1.

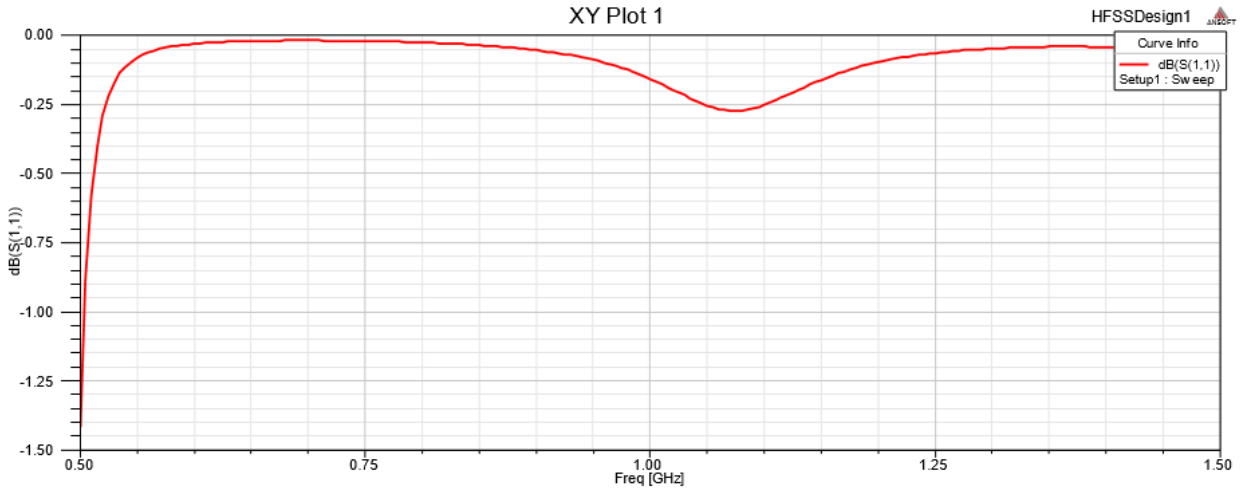

Figure 3.6 .Simulated S_{11} against frequency. Antenna in free space.

The single resonant frequency is around 1GHZ (1.058 GHz) for the multilayer typology. The dielectric loading effect, due to the presence of dielectric substrates, bio-compatible insulation and body phantom will consequently shift the resonant frequency towards lower frequencies, close to the MedRadio band.

3.2 Antenna design in the MedRadio band

3.2.1 Antenna inside the muscle model

Given the dimensions of substrates and metallizations presented in Table 2, the antenna is re-designed using the HFSS Ansoft Software environment. (Fig.7). Then, the structure is placed inside a canonical model imitating the dielectric properties of a human muscle. (ε'_r = 57.09, tanδ=0.621) (Fig.8).

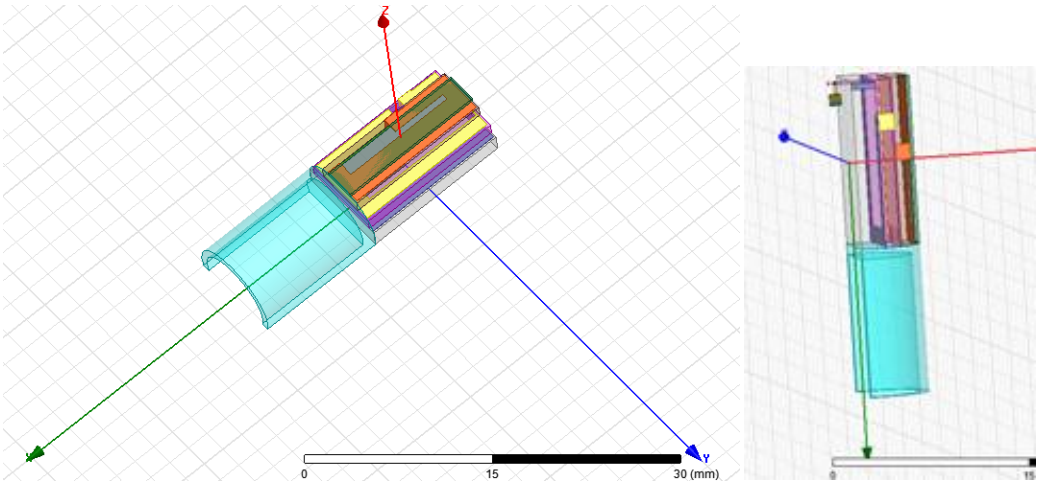

Figure 3.7.Top view and side view of the antenna designed in the HFSS environment .

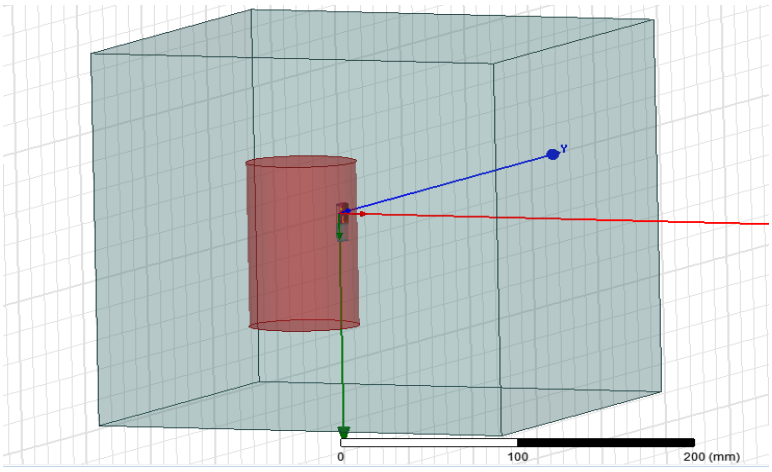

Figure 3.8.Antenna placed inside the cylindrical muscle phantom .

The FE solver of HFSS performs iterative tetrahedron-meshing refinement automatically with the mesh being perturbed by 30% between each pass. The mesh refinement procedure has been set to stop when the maximum change in the reflection coefficient magnitude ($|S_{11}|$) between two consecutive passes is less than 0.02, or when the number of passes exceeds 10. The solver performs a 400 point-frequency sweep by $\pm$100MHz around the center frequency of MedRadio band (401-406 MHz). The results are presented below.

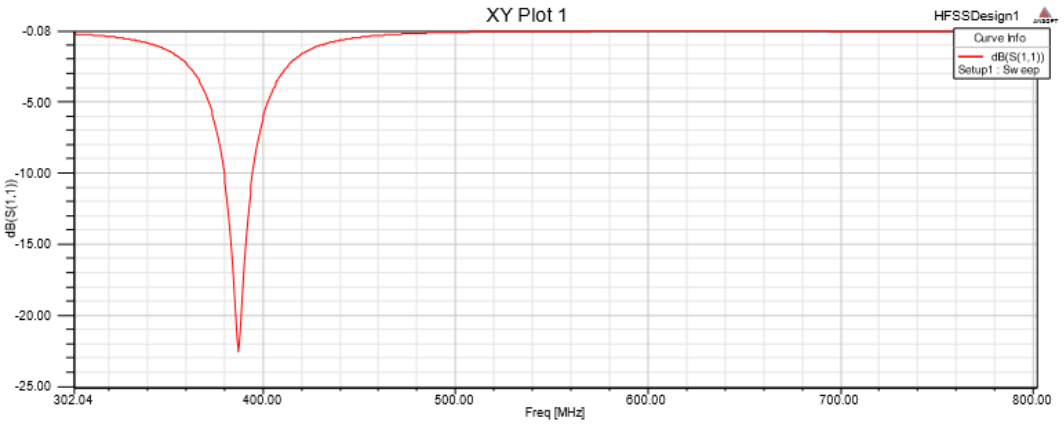

Figure 3.9.Reflection coefficient response for the Multilayer PIFA in muscle homogenous model.

As shown in Fig.9 the antenna resonates around 390MHz with a 6 MHz bandwidth .The magnitude of the return loss is lower than -20dB (≃-23dB) and the maximum values of the Realized Gain and Directivity are -25.96dB and 4.46dB respectively.

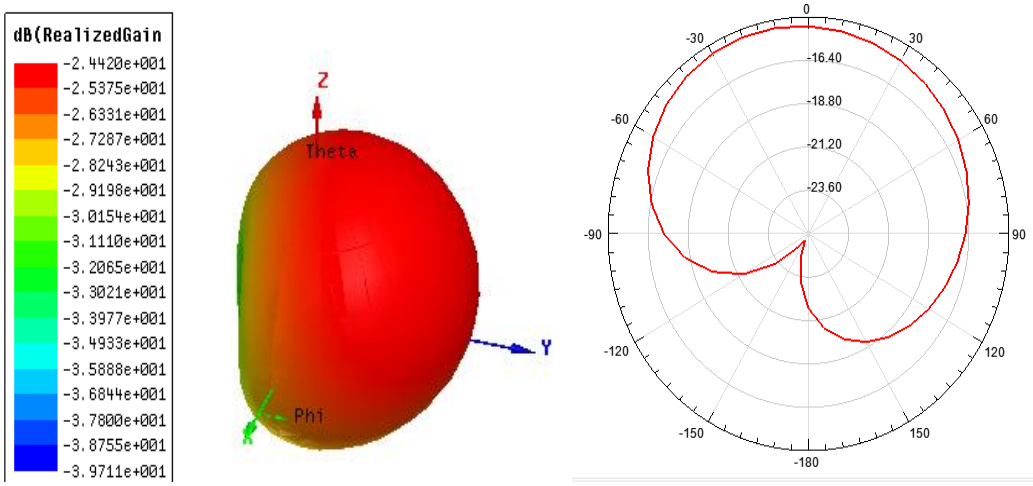

Figure 3.10. Simulated 3D gain polar plot at: (a) 404.5 MHz and (b) Radiation pattern.

3.2.2 Antenna inside the head model

The implant, is now located inside a canonical model imitating the dielectric properties of the human head.(ε'_r = 43.5 , tanδ=0.799)

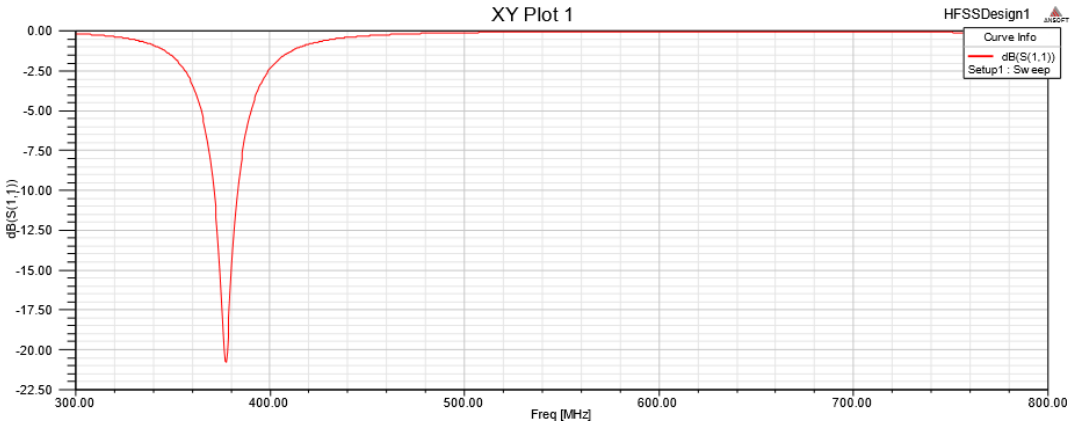

Figure 3.11 .Reflection coefficient response for the Multilayer PIFA in head homogenous model

As shown in Fig.12 the antenna resonates slightly lower than 390MHz with a 6 MHz bandwidth ,while the magnitude of the return loss is higher than -20dB (≃-21dB).

3.2.3. Antenna inside the 3 layer model

Lastly, the antenna is placed inside a 3-layered structure made of muscle-fat-skin(dry),whose radii are 32, 36, and 40mm, respectively(Fig.11). Dielectric properties are taken from Table 2, Chapter 2. (fat: ε'_r = 5.58, tanδ=0.328, skin: ε'_r =46.71, tanδ=0.658).

The resonant frequency is anticipated to shift slightly to the right ,due to the low loss tangent of the fat tissue, that interacts proximately with the antenna .The magnitude of the simulated reflection coefficient $|S_{11}|$ is smaller in this case, because of this frequency alteration. Results are depicted in Fig.14.

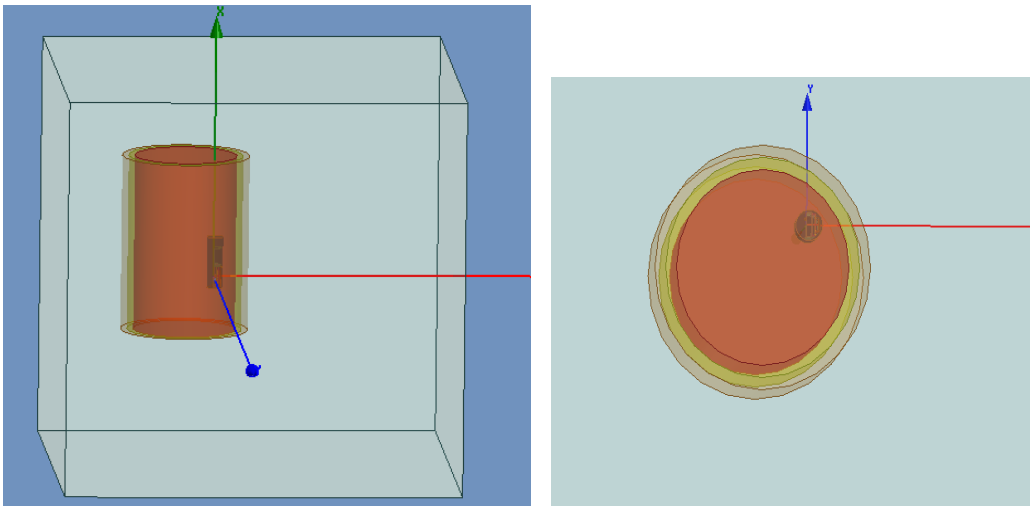

Figure 3.12.Aspects of the three layer model, used for the simulation.

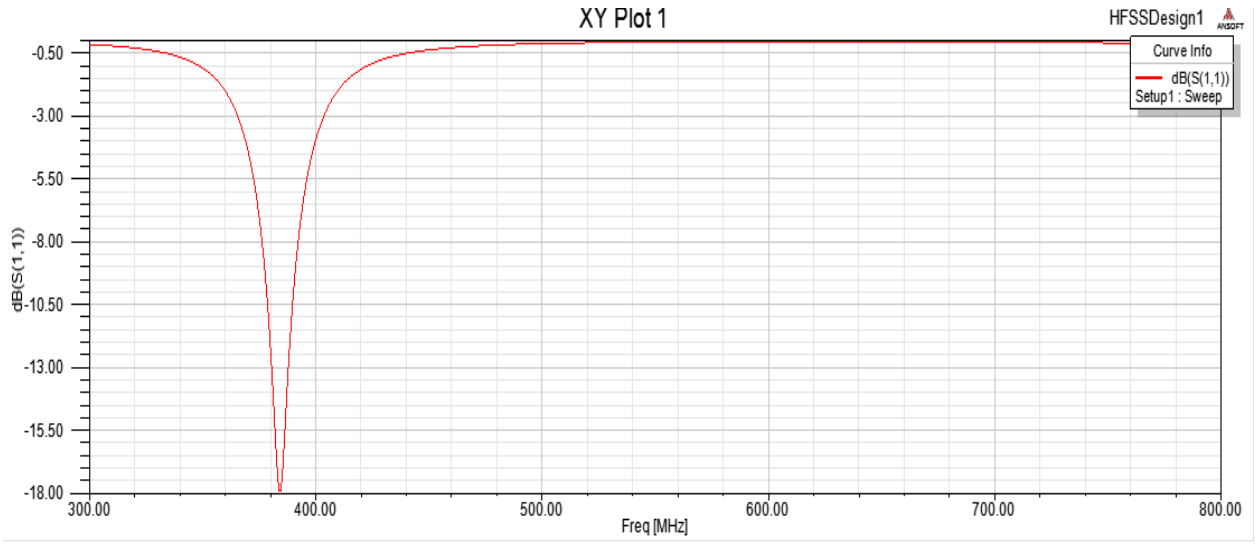

Figure 3.13.Reflection coefficient response for the Multilayer PIFA in three layer (muscle-fat-skin) canonical model.

•Observations

In this set of simulations the antenna resonated ≃-20MHz lower of the MedRadio Band (i.e. 385MHz).Although all stages were strictly followed as depicted in [132], this frequency shift seems unattainable to achieve. Amongst many alterations that were considered to be implemented on the original design in order to achieve resonance in the MedRadio band (i.e. epoxy glue etc.), the most appealing one was the change in the substrate material. Instead of Roger TMM 10 (of dielectric permittivity $\varepsilon'_r = 9.8$) , Roger

TMM 6 (ε'_r = 6) material was used .The results in the three different canonical models are presented below.

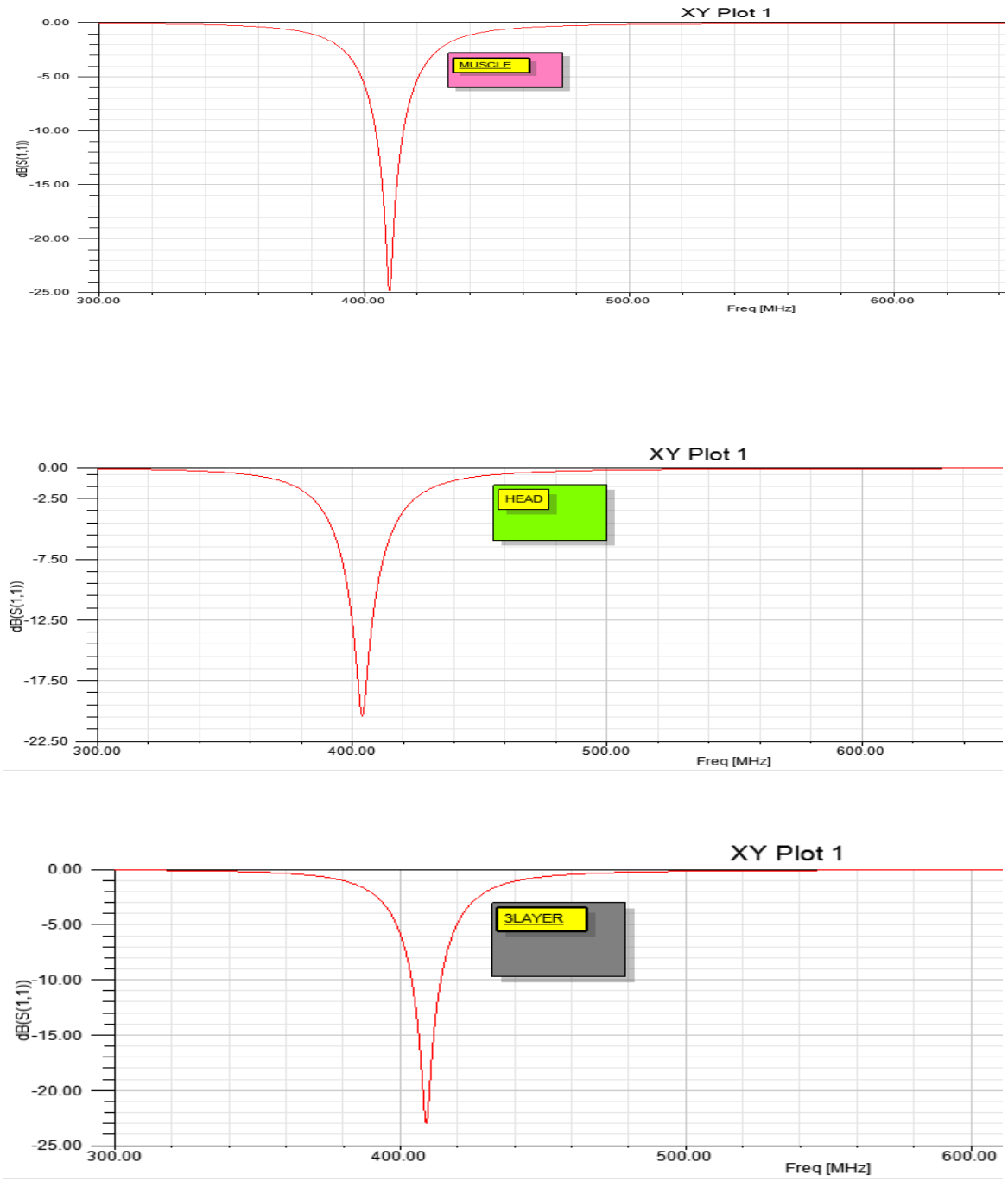

Figure 3.14.Reflection coefficient response for the Multilayer PIFA in the three canonical models. Resonance is achieved inside the MedRadio range.

3.3 Antenna design in the ISM band

Later on, the multilayer spiral structure is being simulated in the ISM band. The FE solver of HFSS performs iterative tetrahedron-meshing refinement automatically with the mesh being perturbed by 30% between each pass. The mesh refinement procedure has been set to stop when the maximum change in the reflection coefficient magnitude (S_{11}) between two consecutive passes is less than 0.02, or when the number of passes exceeds 10. The solver performs a 1600 point-frequency sweep by $\pm$400MHz around the center frequency of ISM Band (2.45 GHz). The results are presented below.

3.3.1 Antenna inside the muscle model

The same procedure was followed, as before and the antenna is placed inside the canonical model, except now the antenna is tested for its tuning in the ISM band. The dielectric properties of the muscle model, in this frequency range, are given in Table 2, Chapter 2; (ε'_r =52.729 , tanδ=0.242)

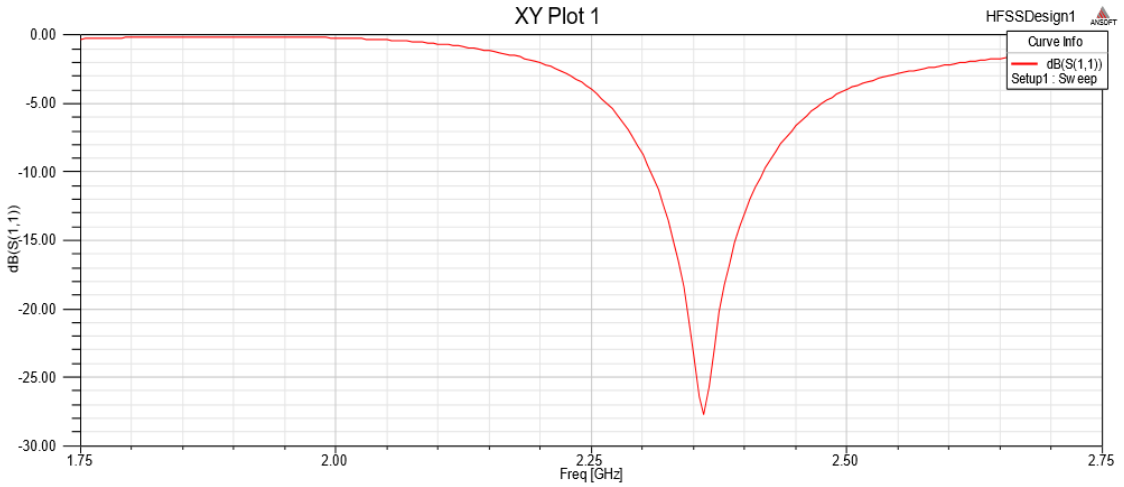

Figure 3.15. Reflection coefficient response for the Multilayer PIFA in muscle canonical model (ISM band).

In agreement with what was claimed in [132], the higher resonance is slightly lower (2.365GHz)than the targeted 2.45GHz. However, the simulated S_{11} depicts a wide working band (6% at -10dB points), which includes a sufficient part of the desired ISM frequency spectrum.

3.3.2 Antenna inside the head model

The antenna is located inside the canonical model, imitating the head dielectric properties. The dielectric properties of the head model, in the ISM frequency range, are given in Table 2,Chapter 2 ; ($\varepsilon'_r = 39.2$, tanδ=0.337)

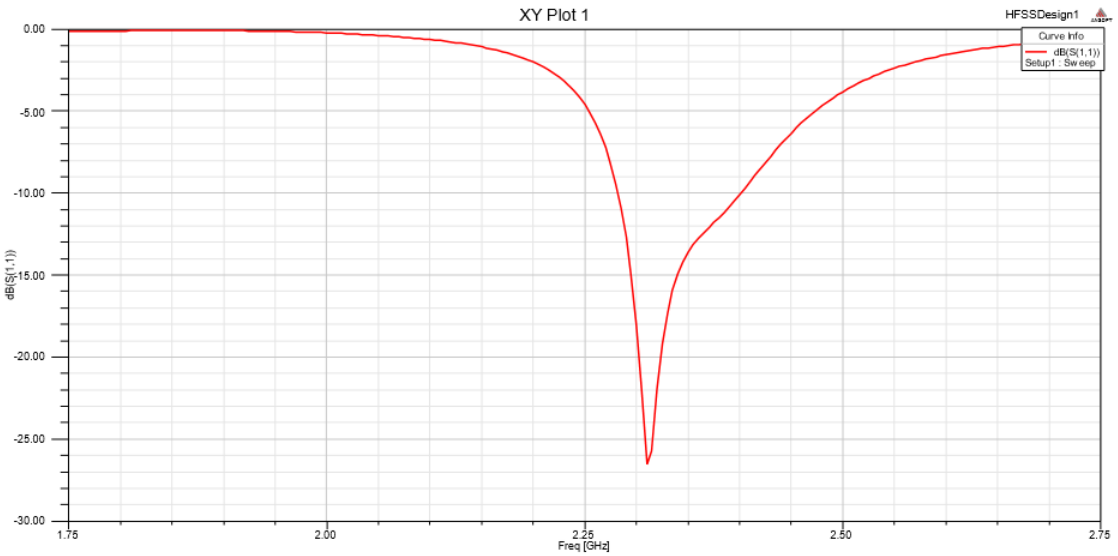

Figure 3.16. Reflection coefficient response for the Multilayer PIFA in muscle canonical model (ISM band).

Same as before, the antenna resonates at a slightly lower frequency (2.345GHz) than the targeted 2.45GHz.The resonant frequency variation is within the 0.3% as shown in Figs.15,16.This reduced sensitivity to the surrounding environmental conditions can be attributed to the lower coupling of the near field with the lossy tissues , since the antenna size is electrically larger in the ISM band. Moreover, the return loss still remains at very satisfying level (over 22dB magnitude).

3.3.3. Antenna inside the 3-layer (muscle-fat-skin) model

Finally, the antenna is located in the middle of the multilayer model (muscle-fat-skin). The dielectric properties of the tissues in the ISM band are given: (fat: $\varepsilon'_r = 5.28$, tanδ=0.145 , skin: $\varepsilon'_r = 38.007$, tanδ=0.283).

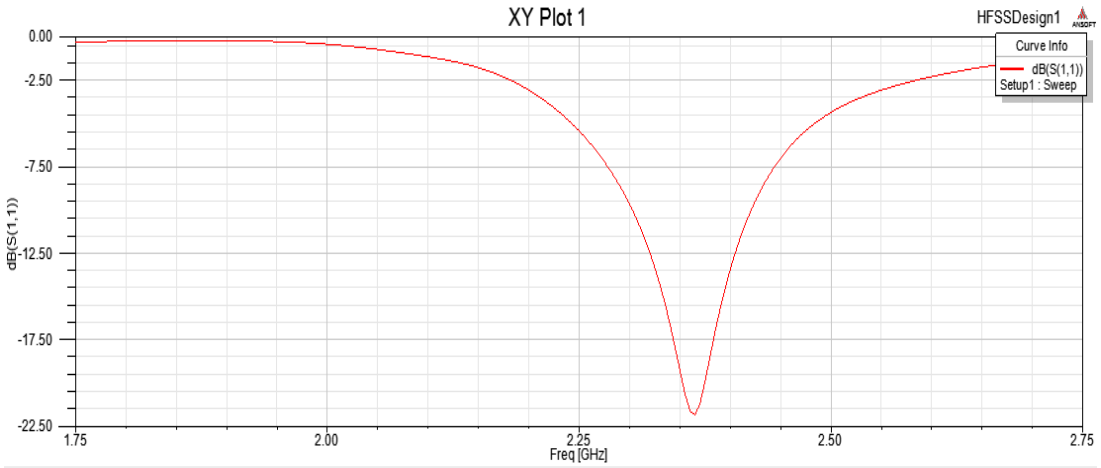

Figure 3.17.Reflection coefficient response for the Multilayer PIFA in muscle canonical model (ISM band).

Resonant Frequency around 2.37GHz.The magnitude of the simulated reflection coefficient $|S_{11}|$ is smaller in this case, which results in greater values of realized Gain (Re_Gain=1-$|S_{11}|^2$). This comes as no surprise, since the antenna is placed closely to the fat tissue, which is characterized by very low permittivity (i.e. 5.28).Because of this fact, the radiated wave undergoes minor attenuation inside this model.

Radiation performances:

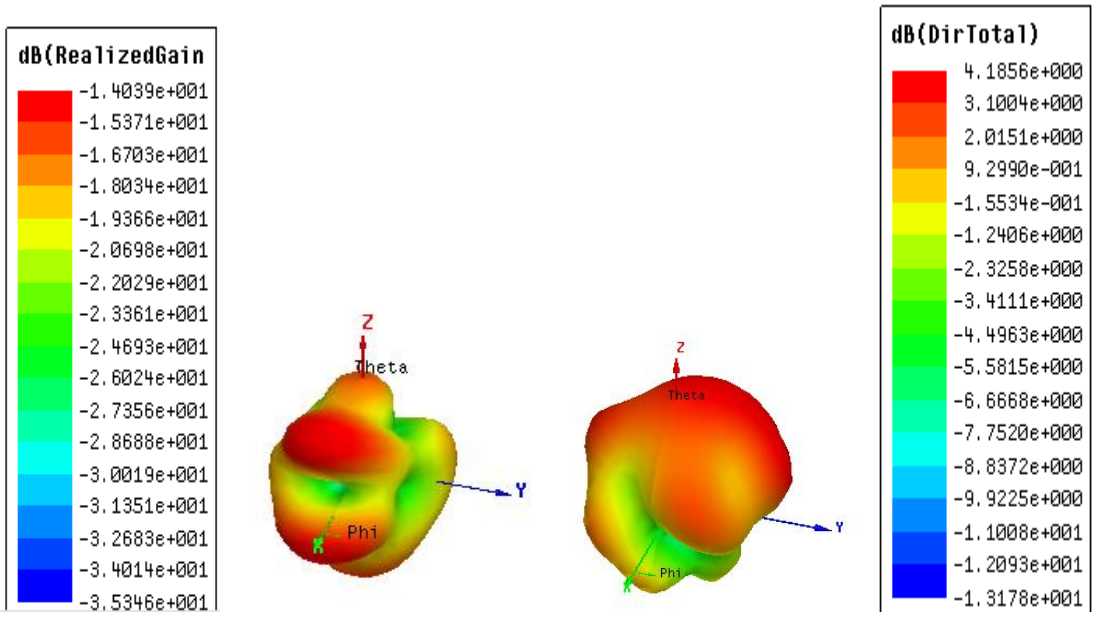

(a) (b)

Figure 3.18. Simulated 3D (a) Realized gain polar plot (*muscle model*) at 2.37GHz. Simulated 3D (b) Directivity plot (*3-layer model)* at 2.37 GHz.

•Observations:

There was a minor deviation between the simulations' results and the ones presented in [132], concerning the maximum values of Realized_Gain obtained(-14.1dB over -18.5dB). Nevertheless, the radiation performances still fulfill the initial requirements providing robust communication in a 2m distance.[137]
Overall, it was presented ,that the corresponding radiation efficiencies of the multilayer spiral PIFA, are rather small but they provide dual operational range , wider than 10m and 5m in the MedRadio and ISM band respectively.

3.4 Parametric Studies of Spiral PIFA - Effects

In this section, the effect of changing different parameters at the Multilayer Spiral PIFA antenna is investigated. As already mentioned the initial design of the multilayer PIFA has been described in section 3.1 of this chapter. The top view and side view of this spiral PIFA antenna are also shown in Figure 7.

•*Effect of the Dielectric Constant (Substrate)*

The effect of altering the electrical permittivity of the substrate is shown below.

Dielectric Material	ε'_r	$f_{res}(MHz)$	$\lvert S_{11} \rvert_{380\,MHz}$
Alumina_96pct	*9.4*	*375*	*35*
Rogerς TMM 10 tm	*9.2*	*380*	*22*
FR4 Epoxy	*4.4*	*442*	*19*
Teflon	*2.1*	*504*	*24*

Table 3.3.Effect of dielectric material on the resonance frequency, and reflection coefficient at 380 MHz.

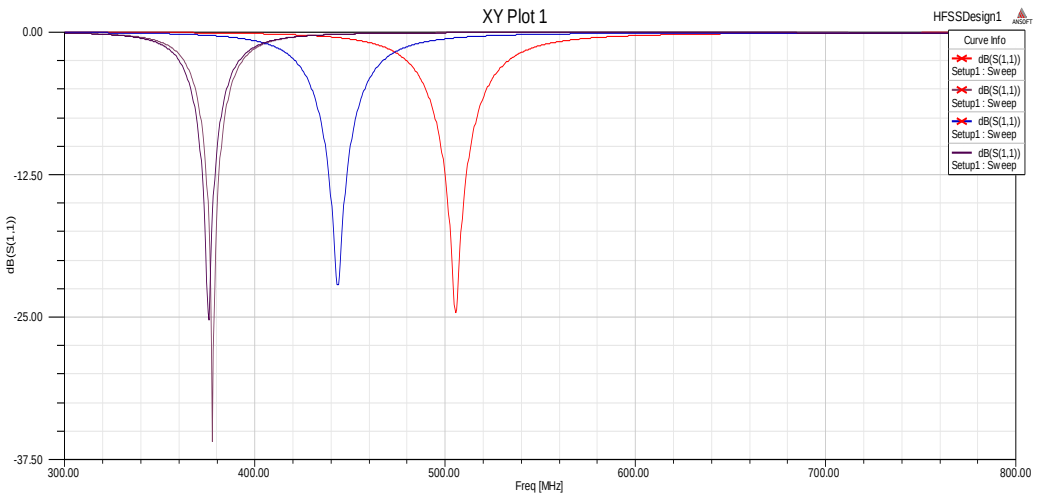

Figure 3.19.Reflection coefficient responses for different dielectric constant materials.

As expected, by increasing the dielectric constant ε'_r, the PIFA's effective wavelength is shortened ,thus the resonant frequency is shifting to the left (the resonant frequency decreases).Simultaneously, the magnitude of the return loss becomes larger. That means that with much larger dielectric constant, the input return loss is higher. Hence, the choice of substrate materials is proved to be highly critical in the design and performance of miniature implantable PIFA.

•*Effect of Strip Width*

The width of the copper metallizations of the three substrates was increased. The parametrization was set by five variables a,b,c (for the 1st substrate), d (for the 2nd substrate) and e (for the 3rd substrate) .

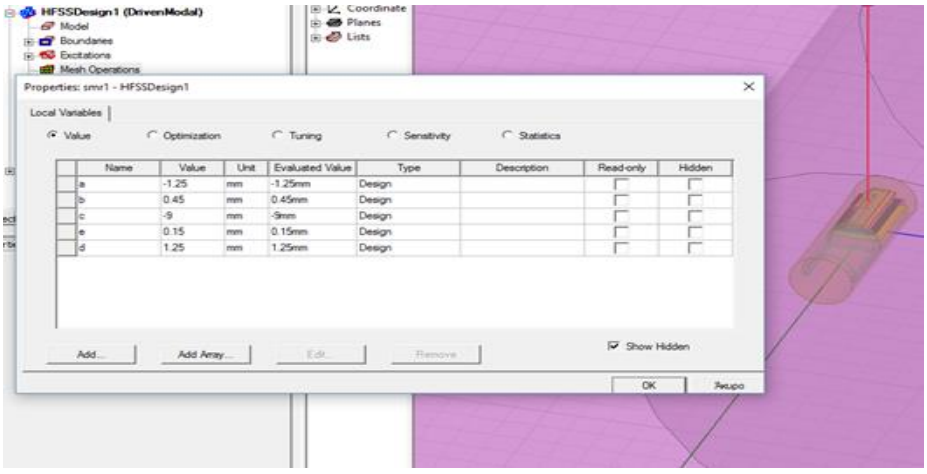

Figure 3.20.Parametric setup; a,b,c,d, variables set.

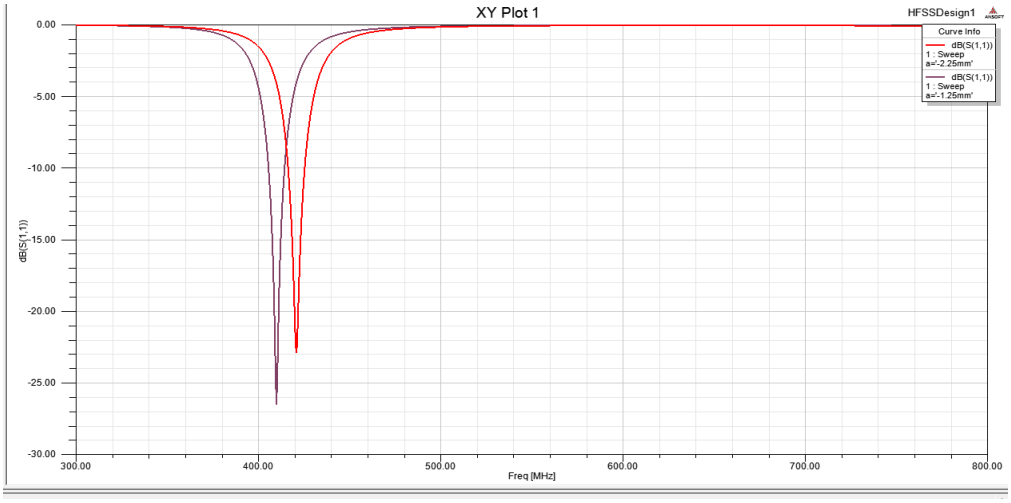

Figure 3.21.Variable a; Increase by 1mm. Small impact on resonant frequency .

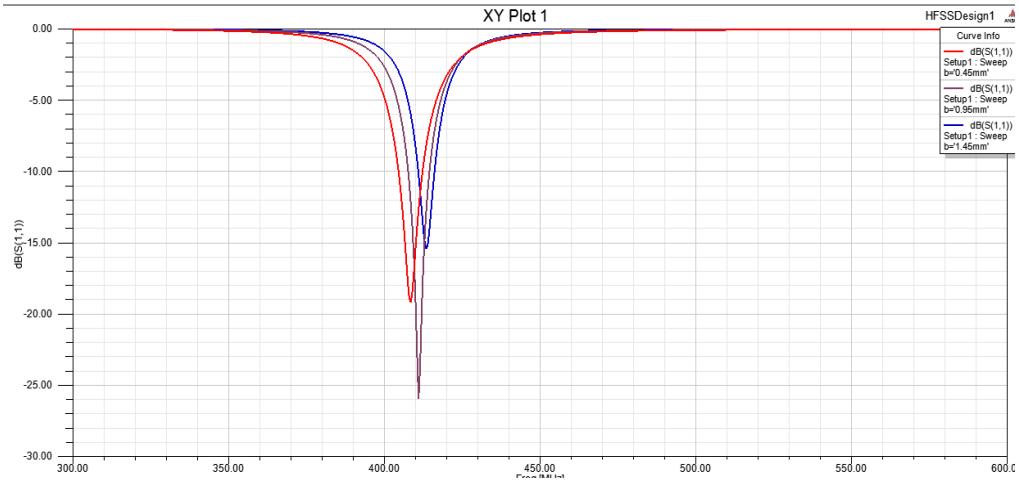

Figure 3.22.Variable b; Increase by 1mm.

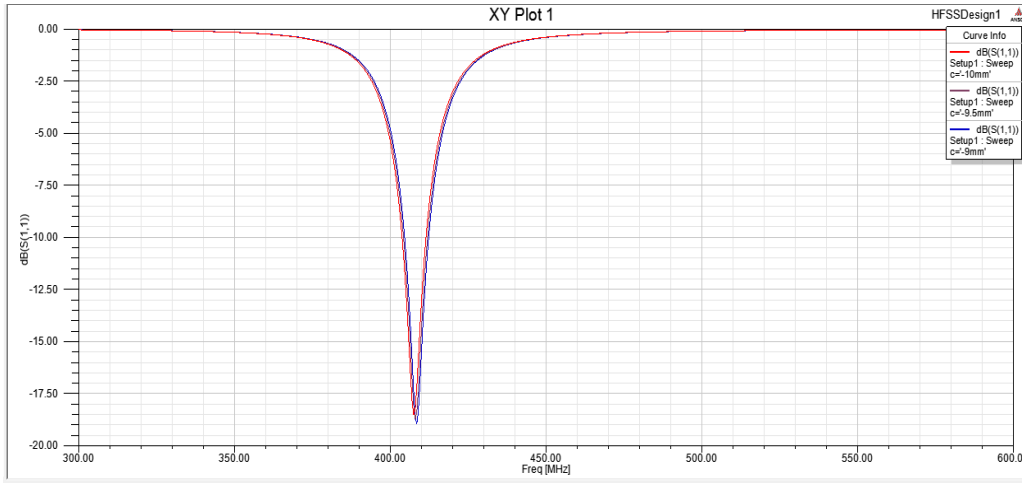

Figure 3.23.Variable c; design limitations - almost identical results .

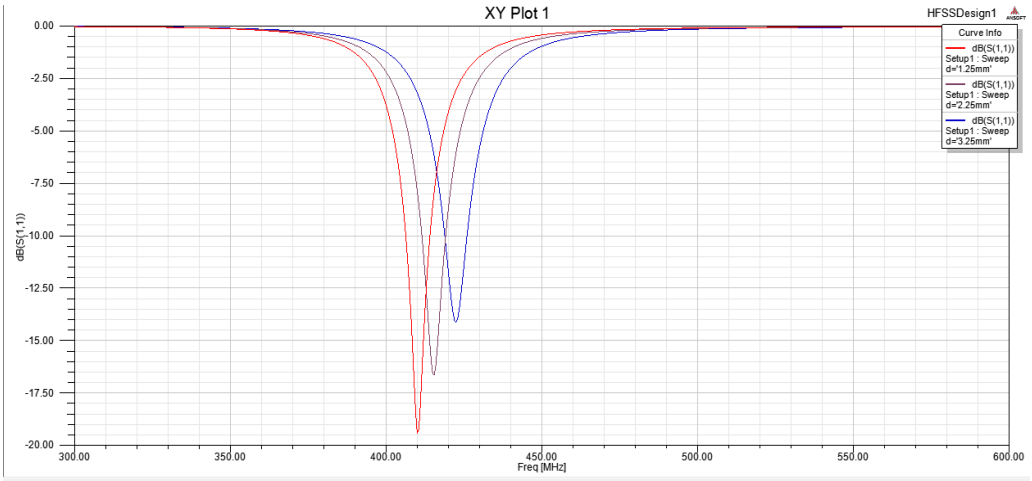

Figure 3.24.Variable d; Increase by 2mm. Shift out of the MedRadio band. Lower return loss S11. Undesirable results.

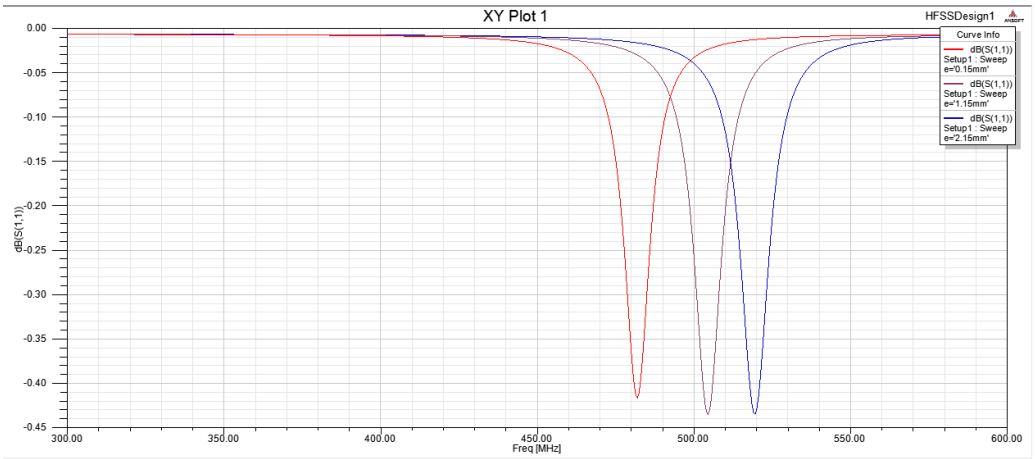

Figure 3.25.Variable e; Increase by 2mm.Great shift on the resonant frequency.

Both the resonant frequency and the magnitude of the reflection coefficient are changed when the strip width is altered. The smaller the width is, the lower the resonant frequency becomes. It can be noted as well that the matching is getting poorer as the strip width is getting smaller.

•*Effect of Feeding Point Position*

The antenna is fed with a standard discrete port, and the location of the feed would be expected to affect the tuning of the antenna. The dependence on the location of feeding point in the resonant frequency is also an interesting parameter. In this case, the feeding

point is placed in different positions along one strip arm (x-axis) and between arms (y-axis).

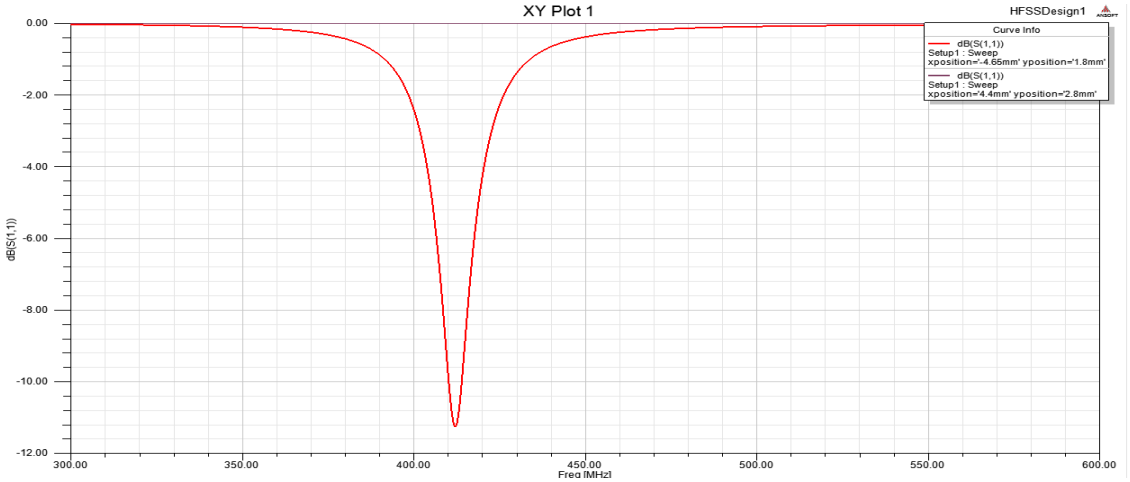

Figure 3.26. Feeding point moved by 0.6mm to the left along the x-axis.

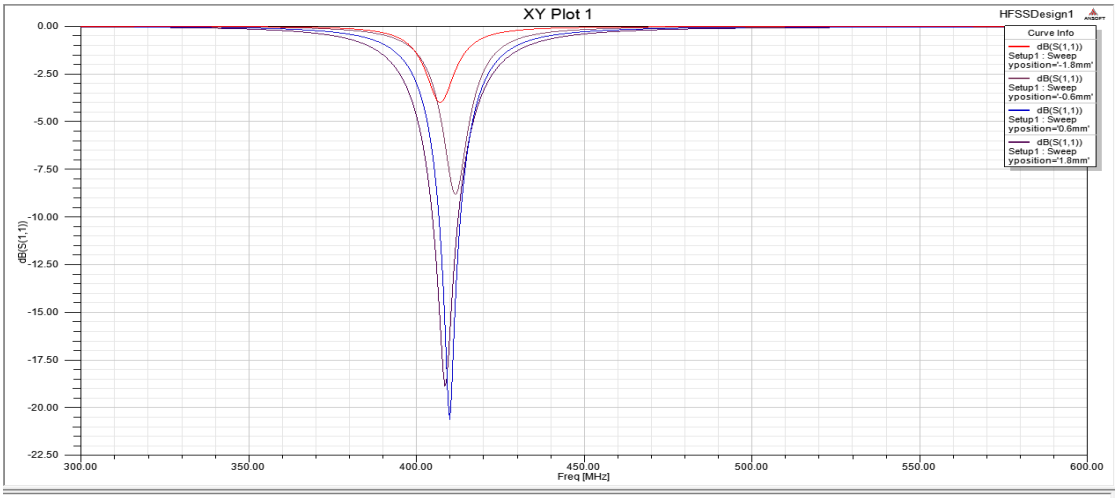

Figure 3.27. Feeding point moved with 0.25mm step, along the y-axis.

As shown in Figures 26-27, the locations of the feed point impact the antenna matching, but have little effect on the resonant frequency. There is no evident difference in the resonant frequency, but there is a change in the propagation. The magnitude of the return loss has become smaller, which indicates worse impedance matching when the distance is being moved from the initial port position by -2 mm

*Note that the parametrization technique of lengthening the electrical path of the substrates was avoided at this stage, because of the complexities occurred from the weldings' interference with the copper strips. It was taken under consideration later on, when setting the max and min values of the copper's dimensions for the optimization analysis.

3.5 Optimization

In the final step, PIFA design is optimized for the implantation scenario under consideration. Quasi-Newton optimization is selected for its speed and accuracy in cases of insignificant numerical noise [138]. Quasi-Newton algorithmic methods are based on Newton's method to find the stationary point of a function, where the gradient is 0. The Quasi Newton optimizer works on the basis of finding a minimum or maximum of a cost function which relates variables in the model to overall simulation goals. The degree of convergence in the desired result , appears in each iteration of the cost function, which returns zero in case the algorithm has satisfied the criteria. If the criteria are not met, QN returns greater numbers.

Optimization is performed inside a canonical muscle model of the intended implantation site. To speed-up design, the position of the coaxial feeding point is kept fixed to that of the initial PIFA as well as the volume of each of the four substrates (i.e. parameters sub1, subw1-subw4 , subz1-subz4, and e1-e2 remain stable).The fifteen variables (w0-w5, l1,l2,l4,l5,l6,l7,l8,10,l11) are only considered as dimensions in the solution space. These are initialized to the values obtained in the first step and vary within the range [0.1mm, 12.7 mm]. The minimum and maximum step values are set to 0.1 and 1 mm, respectively. The cost function is defined as the magnitude of the reflection coefficient (S_{11}) at the desired operating frequency (f_0), i.e.,[139]

$$\text{cost}=\left|S_{11@\, f_0(incanonicalmodel)}\right| , \qquad (2)$$

and optimization terminates when (2) is minimized, or when thenumber of iterations exceeds 350. Noise involved in the calculation of the cost function is small enough (uncertainty in the calculation of the cost function is given by 0.02), justifying the choice for Quasi-Newton optimization.

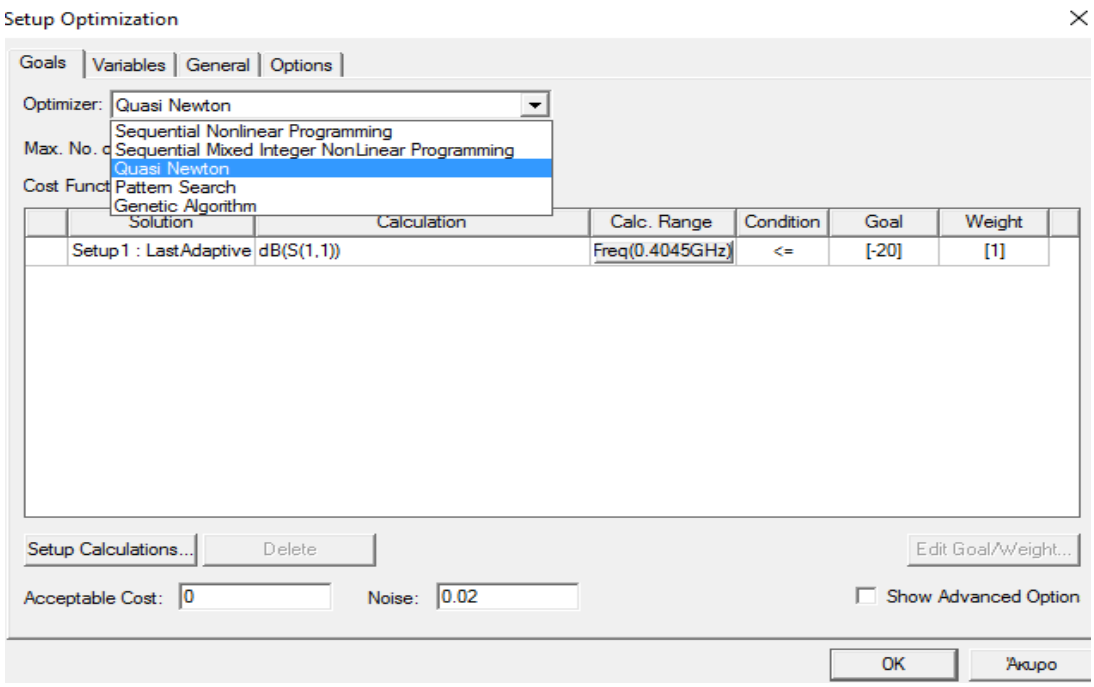

Figure 3.28.Selection of QN algorithm and noise settings.

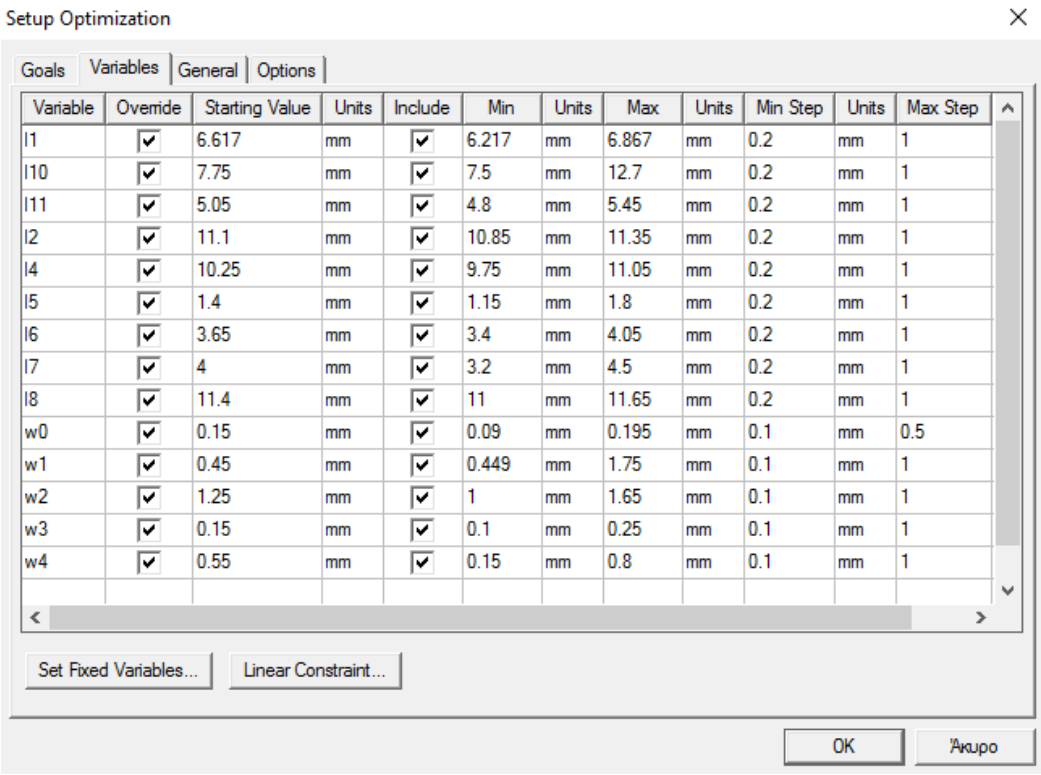

Figure 3.29.Parameters settings for optimization.

Major aim of the procedure, is for the cost function to verify the form: $|S_{11}|_{4045MHz} \leq -20dB$. Since in none of the iterations the terminal criterion was satisfied (cost=0), the optimal solution to the problem, was chosen to be the one corresponding to the lowest cost (cost=2.835 as depicted in Fig.31).For that cost value, the parameters of the metallizations were respectively:

W0=0.149mm	W3=0.148mm	l1=6.617mm	l5=1.4mm	l8=11.4
W1=0.491mm	W4=0.55mm	l2=11.1mm	l6=3.65mm	l10=7.82
W2=1.25mm	W5=2.2mm	l4=10.25	l7=4mm	l11=4.94

*Note that some of the dimensions of the parameters remain the same after the optimization. This is expected since, the antenna simulated in the HFSS Software environment, was already realized [132], so only small improvements are anticipated.

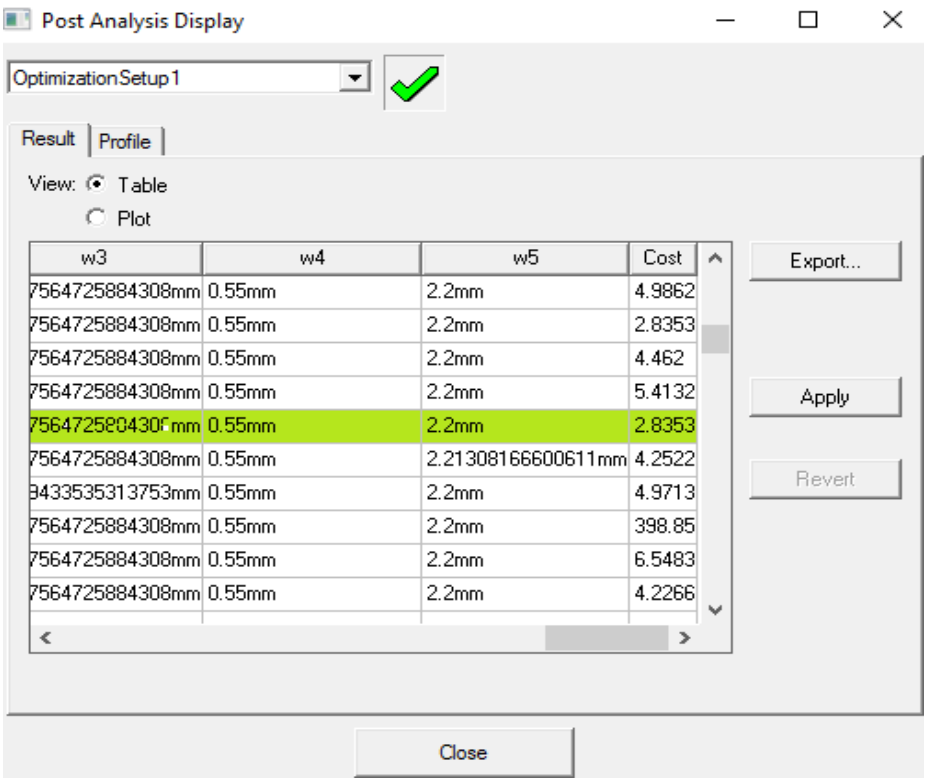

Figure 3.30.Lowest cost value.

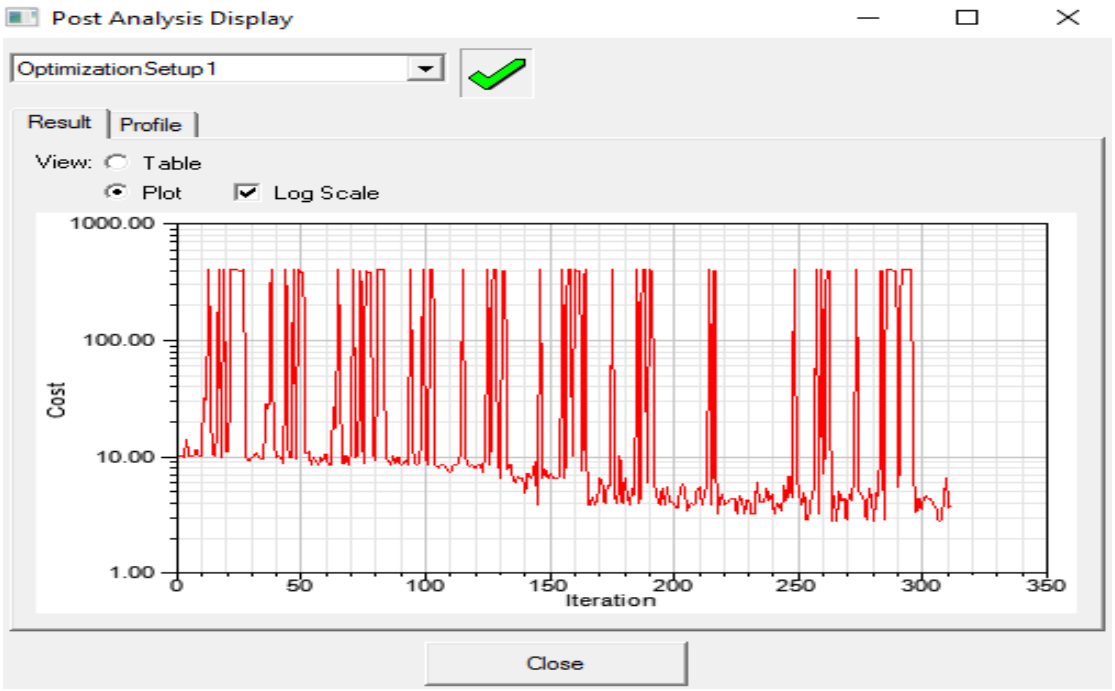

Figure 3.31.Analysis result of the optimization setup. Plot cost function VS number of iterations.

Chapter 4

Novel Spiral Antenna Design

4.1 Concept of the novel antenna

In section 3.2 of the previous chapter, a multilayer PIFA that performed both at the MedRadio and the ISM frequency range was studied. It had the optimal size of $\pi \text{ x} 5^2 \text{ x } 32.1$ mm. In this chapter a further miniaturization of an antenna design is attempted, which will perform at 401-406 MHz (MedRadio band). In order for the electrical length to be maximized and profound miniaturization to be achieved, the rectangular spiral, in multilayer structure, topology is selected .This is mainly ascribed to the fact that, longer strip lines can be design in more compact area.

After the analysis of various parametric studies performed on the previous chapter, attention was drawn to how more densely packed antennas could be designed based on the former typology for implantable or ingestible use. In order to reduce the volume of the antenna the fourth substrate of the initial antenna design, depicted in Fig 2- Chap 3, was removed. The antenna now consists of three Roger TMM 10(tm) substrates packed inside a biocompatible insulation made out of PEEK. Further ahead, the thickness of each substrate is diminished in order for extra miniaturization along the z-axis to be achieved. Last but not least the conformal ground plane was reduced by 2mm and as a result the coating made out of PEEK did too.

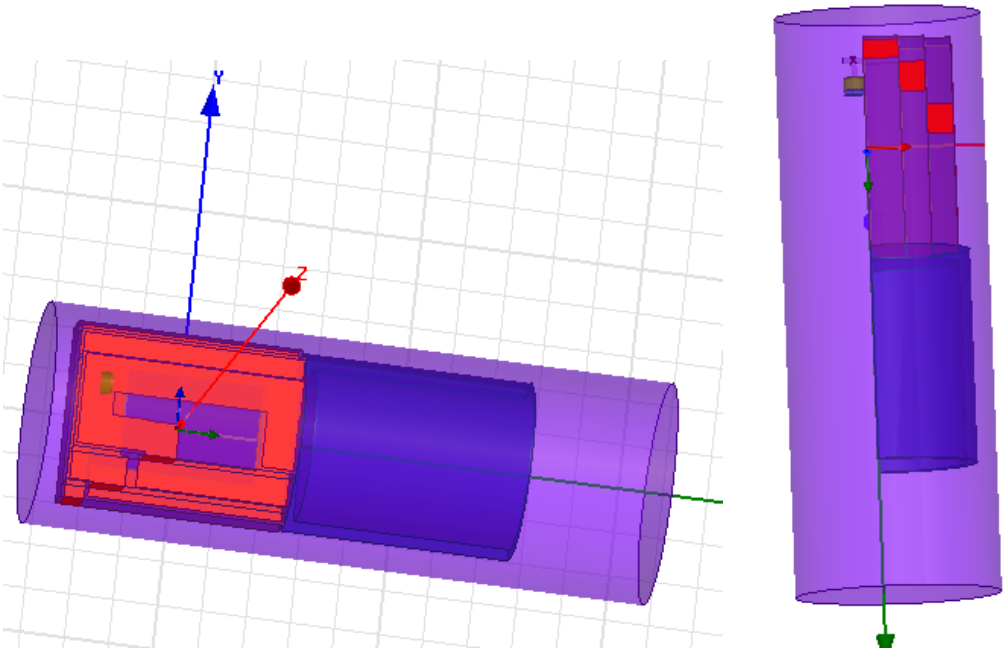

Figure 4.1.Different aspects of the novel multilayer antenna

The new conformal multilayer antenna has a total optimal size of $2018\,mm^3$ instead of the initial $2529\,mm^3$.Because of the curtailment of the total structure the resonant frequency shifted to the right, out of the desirable MedRadio band (Fig 2).

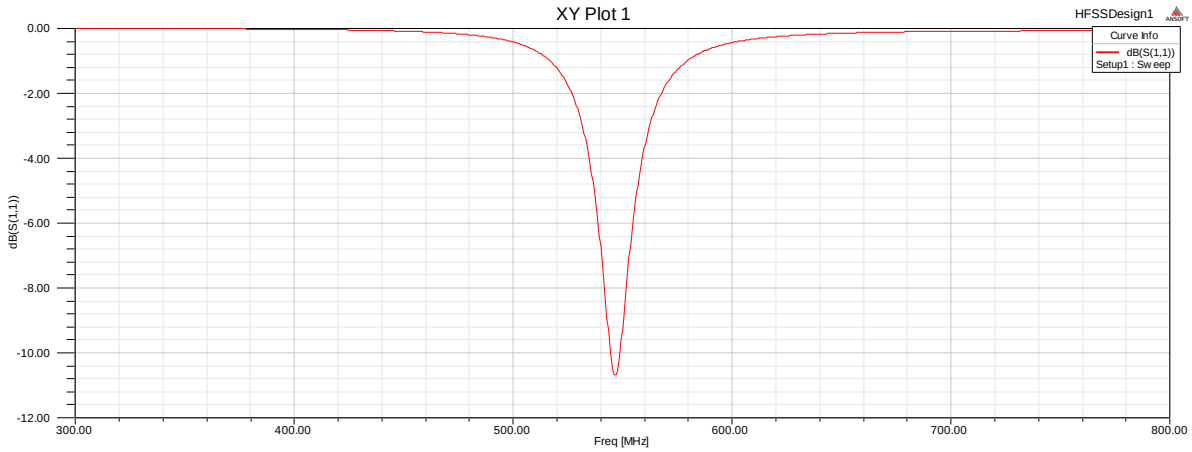

Figure 4.2.Antenna undesirable right frequency shift.

For that reason new arrangements had to be designed concerning the metal strips of the structure. In order to decrease the resonance in lower frequency levels, the length of the metallic strips had to be extended. Hence, alterations had to be made regarding both the

width of the copper and its length in the third substrate .In the other two substrates, limitations were met due to the proximity of the weldings with the metallic strips of the next levels. The values of the design parameters (i.e. Chapter 3, Table 2.), that were modified are presented below.

Table 4.1.New values of the altered dimensions of the novel 3-layer antenna

sub1 (mm)	subz1 (mm)	subz2 (mm)	subz3 (mm)	w2 (mm)	hg (mm)
12.1	**1.705**	**1.17**	**1.17**	**1.25**	**9.75**

4.2 Novel Antenna for Implantable Application

Simulations ran firstly with the novel conformal antenna been located in a canonical model (80 x 110 mm) with muscle equivalent dielectric properties.

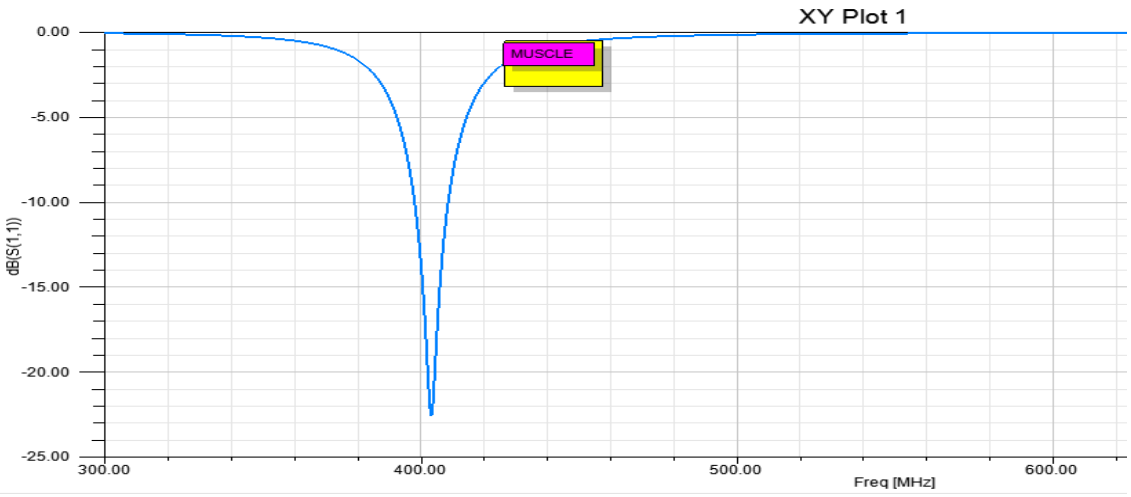

Figure 4.3.Novel antenna's reflection coefficient response at 405MHz

There has been observed, that the antenna resonates successfully at 405MHz with a sufficient bandwidth , as well as with a magnitude of return loss $|S_{11}|$ exceeding the 20dB.The antenna performances are being cited (Figs 3-4).

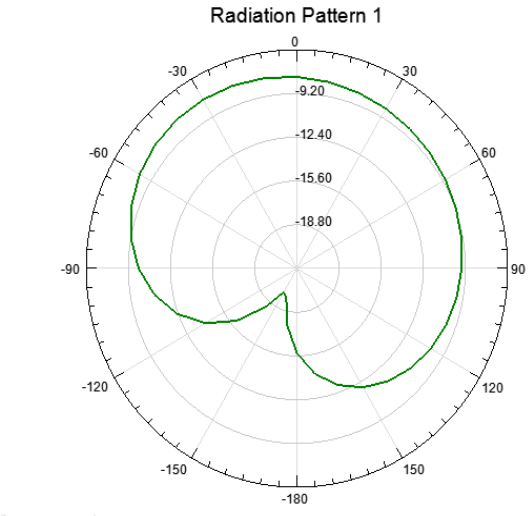

Figure 4.4.Simulated normalized radiation pattern [dB] at the measured resonant frequency (i.e. 405MHz)

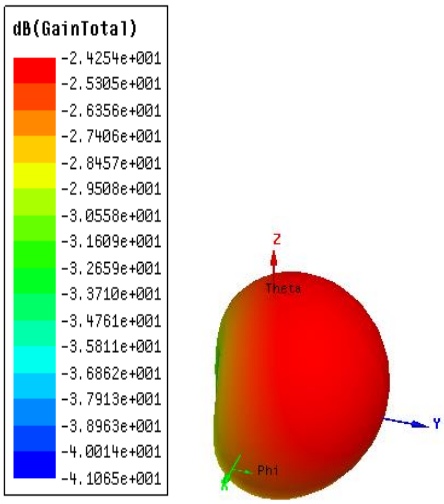

Figure 4.5.Novel conformal 3D Gain plot.

Later on, the antenna is being tested inside both head, and 3-layered (mucle-fat-skin) canonical models. The novel structure appears to be robust inside all different phantoms.

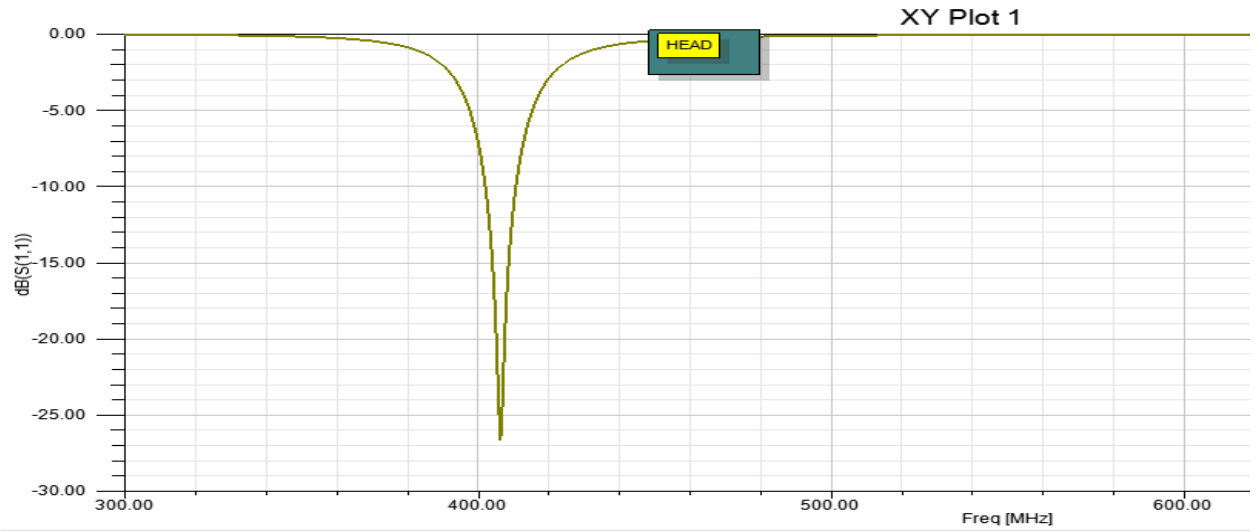

Figure 4.6.Novel Antenna in simulation environment imitating the human head.

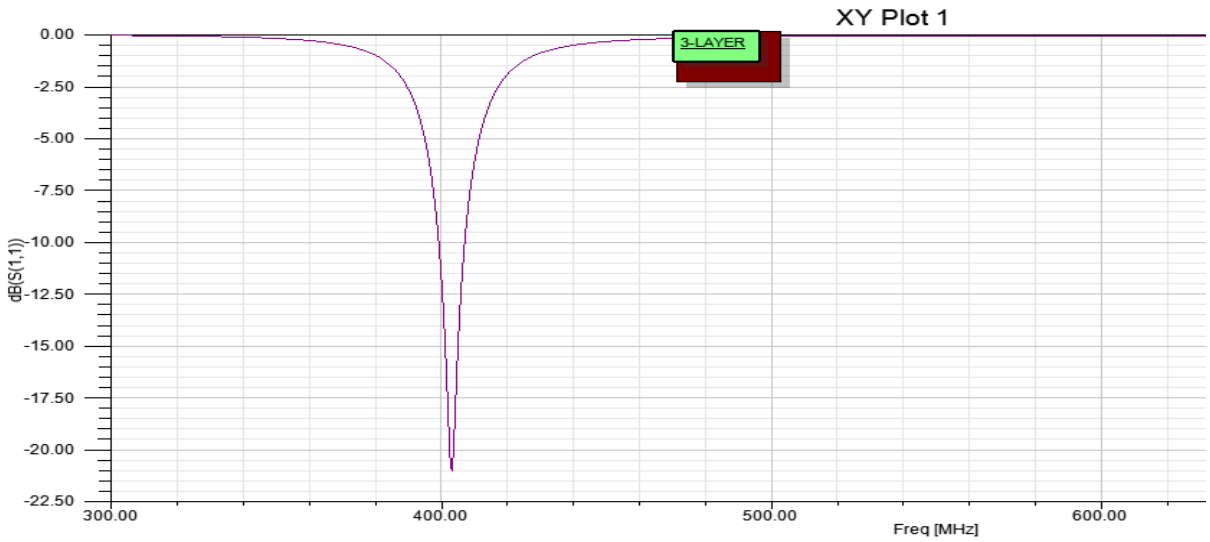

Figure 4.7.Novel antenna's response inside the muscle-fat-skin canonical model.

Radiation performances for the two former models:

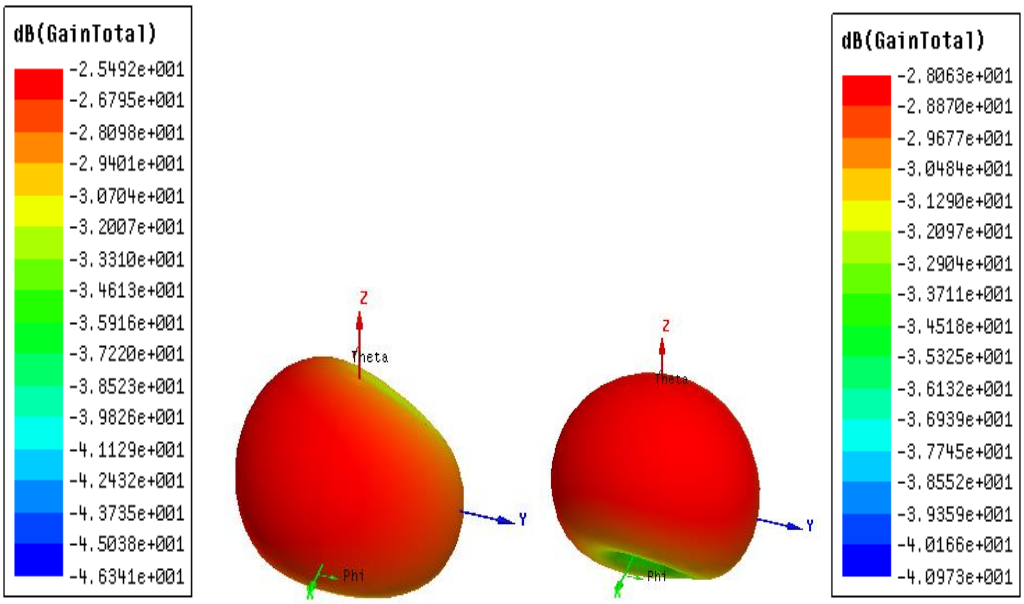

(a) **(b)**

Figure 4.8.Simulated 3D gain polar plot at 405MHz : (a) 3-layer model and (b) head model

4.3 Novel Antenna for Ingestible Application

Due to its compact size and omnidirectional radiation, the antenna was also tested for ingestible utilization. As mentioned in Chapter 1, a Wireless Capsule (WC), except from the antenna incorporates several microelectronic circuits, sensors, a CMOS camera, LEDs, batteries and even, in some experimental cases, sophisticated systems for active locomotion inside the GI tract .As depicted in Fig.2 these items could be integrated in the free space that exists under and behind the volume that the antenna consumes. For the simulation, the multilayer structure – which is encapsulated by biocompatible PEEK coating ,was firstly placed inside a canonical cylindrical model (20 x 260mm) with equivalent dielectric properties of an esophagus (ε'_r = 67.454, σ=1.004, tanδ=0.662, mass density [kg/ m^3]=1040)

The FE solver of HFSS performed iterative tetrahedron-meshing refinement automatically with the mesh being perturbed by 30% between each pass. The mesh refinement procedure had been set to stop when the maximum change in the reflection coefficient magnitude (|S11|) between two consecutive passes is less than 0.02, or when the number of passes exceeds 10. The solver performed a 400 point-frequency sweep by ±100MHz around the center frequency of MedRadio Band (404.5 MHz). Radiation boundaries are set λ_o /4 (λ_o is the free space wavelength, f_o = 404.5 MHz) away from all simulation set-ups to extend radiation infinitely far into space. The results are presented below.

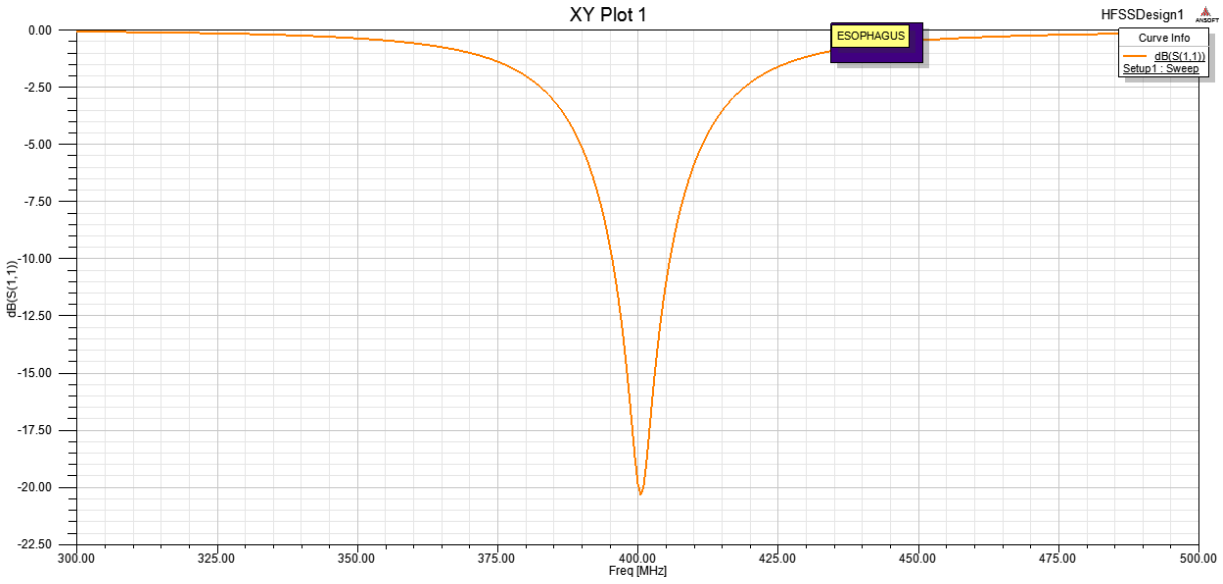

Figure 4.9.Reflection Coefficient (|S11|) frequency response of the antenna inside esophagus model.

Next, the antenna is located inside a sphere of 50 mm in radius that mimics the dielectric properties of the stomach (ε'_r = 67.444, σ=1.004, tanδ=0.6618, mass density [kg/m^3] =1050)

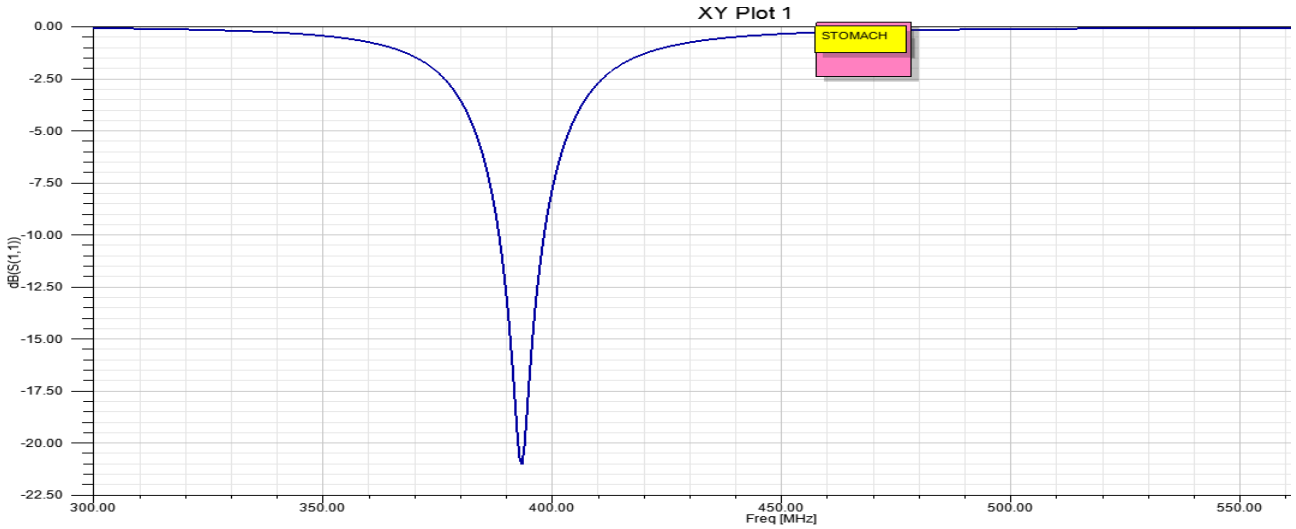

Figure 4.10.Reflection Coefficient (|S11|) frequency response of the antenna inside stomach model.

Later on the 3-layer structure was located inside a canonical box (100 x 100 x400 mm) imitating the dielectric properties of the colon. Its dielectric properties are cited; (ε'_r =62.51, σ=0.86, tanδ=0.611, mass density [kg/m^3] =1044). Following the same procedure with HFSS Software, the simulations gave the reflection coefficient response, as follows .

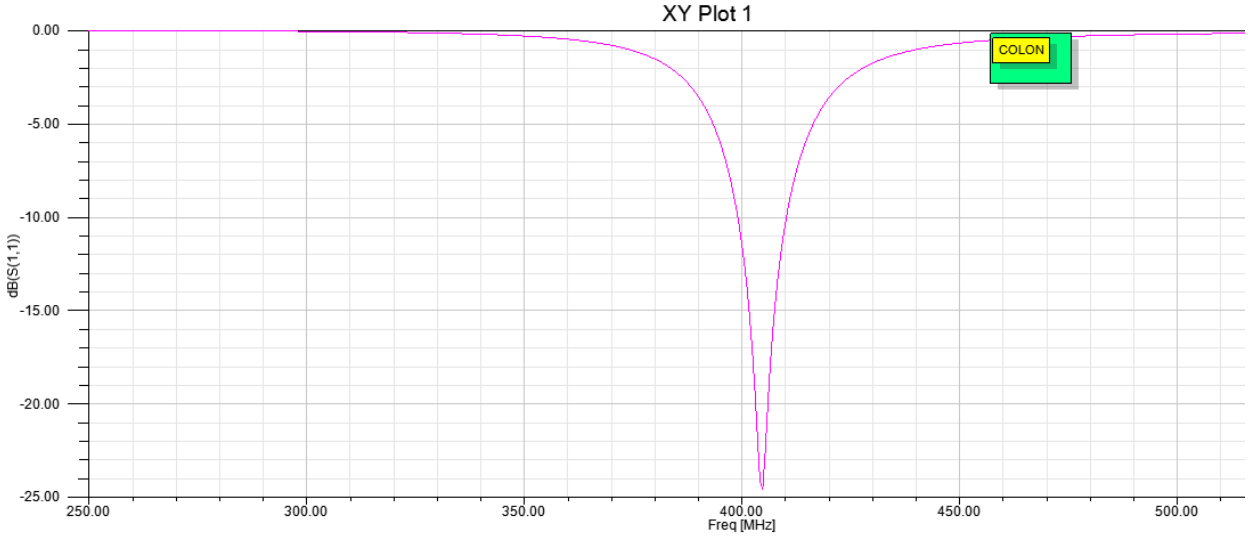

Figure 4.11.Reflection Coefficient (|S11|) frequency response of the antenna inside colon model.

Finally, the conformal antenna was placed inside a canonical model in the shape of a box (200 x 200 x 400mm) with small intestine equivalent dielectric properties (ε'_r = 66.02, σ=1.905, tanδ=1.282, mass density [kg/ m^3]=1044)

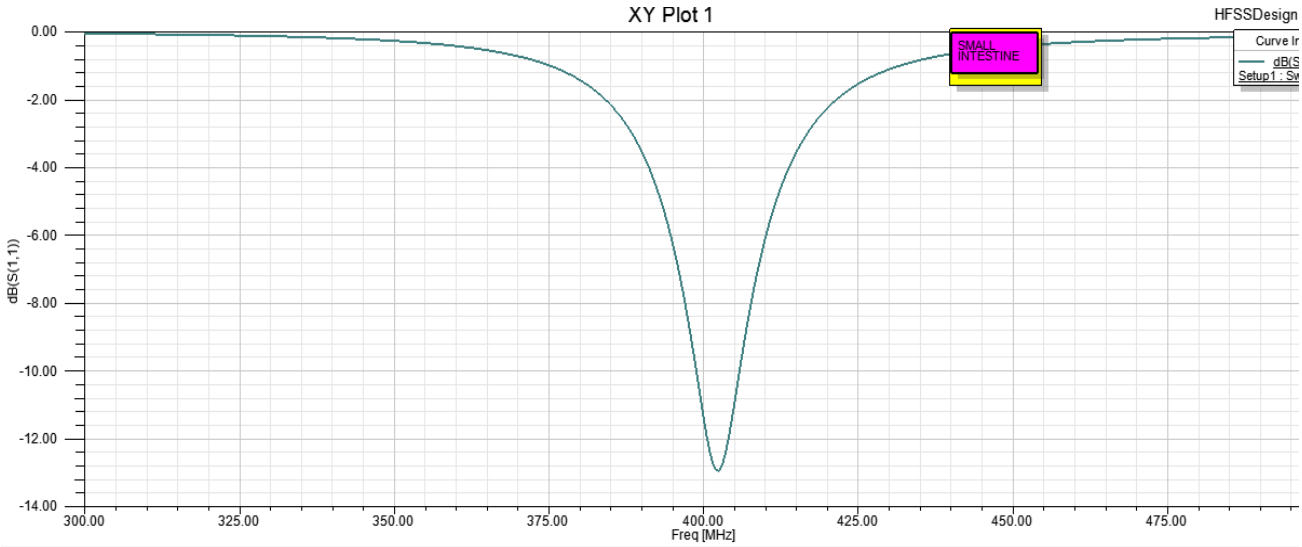

Figure 4.12.Reflection Coefficient (|S11|) frequency response of the novel antenna when placed at the center of the small intestine model

The Radiation Efficiencies of the corresponding simulations in the three models are being presented.

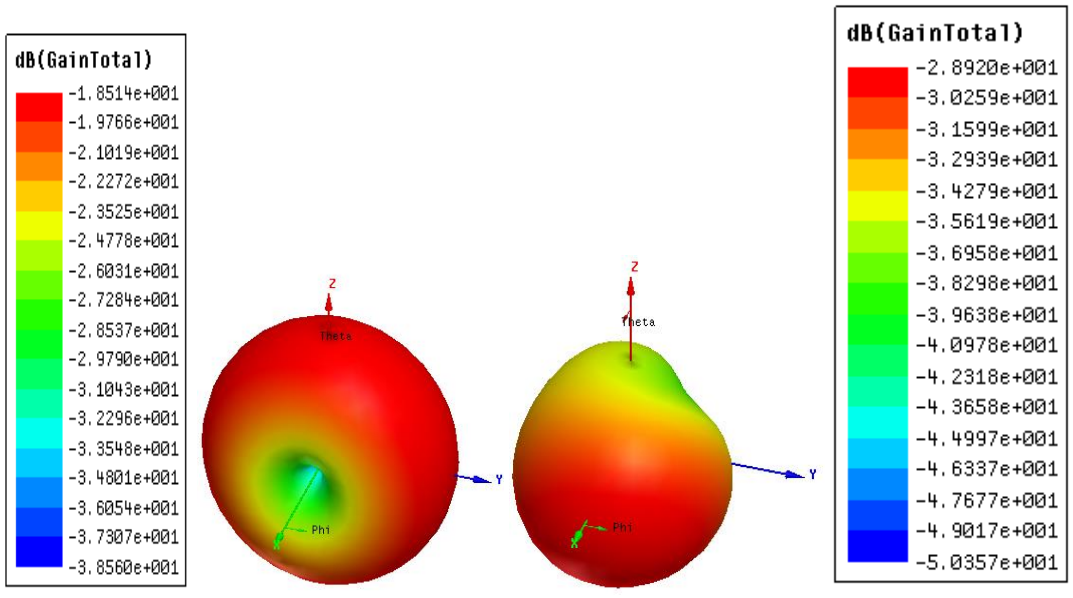

(a) **(b)**

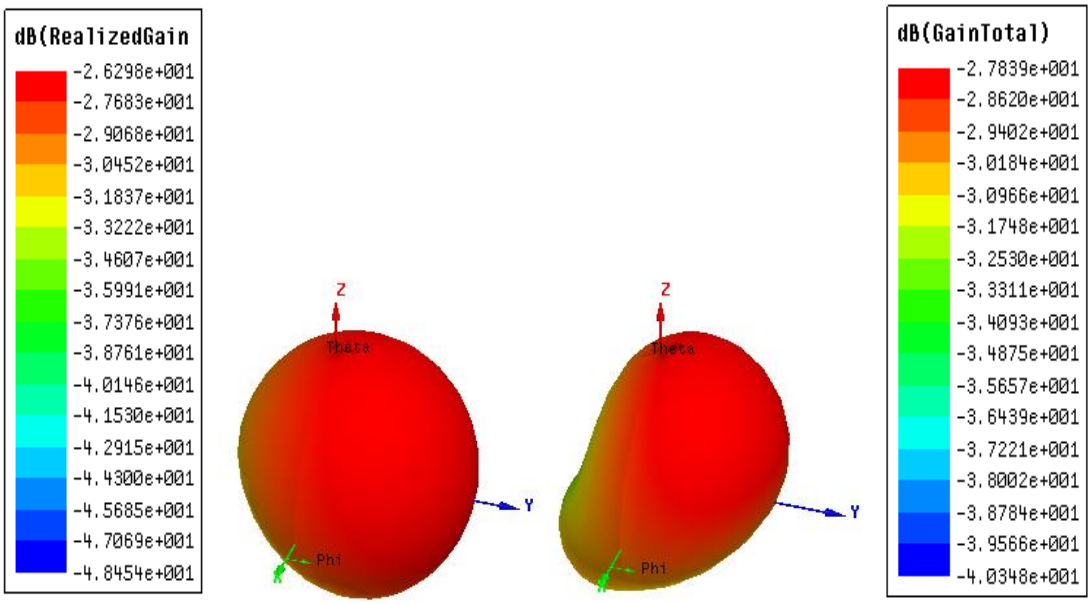

(c) (d)

Figure 4.13. Radiation performance of tuned antenna. 3D Radiation pattern while placed in the center of (a) esophagus (b) stomach (c) small intestine (d) colon (large intestine).

Observations:

•The novel antenna performs sufficiently inside the esophagus model. It resonates around 401-402MHz with a Total Gain value over -18dB.

•Inside the spherical canonical model of the stomach, the novel antenna resonates slightly under the MedRadio band (at ≃395MHz).Since the dielectric properties of the stomach and the esophagus are quite similar that might be owed to the shape and dimensions of the canonical models used.

•In the canonical model of the colon (large intestine) the antenna appears to have a very robust performance. It resonates successfully at 405MHz, with magnitude of return loss greater than 20dB , and sufficient total gain(-27.83dB).

•In the canonical model of the small intestine, the ingestible antenna appears to be affected by more intense detuning phenomena. Given the fact that the permittivity value of the small intestine is close to those of the other examined tissues (i.e. ε'_r = 66.02 Vs ε'_r =62.51 for the colon), the detuning effect can be ascribed to the high conductivity magnitude of the small intestine (almost twice as high as the conductivity of the other tissues).This leads to the antenna exhibiting lower reflection coefficient ($|S_{11}|$) response.

Nonetheless, in more realistic implementations, that multi-layer canonical models or anatomical models will be used, the effect of the high conductivity of the small intestine is expected to fade due to the adjacent tissues (muscles, fat, skin etc.).
Overall, simulations have shown that the novel antenna could perform adequately as a component of a WCE system too. Further testing is indicated in order to assure operation as intended in all the tissues of the GI tract, with extra speculation in the stomach and small intestine tissues.

Chapter 5

Conclusions and future work

In the contexts of this thesis the following were presented:

▪the potentials of biomedical technology and the significant advancements which can contribute to the enhancement of the medical field .
▪the scientific orientation towards more flexible implants and injectable medical devices for less discomfort of the patient.
▪several implantable and ingestible devices that are applicable today and the limitations met in their use.
▪the state of the art in IMDS and antennas in WCE field (i.e. regarding energy issues, improvement of the radiation performances etc.).
▪main principles in the microstrip antenna theory as well as their miniaturization and broadbanding techniques.
▪the properties of the biological tissues, and how they affect the operation of the antenna.
A multilayer rectangular PIFA was introduced, operating in MedRadio and ISM bands. Used for Implantable Applications, its performance was studied inside different body phantoms. Both Parametric and Optimization Analysis also took place.
Based on this structure a novel multilayer antenna was designed, smaller than the former one, for almost 500 mm^3. Thus a 80.33 % reduction in size of the initial antenna is achieved The new 3-layer spiral PIFA operates at 401-406 Med Radio band .The antenna is tested for both implantable and ingestible use. Inside the muscle, head and 3-layer (muscle-fat-skin) models the antenna is well matched at 405MHz with better than -20dB reflection coefficient values. Testing of the antenna in canonical models of GI tract equivalent dielectric properties proved a more challenging procedure, however satisfying results were extracted from the simulation, concerning the reflection coefficient response and the antenna performance.

Future work could include antenna re-design in order to obtain:

•further miniaturization.

•fine tuning in order to operate as intended in all simplified models with sufficient performance needed.

•Study of other dielectric materials to be potentially used for enhancement of the antenna's performance.

• experimental testing of the antenna and the proposed simplified models.

Chapter 6

Referenences

[1] Gerald - Mark Breen & Jonathan Matusitz, An Evolutionary Examination of Telemedicine : A Health & Computer-Mediated Communication Perspective, Social Work in Public Health, 25: 59- 71, 2010.

[2] K.S. Nikita (Ed), Handbook of Biomedical Telemetry, Wiley-IEEE Press Publications, 2014

[3] M. Akay, D.I. Fotiadis, T. Exarchos, K.S. Nikita, Special Issue on Emerging Technologies for Patient-Specific Healthcare, IEEE Transactions on Information Technology in Biomedicine, vol. 16(2), 2012

[4] K.S. Nikita, J.C. Lin, D. I Fotiadis, M.T. Arredondo, "Editorial: Special Issue on Mobile and Wireless Technologies for Healthcare Delivery", IEEE Transactions on Biomedical Engineering, vol 59, no. 11, pp. 3083-3089, November 2012.

[5] M. Akay, G. Coatrieux, Y. Hao, D. I. Fotiadis, A. Laine, B. Lo, K. S. Nikita, N. Noury, J. Rodrigues, M. D. Wang, "The patient always at the center: from patient monitoring, m-health solutions, networking and security to collaborative environments, multiple source data analysis and predictive modeling", IEEE Journal of Biomedical and Health Informatics, vol. 20, no. 3, pp. 731-732, May 2016

[6] R. Ritter, J. Handwerker, T. Liu, and M. Ortmanns, "Telemetry for Implantable Medical Devices," IEEE solid-state circuits magazine, vol. 6,Issue. 2, pp. 47-51,Spring 2014.

[7] U.S. Department of Health & Human Services, National Institutes of Health, "How Does a Pacemaker Work?" [Online] . Available: "http://www.nhlbi.nih.gov/health/healthtopics/topics/pace/howdoes.html."

[8] Blake S. Wilson & Michael F. Dorman, Cochlear implants: Current designs and future possibilities, Journal of Rehabilitation Research & Development, Volume 45, Number 5, Pages 695–730, 2008

[9] Cochlear®, **"**Cochlear implants & cochlear implant technology [Online]. Available:"http : //www.cochlear.com/wps/wcm/connect/uk/home/understand/hearing-and-hl/hltreatments/cochlearimplant"

[10] National Institute of Deafness and other communication disorders, "What is a cochlear implant?"[Online]. Available:" https://www.nidcd.nih.gov/health/cochlear-implants"

[11] Retinal Implant Technology, "*Fighting Blindness"* ,[Online].Available: "https://www.fightingblindness.ie/cure/retinal-implant-technology/"

[12] Medtronic, *Continuous Glucose Monitoring*,[Online]. Available : "https://www.medtronicdiabetes.com/treatments/continuous-glucose-monitoring"
[13] Shabir Bhimji,et al. (2015), Diaphragm Pacing,Medscape. [Online].Available: "http://emedicine.medscape.com/article/1970348-overview
[14] Daniel Kantor,et al (2015), Intracranial pressure monitoring,MedlinePlus [Online].Available:" https://medlineplus.gov/ency/article/003411.htm"
[15] Strojnik, P.,Peckham. Implantable Stimulators for Neuromuscular Control , s.l. : CRC Press LLC, 2000.
[16] OAKLEAF Medical Network, "Spinal Cord Stimulation" [Online].Available: "http://www.carolsuecarlsonmd.com/spinal-cord-stimulation-chippewa-falls/"
[17] OAKLEAF Medical Network, "Spinal Cord Stimulation" [Online].Available: " http://www.salisburyfes.com/STIMuSTEP%20for%20web%20page.htm
[18] Yangzhe Liao, Mark S. Leeson, Matthew D. Higgins et al.(2016)." A Communication Link Analysis Based on Biological Implant Wireless Body Area Networks, Applied Computational Electromagnetics Society Journal 31(6):619-628
[19] G. Ntouni, A. Lioumpas, K.S. Nikita, "Reliable and Energy Efficient Communications for wireless Biomedical Implant Systems", IEEE Journal of Biomedical and Health Informatics, vol. 99, no. 1,2014.
[20] M. Seyedi, B. Kibret, D. T. Lai, and M. Faulkner, "A survey on intrabody communications for body area network applications," IEEE Transactions on Biomedical Engineering, vol. 60, no. 8, pp. 2067-2079, 2013.
[21] S. Ullah, et al, "A comprehensive survey of wireless body area networks," Journal of medical systems,vol. 36, pp. 1065-1094, 2012.
[22] F. Merli, "Implantable Antennas for Biomedical Applications," Ecole Polytechnique Federale De Lausanne,2011.
[23] FCC, "Medical Device Radiocommunications Service (MedRadio)",[Online]. Availiable:"https://www.fcc.gov/general/medical-device-radiocommunications-service-medradio"
[24] Fatih Mehmet Yurdal,*"* Short range devices (SRDs) & Ultra Wide Band, ITU,Geneva, 3 June 2014
[25] Xiao S., Liu C., Li Y., Yang M. X.,Liu X. ," Small-Size Dual-Antenna Implantable System for Biotelemetry Devices",IEEE Antennas and Wireless Propagation Letters, Vol 15, pp.1723 – 1726, February 2016
[26] Wang Z., JIANG H., "Developing Innovation -Wireless Transceiver Design for Implantable Medical Devices",RF & Wireless Technologies for Biomedical & Healthcare Applications (IMWS-BIO),2015 IEEE MTT-S 2015 International Microwave Workshop Series on, 21-23 Sept.2015
[27] D. Porcino and W. Hirt, "Ultra-wideband radio technology: potential and challenges ahead," IEEE Communications Magazine, vol. 41, no. 7, pp. 66-74, 2003.
[28] Chauhan Amadeep, et al. (2015),''Implantable Antennas in Biomedical

Applications'' , 2015 International Conference on Computational Intelligence and Communication Networks
[29] P. Soontornpipit, C.M.Furse,Y.C Chung.''Design of Implantable microstrip antenna for communication with medical implants",IEEE Transactions on Microwave theory & techniques, vol.52,pp.1944—1951,Aug2004
[30] A. Kiourti, J.R. Costa, C.A. Fernandes, A.G. Santiago, K.S. Nikita, "Miniature Implantable Antennas for Biomedical Telemetry: from Simulation to Realization", IEEE Transactions on Biomedical Engineering, vol. 59, no. 11, pp. 3140-3147, November 2012
[31] A. Kiourti, K.S Nikita, "Implantable Antennas: A Tutorial on Design, Fabrication, and In Vitro/In Vivo Testing", IEEE Microwave Magazine, vol. 15, issue. 4, pp. 77-91, 2014
[32] A. Kiourti, K.S. Nikita, "A Review on Implantable Patch Antennas for Biomedical Telemetry: Challenges and Solutions", IEEE Antennas and Propagation Magazine, vol. 54, no. 3, pp. 210-228, June 2012.
[33] Chen K., Yang Z., Hoang L., Weiland J., Humayun M., Liu W. An integrated 256-channel epiretinal prosthesis.IEEE J. Solid State Circuits. 2010;45:1946–1956
[34] Achraf Ben Amar, Ammar B. Kouki ,Hung Cao2 ,et al. (2015),"Power Approaches for Implantable Medical Devices", US National Library of Medicine National Institutes of Health,Sensors (Basel). 2015 Nov; 15(11):28889–28914.
[35]A.Kiourti, K.A. Psathas, K.S. Nikita, "Imlantable and ingestible medical devices with wireless telemetry functionalities: A review of current status and challenges", Bioelectromagnetics, vol. 35, no. 1, pp. 1-15, 2014
[36] Eng Gee Lim, Zhao Wang, Fang Zhou Yu, Tammam Tillo, Ka lok Man, Jing Chen Wang, Meng Zhang,Transmitter Antennas for Wireless Capsule Endoscopy,SoC Design Conference (ISOCC), 2012 International
[37] A. Glukhovsky, "Wireless capsule endoscopy," Sensor Rev., vol. 23, no. 2, pp. 128–133, 2003.
[38] Medtronic,Given,Imaging, M2A [Online]. Available: http://www.givenimaging.com/
[39] D.S. Mishkin, R. Chuttani, J. Croffie, J. Disario, J. Liu, R. Shah, L.Somogyi, W.Tierney, L.M.Song, and B.T.Petersen, Gastrointest. Endosc. 63, 539 (2006).
[40] Eliakim R, Yassin K, Shlomi I, Suissa A, Eisen GM. A novel diagnostic tool for detecting oesophageal pathology: the PillCam oesophageal video capsule. Aliment Pharmacol Ther 2004;20:1083–9.
[41] Cave DR. Reading wireless video capsule endoscopy. Gastrointest Endosc Clin N Am 2004;14:17–24.
[42] Lewis B. Capsule endoscopy-transit abnormalities.Gastrointest Endosc Clin N Am 2004;16:221–8.
[43] Andrea Moglia, Arianna Menciassi, Marc Oliver Schurr, Paolo Dario,"Wireless capsule endoscopy: from diagnostic devices to multipurpose robotic systems", Biomed Microdevices (2007) 9:235–243

[44] Saurin JC. Capsule endoscopy. Endoscopy 2007;39:986–91.
[45] Byungkyu Kim, Sunghak Lee, Jong Heong Park, Member, Jong-Oh ,"ParDesign and Fabrication of a Locomotive Mechanism for Capsule-Type Endoscopes Using Shape Memory Alloys (SMAs)",IEEE Trans on Mechatronics, vol. 10, no. 1, February 2005
[46] Gurveer Kaur, "Antennas for Biomedical Applications", The Korean Society of Medical & Biological Engineering and Springer 2015,Biomed Eng Lett (2015) 5:203-212
[47] Basar MR, Malek F, Juni KM, Idris MS, Saleh M. Ingestible wireless capsule technology: a review of development and future indication. Int J Antenn Propag. 2014; 12:1-14.
[48] Xu L, Meng MQH, Chan Y,et al. 2009, "Effects of dielectric parameters of human body on radiation characteristics of ingestible wireless device at operating frequency of 430 MHz", IEEE Trans. Biomed. Eng., 6:2083–2094.
[49] Lee SH, Lee J, Yoon YJ, Park S, Cheon C, Kim K, Nam S.,et al. 2011" A wideband spiral antenna for ingestible capsule endoscope systems: Experimental results in a human phantom and a pig." IEEE Trans.Biomed. Eng., 58(6):1734–1741.
[50] A. K. Hara, J. A. Leighton, V. K. Sharma, R. I. Heigh, and D. E. Fleischer, "Imaging of small bowel disease:comparison of capsule endoscopy, standard endoscopy, barium examination, and CT," Radiographics, vol. 25,no. 3, pp. 697–711, 2005.
[51] Ciuti G, Menciassi A, Dario P (2011) Capsule endoscopy: from current achievements to open challenges. IEEE Rev Biomed Eng 4:59–72
[52] Sliker LJ, Ciuti G (2014) Flexible and capsule endoscopy for screening, diagnosis and treatment. Expert Rev Med Devices 11: 649–666
[53] E. Rondonotti, J. M. Herrerias, M. Pennazio, A. Caunedo, M. Mascarenhas-Saraiva, and R. De Franchis,"Complications, limitations, and failures of capsule endoscopy: a review of 733 cases," Gastrointestinal Endoscopy, vol. 62, no. 5, pp. 712–716, 2005.
[54] Moglia A., et al(2007),"Wireless capsule endoscopy: from diagnostic devices to multipurpose robotic systems",Biomed Microdevices (2007) 9:235–243
[55] Ciuti G, et al.(2016,)"Frontiers of robotic endoscopic capsules: a review", J Micro-Bio Robot
[56] Farnbacher MJ, Krause HH, Hagel AF, et al. QuickView video preview software of colon capsule endoscopy: reliability in presenting colorectal polyps as compared to normal mode reading. Scand J Gastroenterol 2014;49:339–346.
[57] Saurin J.C ,"Challenges and Future of Wireless Capsule Endoscopy", Clin Endosc.. 2016 Jan; 49 (1): 26–29.
[58] Valdastri P, Quaglia C, Susilo E, et al. Wireless therapeutic endoscopic capsule: in vivo experiment. Endoscopy 2008; 40:979–982.
[59] Koulaouzidis A, "Wireless endoscopy in 2020: Will it still be a capsule?", World J Gastroenterol.2015 May 7;21(17): 5119–5130.
[60] Xin W, Yan G, Wang W. Study of a wireless power transmission system for an active capsule endoscope. Int J Med Robot 2010; 6:113–122.

[61] Philip R. Troyk,(1999) Injectable Electronic Identification, Monitoring, and Stimulation Systems, Annu. Rev. Biomed. Eng. 1999. 01:177–209
[62] G.E. Loeb, F.J.R. Richmond, S. Olney, T. Cameron, A.C. Dupont, K. Hood, R.A. Peck,1998, BIONTM Bionic Neurons for Functional and Therapeutic Electrical Stimulation, Proceedings of the 20th Annual International Conference of the ZEEE Enpineering in Medicine and Bioloav Society, Vol. 20, NO 5
[63] R. Carbunaru, T. Whitehurst, K. Jaax, J. Koff and J. Makous,(2004), Rechargeable Battery-Powered bion® Microstimulators for Neuromodulation, IEEE EMBS, September1-5.
[64] G. E. Loeb, F.J.R. Richmond, J. Singh, R.A. Peck, W. Tan, Q. Zou, and N. Sachs,(2004) ,RF- Powered BIONs™ for Stimulation and Sensing,26th Conference, IEEE EMBS,September1-5.
[65] Djordje Popovic, Lucinda L. Baker, and Gerald E. Loeb,(2007), Recruitment and Comfort of BION Implanted Electrical Stimulation: Implications for FES Applications,IEEE Trans on neural Systems and Rehabilitation Engineering, vol 15, no.4, December 2007
[66] Loeb G.E. et al (1991) Injectable microstimulator for functional electrical stimulation .Med. Bio.Eng. Comput.29 ,NS13-NS19
[67] Xiaolong Li , Wouter A.Serdijn, Wei Zheng, Yubo Tian & Bing Zhang, The injectable neurostimulator: an emerging therapeutic device, article in Press, CellPress , 2015
[68] Warren M. Grill, Sharon E. Norman,and Ravi V. Bellamkonda3,et al.(2009) Implanted Neural Interfaces: Biochallenges and Engineered Solutions, Annu Rev Biomed Eng.:1-24.
[69] Sanketh R. Gowda,Arava Leela Mohana Reddy, Xiaobo Zhan,Huma R. Jafry, and Pulickel M.Ajayan,e t al.(2012), 3D Nanoporous Nanowire Current Collectors for Thin Film Microbatteries, ACS Nano Lett12,1198-1202
[70] Honghao Chen, Samuel Cartmell, Qiang Wang, Terence Lozano, Z. Daniel Deng, Huidong Li, Xilin Chen,Yong Yuan, Mark E. Gross, Thomas J. Carlson & Jie Xiao,et al(2014) Micro-battery Development for Juvenile Salmon Acoustic Telemetry System Applications. Scientific Reports 4,3790
[71] Loeb,G.E. et al. (2006)The BION devices :injectable interfaces with peripheral nerves and muscles.Neurosurg.Focus 15,E2
[72] Sahin M et al. (2011) Wireless microstimulators for neural prosthetics .Crit. Rev. Biomed.Eng.39,63-77
[73] Dunne S.M,et al. (2000) Dental post-operative sensitivity assosiated with a gallium-based restorative material.Br. Dent. J. 189,310-313
[74] Kim, D. et al.(2009) Silicon electronics on silk as a path to bioresorbable ,implantable devices . Appl. Phys.Lett 95,133701
[75] Zaraska, W. et al.(2005) Design and fabrication of neurostimulator implants-selected

problems. Microelectron.Reliab. 45,1930-1934
[76] Chao Jin, Jie Zhang, Xiaokang Li, Xueyao Yang, Jingjing Li & Jing Liu,(et al 2013), Injectable 3-D Fabrication of Medical Electronics at the Target Biological Tissues, Scientific Reports 3,3342
[77] Howes,P.D. et al.(2014) Colloidal nanoparticles as advanced biological sensors. Science 346,1247390
[78] Yibo,L. et al. (2010) Implantable magnetic relaxation sensors measure cumulative exposure to cardiac biomarkers. Nat. Biotechnol. 29,273-277
[79] Patek, S.N. (2014) Biomimetrics and evolution. Science 345,1448-1449
[80] Quiney,H. M. et al. (2011) Biomolecular imaging and electronic damage using X-Ray free- electron lasers.Nat Phys. 7,142-146
[81] Hillel, A.T. et al. (2011) Photoactivated composite biomaterial for soft. tissue restoration in rodents and in humans, Sci. Transl. Med. 3,93ra67
[82] C. A. Balanis, Antenna Theory, Analysis and Design, 3rd ed. John Wiley & Sons, INC, 2005.
[83] Kin-Lu Wong, Compact and Broadband Microstrip Antennas, John Wiley & Sons, INC,2002
[84] D. H. Schaubert, F. G. Farrar, A. Sindoris, and S. T. Hayes, "MicrostripAntennas with Frequency Agility and Polarization Diversity," IEEE Trans. Antennas Propagat., Vol. AP-29, No. 1, pp. 118–123, January 1981.
[85] Bhattaacharyya, K. and L. Shafai, "Surface wave coupling between circular patch antennas,"Electronic Letters, Vol. 22, No. 22, 1986.
[86] D. M. Pozar, "Microstrip Antennas," Proc. IEEE, Vol. 80, No. 1, pp. 79–81, January 1992
[87] Medikonda A.K, N. RAJU, S. MISRA," Rectangular Micro strip Patch Antenna using Coaxial Probe Feeding Technique to Operate in MICS-Band", International Journal of Advanced Technology and innovative Research IJATIRVol.08 ,Issue.10, pp:2065-2068, Aug.2016
[88] W.-C. Liu, F.-M. Yeh, and M. Ghavami, "Miniaturized implantable broadband antenna for biotelemetry communication," Microw Opt Technol Lett, vol. 50, pp. 2407–2409, Sep. 2008.
[89] Chandra Prakash , R.P.S. Gangwar , "Six Layers Circular Microstrip Antenna Implanted in a Phantom of Vitreous Humor", RF and Wireless Technologies for Biomedical and Healthcare Applications (IMWS-Bio), 2014 IEEE MTT-S International Microwave Workshop Series on,pp.1-3,Dec. 2014
[90] Rupam Das; Hyoungsuk Yoo,"Wireless power transfer and biotelemetry in a leadless pacemaker",2015International Workshop on Antenna Technology (iWAT), March 2015
[91] Mai O. Sallam , Ashraf Badawi , Ezzeldin A. Soliman, "Design of an Implantable Miniaturized Meander Line Antenna for Biomedical Telemetry", 2016 10th European Conference on Antennas and

Propagation (EuCAP), pp1-4, Octob. 2016
[92] Kiourti A, Tsakalakis M, Nikita KS. “Parametric study and design of implantable PIFAs for wireless biotelemetry”. Proceedings of the 2nd ICST Intern Conference on Wireless Mobile Communication and Healthcare (MobiHealth 2012), Kos Island, Greece, October 2011.
[93] Imran Gani , Hyoungsuk Yoo, “Miniaturized scalp-implantable antenna for wireless biotelemetry”,Antenna Technology (iWAT), 2015 International Workshop on, March 2015
[94] Kiourti A, Christopoulou M, Nikita KS. “Performance of a novel miniature antenna implanted in the human head for wireless biotelemetry”. IEEE Intern Symposium on Antennas and Propagation, Spokane, Washington, July 2011.
[95] Zetao Wu, XiongYing Liu, YunHui Di ,”A novel stacked inverted-F antenna for implanted bio-devices in the MICS band”. Computational Electromagnetics (ICCEM), 2015 IEEE International Conference on, Feb. 2015
[96] Damla Alptekin, Lale Alatan, Nevzat G. Gencer,” Dual band PIFA design for biomedical applications,Antennas and Propagation (EuCAP)”, 2016 10th European Conference on,pp. 1-4, April 2016
[97] M. A. Youssef, M. M. A. Allam,” Implanted Antenna on Human Breast”, 2014 International Conference on Engineering and Technology (ICET),PP. 1-4, April 2014
[98] Vidal, N., Villegas, J.M.L., Curto, S., and Sieiro, J., “Design of a LTCC compact implantable broadband antenna for wireless biotelemetry,” Antennas Propag. Soc. Int. Symp. Apsursi 2012 Ieee, pp. 1–2, Jul. 2012.
[99] Permana H, Fang Q, Cosic I. “3-Layer implantable microstrip antenna optimized for retinal prosthesis system in MICS band”. Proceedings of the IEEE Intern Symposium on Bioelectronics and Bioinformatics (ISBB 2011), November 2011.
[100] A. Garcia-Miquel, N. Vidal J., M. Lopez-Villegas, J. J. Sieiro, F. M. Ramos, ”Miniaturization effects on implantable antennas for biomedical applications”,2015 9th European Conference on Antennas andMPropagation (EuCAP),pp.1-4,Aug 2015
[101] Jae-Ho Lee Dong-Wook Seo Hyung-Soo Lee ,“Design of implantable antenna on the dielectric/ferrite substrate for wireless biotelemetry “.Antennas and Propagation (ISAP), 2015 International Symposium ,Nov. 2015
[102] P. S. Neelakantra and R. Chatterjee, Antennas for Information Super Skyways: An Exposition on Outdoor and Indoor Wireless Antennas. Research Studies Press Ltd., 2002.
[103] Mohammed N. Shakib, Mahmoud Moghavvemi Wan N. L. Mahadi, Muhammad R. Ahmed, ”Design of a Broadband Implantable Antenna in the Rat for Biotelemetry Applications”, 2015 IEEE MTT-S 2015 International Microwave Workshop Series on RF and Wireless Technologies for Biomedical and Healthcare Applications (IMWS-BIO),pp. 239 – 240, Sept. 2015
[104] Sanchez-Fernandez CJ, Quevedo-Teruel O, Requena-Carrion J, Inclan-Sanchez L, Rajo-Iglesias E. , “Dual-band microstrip patch antenna based on short-circuited ring and

spiral resonators for implantable medical devices". IET Microw Antenn P. 2010; 4(8):1048-55.
[105] A. A. Abdelaziz, "Bandwidth Enhancement of Microstrip Antennas", Progress In Electromagnetics Research, PIER 63, 311–317, 2006
[106] James, J. R. and P. S. Hall, Handbook of Microstrip Antennas, Peter Peregronic Ltd., London, 1989.
[107] R. Garg, P. Bhartia, I. Bahl, A. Ittipiboon,Microstrip Antenna Design Handbook, Artech House INC,2001
[108] Pozar, D. M. and D. H. Schaubert, "Scan blindness in infinite phased arrays of printed dipoles," IEEE Trans. Ant. Prop., Vol. AP-32, No. 6, 1984.
[109] A. Kiourti, J.R. Costa, C.A. Fernandes, K.S. Nikita, "A Broadband Implantable and a Dual-Band On-Body Repeater Antenna: Design and Transmission Performance", IEEE Transactions on Antennas and Propagation, vol. 62, no. 6, pp. 2899-2908, 2014.
[110] K.W. Loi, S. Uysal, and M. S. Leong, "Design of a wideband Microstrip bowtie patch antenna" Proc.Inst. Elect. Eng. Microwave Antennas propagation vol. no. 145,pp. 137-140, 1998.
[111] Shing-Lung Steven Yang , Ahmed A. Kishk ,and KaiFong Lee "Frequency Reconfigurable U-slot Microstrip Antenna" IEEE antenna and wireless propagation letters vol. no. 7, 2008.
[112] D.D.Ahire, S.R.Bhirud."Performance Enhancement of Microstrip Patch Antennas Using Slotting : A Review", International Journal of Advance Foundation and Research in Computer (IJAFRC) Volume 2, Issue 8, August - 2015.
[113] Tej Raj , Brajlata Chauhan ,"Single Layer Dual band Microstrip Patch Antenna using Probe Feed",International Journal of Computer Applications (0975 – 8887) Volume 92 – No.12, April 2014
[114] C. K. Wu and K. L. Wong, "Broadband microstrip antenna with directly coupled and gap-coupled parasitic patches", Microwave Opt. Technol. Lett. 22, 348–349, Sept. 5, 1999.
[115] Sharif I.Mitu Sheikh, W. Abu-Al-Saud, and A. B. Numan"Directive Stacked Patch Antenna for UWB Applications" Hindawi Publishing Corporation International Journal of Antennas and Propagation Volume 2013
[116] Hatem H. Abbas , Jabir S. Aziz, "Bandwidth Enhancement of Micro-Strip Patch Antenna ",Journal of Mobile Communication, Volume 4,pp. 54-59,2010
[117] Asimina Kiourti,"Implantable Antennas for Biotelemetry Applications, Dissertation, July 2013
[118] R. W. P. King and G. S. Smith, Antennas in Matter: Fundamentals, Theory, and Applications, 1st ed.Cambridge, Massachusetts, and London, England: The MIT Press, 1981
[119] C.Gabriel, "Compilation of the dielectric properties of body tissues at RF and microwave frequencies," Brooks Air Force Base, Texas (USA), Tech. Rep. Report

N.AL/OE-TR-, June1996. [Online]. Available:
http://niremf.ifac.cnr.it/tissprop/htmlclie/htmlclie.htm
[120] Konstantinos A. Psathas, Anastasis P. Keliris, Asimina Kiourti, Konstantina S. Nikita, "Operation of Ingestible Antennas along the Gastrointestinal Tract: Detuning and Performance", Bioinformatics and Bioengineering (BIBE), 2013 IEEE 13th International Conference, Nov. 2013
[121] A.Kiourti, K. Psathas, P. Lelovas, N. Kostomitsopoulos, K.S. Nikita, "In Vivo Tests of Implantable Antennas in Rats: Antenna Size and Inter-Subject Considerations", IEEE Antennas and Wireless Propagation Letters, vol. 12, pp. 1396-1399, 2013.
[122] A. Kiourti and K. S. Nikita, "Miniature Scalp-Implantable Antennas for Telemetry in the MICS and ISM Bands: Design, Safety Considerations and Link Budget Analysis," IEEE Transactions on Antennas and Propagation
[123] P. Soontornpipit, C. M. Furse, and Y. C. Chung, "Design of Implantable Microstrip Antenna for Communication with Medical Implants," IEEE Transactions on Microwave Theory and Techniques,52, 8, August 2004, pp. 1944-1951
[124] A. Kiourti and K. S. Nikita, "Meandered Versus Spiral Novel Miniature PIFAs Implanted in the Human Head: Tun ing and Performance," Proceedings of the 2nd ICST International Conference on Wireless Mobile Communication and Healthcare (MobiHealth 2012), Kos Island, Greece, October 2011.
[125] A. Kiourti, K.S. Nikita, "Numerical Assessment of the Performance of a Scalp-Implantable Antenna: Effects of Head Anatomy and Dielectric Parameters", Bioelectromagnetics, vol. 34, issue 3, pp. 167- 179, April 2013.
[126] C. Miry, R. Gillard, and R. Loison, "An application of the multi-level DG-FDTD to the analysis of the transmission between a dipole in free-space and an implanted antenna in a simplified body model with various positions," in Proc. 3rd European Conference on Antennas & Propagation EuCAP 2009, 23–27 Mar. 2009, pp.67–70
[127] A. Kiourti, K.S. Nikita, "Design of Implantable Antennas for Medical Telemetry: Dependence Upon Operation Frequency, Tissue Anatomy, and Implantation Site", IGI Global International Journal of Monitoring and Surveillance Technologies Research (IJMSTR) vol. 1, issue 1, pp. 16-33, 2013.
[128] W. C. Liu, S. H. Chen, and C. M. Wu, "Implantable Broadband Circular Stacked PIFA Antenna for Biotelemetry Communication," Journal of Electromagnetic Waves and Applications, 22, 13, 2008, pp. 1791-1800.
[129] W. Huang and A. A. Kishk, "Embedded Spiral Microstrip Implantable Antenna," Hindawi International Journal of Antennas and Propagation, 2011
[130] Kiourti, K.S. Nikita, "Accelerated design of optimized implantable antennas for medical telemetry", IEEE Antennas and Wireless Propagation Letters, vol. 11, pp. 1655-1658, 2012
[131] HFSS user's guide – High Frequency Structure Simulator, ANSOFT CORPORATION Pittsburgh, PA 15219-1119, 2005

[132] Francesco Merli, Jean-Francois Zurcher, Giancarlo Corradini, Eric Meurville,Anja K.Skrivervik, ”Design, Realization and Measurements of a Miniature Antenna for Implantable Wireless Communication Systems”, IEEE Trans on Antennas and Propagation, vol.59, n0.10, October 2011
[133] K.Gosalia,G.Lazzi,andM.Humayun,“Investigation of a microwave data telemetry link for a retinal prosthesis,” IEEE Trans. Microwave Theory Tech., vol. 52, no. 8, pp. 1925–1933, Aug. 2004.
[134] J. Kim and Y. Rahmat-Samii, “Planar inverted-f antennas on implantable medical devices: Meandered type versus spiral type,” Microw.Opt.Technol.Lett., vol.48,no.3,pp.567–572,2006.
[135] P. Soontornpipit, C. Furse, and Y. C. Chung, “Design of implantable microstrip antenna for communication with medical implants,” IEEE Trans. Microwave Theory Tech., vol. 52, no. 8, pp. 1944–1951, Aug. 2004.
[136] P.D. Bradley, “An ultra low power, high performance medical implant communication system (MICS) transceiver for implantable devices,” in Proc. IEEE Biomedical Circuits and Systems Conf. BioCAS 2006, Nov. 2006, pp. 158–161.
[137] Handbook of Materials for Medical Device. Materials Park, OH: ASM international, 2003, ch. 1.
[138] W. Sun and Y.-X. Yuan, Optimization Theory and Methods. NewYork: Springer, 2006, ch. 5, Ed.
[130] A. Kiourti, K.S. Nikita, “Recent Advances in Implantable Antennas for Medical Telemetry”, IEEE Antennas and Propagation Magazine vol. 54, no. 6, pp. 190-199, December 2012.
[140] A.Kiourti, K.S. Nikita , “A Review of In-Body Biotelemetry Devices: Implantables, Ingestibles, and Injectables”, IEEE Transactions in Biomed Eng. 2017 Feb 14